HOST UNIVERSITY: ETH Zürich

FACULTY: Civil, Environmental and Geomatic Engineering

DEPARTMENT: Institute of Structural Engineering (IBK)

Academic Year 2021-2022

Modelling of Timber Pyrolysis with FDS

Sabrina Spörri

Supervisors:

Prof. Dr. Bart Merci (Ghent University), Dr. Andrea Lucherini (Ghent University),

Prof. Dr. Andrea Frangi (ETH Zürich), Karannagodage Chamith (ETH Zürich)

Master thesis submitted in the Erasmus+ Study Programme

International Master of Science in Fire Safety Engineering

DISCLAIMER

This thesis is submitted in partial fulfilment of the requirements for the degree of *The International Master of Science in Fire Safety Engineering (IMFSE)*. This thesis has never been submitted for any degree or examination to any other University/programme. The author(s) declare(s) that this thesis is original work except where stated. This declaration constitutes an assertion that full and accurate references and citations have been included for all material, directly included and indirectly contributing to the thesis. The author(s) gives (give) permission to make this master thesis available for consultation and to copy parts of this master thesis for personal use. In the case of any other use, the limitations of the copyright have to be respected, in particular with regard to the obligation to state expressly the source when quoting results from this master thesis. The thesis supervisor must be informed when data or results are used.

Read and approved,

Sabrina Spörri

(10th May 2022)

Abstract

Timber is experiencing a revival in the construction area. However, as a combustible material it poses a risk in case of fire. The understanding of how it burns in non-standardized fires is actually limited, but with the evolution towards performance-based designs, such knowledge is of huge importance.

Wood burning is a complex process because of its inhomogeneous structure and the interlinked processes of material decomposition and gas-phase combustion. Further, the burning products such as char influence the fire dynamics. Therefore, this work studies the charring properties during the burning of timber by a FDS (Fire Dynamics Simulator) simulation. The goal is to use the complex pyrolysis model in FDS with appropriated input parameters together with gas phase combustion in simulations with a non-standardized environment and analyse the simulation results in view of the charring properties as well as compare them to experimental data. Additionally, the study also changed some input parameters to assess their influence on the simulation results and the usefulness of such changes compared to the experimental results.

The main finding of this study was that an appropriated mesh resolution is needed inside the timber sample to perform theses simulations. The simulation outputs showed relatively good values for the charring rates and the surface temperatures of the timber compared with the experimental results. However, the charring depth was overestimated. The changed input parameters for the simulations did not result in huge differences compared to the experimental data.

To conclude, the ability of FDS to include different submodels and to be used with different complexities, makes it an interesting tool to study charring properties during the burning of timber, even if until now the setup of the FDS code needs a lot of input data and is relatively time-consuming.

Keywords: Pyrolysis; timber; simulation; FDS; charring rate; charring depth

Zusammenfassung

Holz erfährt im Moment einen neuen Aufschwung im Baugewerbe. Allerdings ist es auch ein brennbares Material, das eine Brandgefahr darstellt. Das Verständnis, wie sich Holz in nicht standardisierten Bränden verhält, ist im Moment begrenzt. Mit der Entwicklung in Richtung performance-basierenden Designen ist solches Wissen jedoch von enormer Wichtigkeit.

Der Abbrand von Holz ist ein komplexer Prozess wegen seiner inhomogenen Struktur und den ineinandergreifenden Prozessen von Materialzersetzung und Gasverbrennung. Zusätzlich beeinflussen Abbrandprodukte wie Kohle die Branddynamik. Daher wird diese Arbeit die Verkohlungseigenschaften während der Holzverbrennung mit dem Simulationsprogram FDS (Fire Dynamic Simulator) studieren. Das Ziel ist es, das komplexe Pyrolysemodel von FDS mit geeigneten Inputparametern sowie der Gasverbrennung und einer nicht-standardisierten Umgebung zu benutzen sowie die Simulationsresultate hinsichtlich der Verkohlungseigenschaften zu analysieren und mit experimentellen Resultaten zu vergleichen. Zusätzlich ändert die Studie auch einige Inputparameter ab, um deren Einfluss auf die Simulationsresultate und deren Nutzen im Vergleich mit den experimentellen Resultaten zu beurteilen.

Das Hauptresultat dieser Studie ist, dass eine geeignete Gitterauflösung in der Holzprobe für die Simulationen notwendig ist. Die Simulationsergebnisse zeigten relativ gute Werte für die Verkohlungsraten und die Oberflächentemperaturen des Holzes verglichen mit den Versuchsresultaten. Hingegen wurden die Verkohlungstiefen überschätzt. Die geänderten Simulations-Inputparameter resultierten in keinen grossen Unterschieden verglichen mit den besagten Versuchsergebnisse.

Abschliessend kann gesagt werden, dass die Fähigkeit von FDS, verschiedene Untermodelle einzubinden und mit verschiedenen Komplexitäten benutzt zu werden, es zu einem interessanten Instrument macht, um die Verkohlungseigenschaften während des Holzbrandes zu studieren, obwohl momentan das Simulationssetup noch eine Menge an Input-Daten braucht und relative zeitintensive ist.

Keywords: Pyrolyse; Holz; Simulation; FDS; Verkohlungsrate; Verkohlungstiefe

Table of content

1 Introduction

Nowadays, the traditional construction material timber is experiencing a renaissance as it is a climate-friendly material which contributes to a sustainable construction, but also satisfies the architectural need for new designs and aesthetics [1]–[6]. However, timber is also a combustible material which adds additional fuel load to a fire [2], [6]. This was also the reason why its use as a construction material was strictly limited for a long time, or even partly forbidden – e.g. for residence buildings [2]. A lot of our actual knowledge about timber behavior in fire situations is derived from standard-temperature exposure approximating a fully developed fire [2], [6]. This is due to the fact that this condition is used for testing in regulations, as for example in the European regulations [7]. But there are designs where this standard temperature exposure is clearly not the right way to assess the safety of a building in a fire situation and such a test would lead either to an overconservative construction or one deemed to fail. In such cases, an evaluation of the design based on its performance in a fire will allow a more accurate judge of its safety (risk-based approach or performance-based design instead of prescriptive design). These performance-based designs are also the long-term objectives of regulations and laws [2]. However, for other stages in a fire or in other fire situations, the actual understanding is limited and more research is needed to be able to assess the contribution of timber-based material on fire dynamics - especially as timber not only contributes to the heat release rate as a combustible material but it also influences the fire dynamics [6]. For example, the danger of a fire for a construction is defined by the combustible material present. If the walls and ceiling are made out of wood, this combustible material should be added to the fire load as they burn [3]. However, experiments showed that in such cases and with a ventilation-controlled fire, “a larger part of the produced pyrolysis gases burned outside of the fire compartment” [6, p. 895] than for environments without exposed timber elements. Therefore, such a methodology would lead to an overconservative design inside and can underpredict the danger outside. Another specialty of the burning of timber is that the produced char has different material properties than the virgin timber and therefore a simple assessment of the amount of timber for the fire load does not give an accurate estimation of the contribution of the wooden elements to the fire [1], [3]. This is why this study will focus on the char properties during the burning of timber. A cost-effective way to do that is by computer simulation. This study will use the software FDS (Fire Dynamic Simulator) which is based on computational fluid dynamic models (CFD) and includes pyrolysis models.

The next section explains what timber is, followed by an introduction to the complex process of timber burning and an overview of the methods of simplification of that process and ends with an introduction to the FDS software.

1.1 Composition of timber

Timber is a substance with an anisotropic structure [8]. Its main components being cellulose, hemicellulose and lignin [8]–[10]. Depending on the wood species, the percentage of these three molecules vary, but a rough approximation for dry wood is 50 % of cellulose, 25 % of hemicellulose and 25 % of lignin [8], [9]. Chemically cellulose is a glucon polymer made out of linear chains of β-(1,4)-D-glucopyranose units. From an engineering perspective, cellulose is responsible for the tensile strength as the wood cell walls are made out of it [11]. Hemicellulose is a mixture of polysaccharides [9] and is placed around the cellulose [11]. Finally, lignin is a ”random polymer of substituted phenyl propane units” [9, p. 3] and keeps the wood cells together. By that, it is responsible for transferring compressive and shear stresses [11].
All the different types of timber can be classified into softwood or hardwood [10]. Table 1 shows some examples (extracted from [10, p. 2]).

Table 1: Classification of timber

Type of timber	Examples
Softwood	Douglas fir, Red pine, Spruce, Western larch, White fir, White pine
Hardwood	Beech, Birch, Cherry, Mahogany, Maple, Oak, Walnut, White ash, Willow

Timber naturally contains some moisture [12]. This can exist either as bound water in the cell wall – named hygroscopic water – or as free water in the voids of the wood – named capillary water. The maximum percentage of bound water in the cell is called fibre saturation point (FSP) and is for wood around 30 % [12]. Above that value, water is present as free water and can be as high as 200 % [12].

1.2 Burning of timber

The burning of timber can be divided into two main processes [9]. First of all, a thermal degradation (pyrolysis) takes place when timber is exposed to a heating source. That process produces, amongst others, flammable volatiles. They are then involved in the second process which is the gas combustion (fuel oxidation) triggered by an ignition condition. The next two subsections present these processes in more detail.

1.2.1 Pyrolysis of timber

Pyrolysis is a process that occurs in the absence of oxygen or under inert atmosphere [13], [14]. [15] cited Bartlett et al. [14] identifies three temperature dependent main stages. The first is below 200 [°C] where dehydration and a very slow pyrolysis happens. Then until up to 300 [°C] is the start of pyrolysis and from then on, fast pyrolysis happens. During pyrolysis, chemical, physical and mechanical processes take place as summarized in figure 1 [4, Fig. 3].

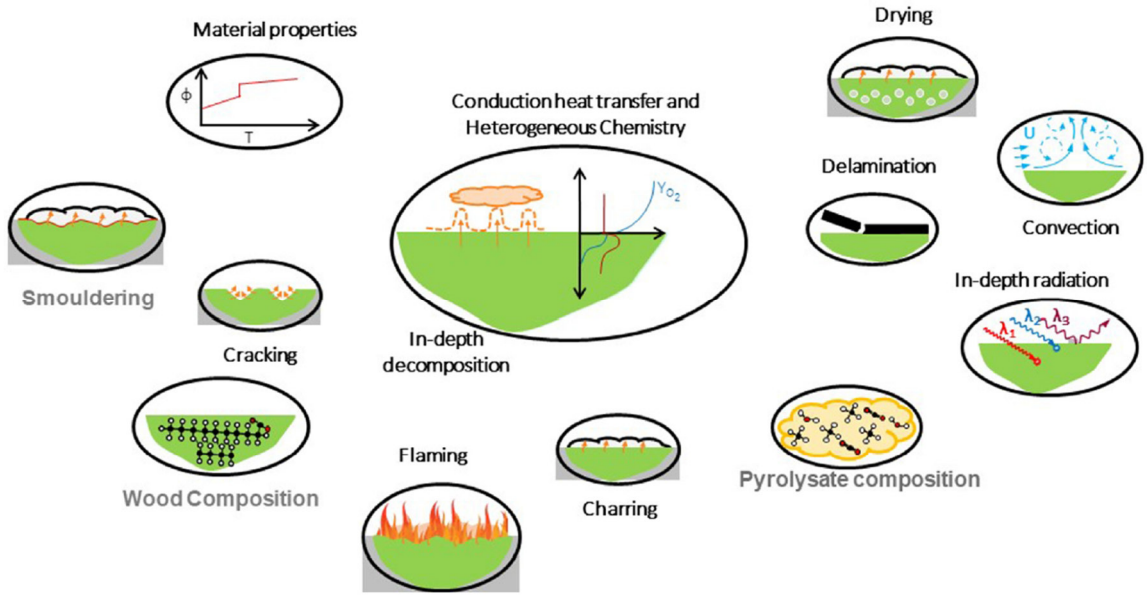

Figure 1: Factors influencing the pyrolysis of wood [4, Fig. 3]

The next two sections explain the chemical and physical processes.

Chemical process

On a general level, pyrolysis is an endothermic reaction and energy is needed to break the polymers into smaller parts able to be present in the gaseous phase [11], [14]. This process produces inert and combustible gases, liquid tar, solid carbon-rich non-volatile char and inorganic nonburning ashes [11], [14] as shown in equation 1.

$$wood \rightarrow gases + tar + char + ashes \qquad (1)$$

The produced gases are mainly CO, CO_2 and H_2O. The combustible gases will further undergo combustion (cf. Chapter 1.2.2 “Gas combustion”). The produced tar is a mixture of high molecular weight molecules, containing many 1,6-anhydro compounds [8]. They can also undergo other reactions as either being broken down into combustible gases or forming char by repolymerization [14].The char are the heavier and larger molecules which stay on the wood surface and are forming a layer which will affect the heat transfer (cf. next subsection “Physical process”). Char can also further react by solid phase oxidation which is visible as smouldering and results in further products. This decomposition creates also a surface regression of the wood and makes the cross-section smaller [3]. The char yield of the reaction is influenced by the presence of organic impurities in the wood sample [14].

As explained in the section before, timber is made out of three main components, each of it reacts at different temperature intervals. The main one, cellulose, decomposes in two different processes depending on the temperature range [9]. The main process for temperatures less than

300 [°C] is a reduction in the polymerization degree. For higher temperatures, the degradation results in the formation of char, tar and gaseous products.
The second main component in wood, the hemicellulose, is very temperature sensitive and degrades between 200 [°C] and 260 [°C] [9]. It also gives rise to more volatiles than the process for cellulose.
The last component, lignin, degrades between 280 [°C] and 500 [°C] and produces around 55 % of char, 20 % of aqueous components, 15 % of tar residue and 10 % of gaseous products [9]. Char formation starts at around 300 [°C] for most situations [14].
During this process, around 77 % by weight of dry wood of volatiles are produced. Table 2 summarizes the overall process of pyrolysis from a chemical point of view [9].

Table 2: Key events in chemical process of pyrolysis

Temperature [°C]	Process
~ 160	All moisture is removed from the wood sample
200 - 280	Decomposition of hemicellulose producing primarily volatiles
280 – 500	Decomposition of cellulose, producing primarily volatiles
300	Onset of fast pyrolysis and char formation
~ 320	Peak of cellulose decomposition
> 320	Increase of lignin decomposition

This is a simplified description of the processes. In reality, several interdependent chemical reactions occur at the same time and the process is further complicated by the inhomogeneity of wood and the influence of the produced char layer [8].

Physical process

The physical process – summarized by Sinha et al. [9] – starts by the heating up of the timber by a heating source leading to an increased temperature inside the timber. This is mainly done by conduction. Once the temperature is high enough, the first pyrolysis reactions start, releasing volatiles and the formation of a char layer begins. The volatiles will flow up and out of the wood surface. On their way out they will exchange heat with the cooler unpyrolysed fuel. Some of them will even condensate which results in the production of tar or undergo secondary pyrolysis reaction changing the heat balance. Hence, the speed of the pyrolysis front and the pyrolysis rate is defined by the in-depth conductive heat transfer from the flaming combustion and the heat loss by convection of the hot pyrolysis gases as is shown in the figure 2 [11].

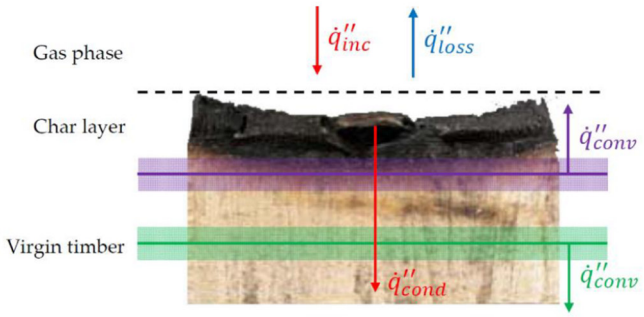

Legend

$\dot{q}''_{inc}$	Incident heat flux
$\dot{q}''_{loss}$	Heat loss
$\dot{q}''_{conv}$	Heat flux by convection
$\dot{q}''_{cond}$	Heat flux by conduction

Figure 2: Simplified summary of heat transfer in a wood sample [11, Fig. 2.7], *© Juan Cuevas*

Figure 3 combines the physical and chemical process of a burning wood sample [14, Fig. 1].

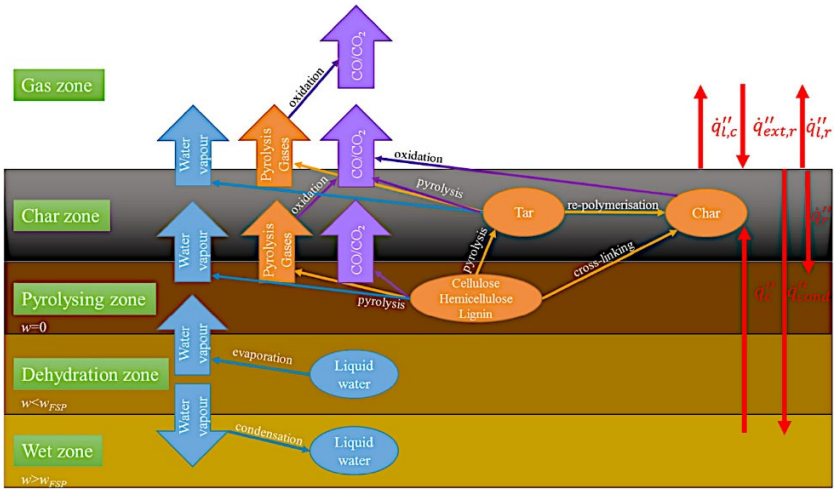

Legend

$\dot{q}''_{l,c}$	Surface heat loss by convection
$\dot{q}''_{l,r}$	Surface heat losses by radiation
$\dot{q}''_{ext,r}$	External heat flux
$\dot{q}''_{r}$	In-depth radiation
$\dot{q}''_{cond}$	Conduction into wood sample
$\dot{q}''_{c}$	Convective heat transfer through cracks in sample
FSP	Fiber saturation point

Figure 3: Summary of chemical and physical process [14, Fig. 1]

The physical processes are further complicated by the moisture transport (figure 2 & 3). As explained by Bartlett et al. [14], the evaporation of water starts at around 100 [°C] and therefore, before pyrolysis begins. Water vapour will leave the wood sample as shown in figure 3. At the same time, a smaller part of the water vapour will move away from the surface, deeper inside the sample and recondense there. This process splits the wood sample in three areas (image 3): the pyrolysis zone which is a dry one, the dehydration zone and the wet zone. Depending on the intensity of the heat flux, dehydration and pyrolysis will take place either independently or at the same time. The last case occurs at high heat fluxes. There, the need of energy to evaporate the water will slow down the temperature rise. Also, the convective mass flow of that vapour will cool the pyrolysis zone.

The formed char layer also affects the heat transfer and hence the fire dynamic. One reason for this are the different material properties between char and timber [14]. Char is a porous material and increases the heating of the wood sample but at the same time it has a higher thermal

conductivity than wood delaying the pyrolysis start. Moreover, the cracks in the char change the type of heat transfer, from a normally conductive dominated one to a radiative one. To summarize, there is an overall consent that char insulates and decreases burning rate [16].

1.2.2 Gas combustion

The mixing of combustible pyrolysis products with air in the right proportion (*flammability limit*) and in the right environmental conditions leads to their oxidation. This process is called combustion [11], [14]. This is an exothermic process producing energy which will further enhance the production of pyrolysis gases [14]. If this heat loop produces enough heat for the production of further volatiles and they end up in the flammability limit, then sustained burning is the result. If the oxidation takes places with the volatiles in a gaseous condition, the process is called *flame combustion*, and if it is for the solid-phase char then *smouldering combustion* [14]. The exact ignition criteria depends on many different factors, as for example "test setup, sample orientation, ambient temperature, heat transfer mode" [14, p. 6], as well as density, moisture content and the thickness of the timber sample. Several researchers, summarized in Bartlett and al. [14], mentioned as a key criteria for ignition the *gas phase temperature*.
The flammable mixture produced by the pyrolysis process needs to reach a temperature at which ignition is possible as it is explained in Bartlett et al. [14]. The time taken to reach that point is called *induction time*. Also, environmental conditions such as flow velocity influence the ignition. Higher flow leads to a shorter time to produce a flammable mixture of pyrolysis products but the induction time will be higher. The presence of moisture will delay the ignition point and requires also a higher heat flux intensity for ignition.

1.3 Pyrolysis models

As the overall process of pyrolysis is too complex to work with, a lot of models have been developed to describe the process in a simplified way adapted to the desired real life application situation. Moghtaderi [12] gives an overview of the different pyrolysis model. He classifies them on the basis of their decomposition reaction as how the conversion from virgin fuel into gaseous products and char residues is described. Distinctions are to be made between *simple thermal models* and *comprehensive models*. These two groups differ in the way they define the conversion of fuel into products, by the *pyrolysis rate*. The thermal models derive the rate only from the energy balance and the comprehensive models by a "combination of kinetic schemes, mass and energy balances" [12, p. 2].

The next two subsections explain the different types of models based on the review of Moghtaderi [12] and the last one discusses the input parameters for such models.

1.3.1 Simple thermal models [12]

To derive the pyrolysis rate (i.e., mass loss rate) from the energy balance, simple thermal models use the criteria of a critical pyrolysis temperature and simultaneously neglecting the physical and chemical processes. The solution method used to solve the equation in the model allows a further division (table 3).

Table 3: Classification of simple thermal models

Type of model	Classification
Simple thermal models	Algebraic models
	Analytical models
	Integral models

Sometimes the resulting equations are directly solvable by an exact analysis resulting in *analytical models*. If further simplifications are necessary to solve them, then they are called *algebraic models*. Equation 2 shows an example of an analytical equation where the mass loss rate is proportional to the net absorbed heat flux for a thermally thin slab exposed to a constant heat flux [12, p. 4].

$$\dot{m} = -\frac{\dot{q}_e'' A_s}{Q_p} \qquad (2)$$

Where:

- $\dot{m}$ Mass loss rate, [kg/s]
- $\dot{q}_e''$ External heat flux, [kW/m^2]
- A_s Surface area for solid material, [m^2]
- Q_p Heat of pyrolysis, [kJ/kg]

The equation can be used under the assumption that no shrinking or swelling happens and ignores the porosity of the material and thermophysical properties.

Equation 3 gives an example for an algebraic model for a thermally thick wood sample again exposed to a constant heat flux. It is based on the transient heat conduction derived for "the thermal location of the pyrolysis front (x_p at which $T = Tp$) and the thermal wave speed ($\mathrm{d}x_p/\mathrm{d}t$)" [12, p. 4].

$$\dot{m} = -A_s(\rho_0 - \rho_c)\left(\frac{\mathrm{d}x_p}{\mathrm{d}t}\right) \qquad (3)$$

Where:

- $\dot{m}$ Mass loss rate, [kg/s]
- A_s Surface area for solid material, [m^2]
- ρ_0 Initial density, [kg/m^3]
- ρ_c Density of char, [kg/m^3]
- x_p Location of the pyrolysis front, [m]
- $\mathrm{d}x_p/\mathrm{d}t$ Thermal wave speed, [m/s]

Both types show the disadvantage of a limited range of applications – but the advantage is that they are relatively simple to use.

The third classification, the *integral model* uses a set of ordinary differential equations of the heat conduction given by the energy conservation with time as an independent parameter. In using that set, temperature distribution and the mass loss rate can be calculated. The method to solve them is to reduce them to ordinary differential equations. This is done "by assuming that the temperature distribution within the solid depends on the space variable (x) in some particular fashion consistent with the boundary conditions" [12, p. 4]. Often a quadratic temperature profile is assumed, but also other polynomial and exponential distributions are published. With that assumption, the heat-balance integral can be obtained by substitution of this temperature distribution into the heat conduction equation followed by an integration with respect to the space variable over a chosen interval. An example of such a model given for a wood sample and exposed to an external heat flux, divides the heating in three stages, and then defines the temperature distribution for each phase. The first phase is before ignition, where conduction will heat up the material (*constant density heat-up phase*). The second phase starts after the pyrolysis temperature is reached and where the wood behaves in a semi-infinite manner (*infinite-body pyrolysis phase*). The last phase is the finite-body pyrolysis phase where the thermal wave reaches the back of the wood sample and the wood is totally converted into char. The derivation of the corresponding equations can be found in [12], [13] and leads finally to a set of 10 equations. Another application of an integral model is described in the article of Spearpoint and Quintere [17] where they develop an integral model for the horizontal burning of several wood species exposed to an incident heat flux between 25-75 [kW/m^2] and depending on the grain direction of the wood.

The advantage of such integral models is that they are relatively simple and easy to use compared to the comprehensive model, but less restrictive than the two other thermal models. However, they have the same disadvantage as the other thermal models in that they rely on a critical temperature for ignition and neglect to consider many chemical processes. The application of a critical temperature makes the simplification that chemical processes are taking place faster than diffusion processes. This is only true for high temperatures. At lower ones, chemical kinetics are the key players.

1.3.2 Comprehensive models [12]

The *comprehensive model* combines chemical and diffusion processes taking place during the pyrolysis. With that, they overcome the basic nature of a simple thermal model. As a consequence, these models are also able to include the thermal degradation processes. Other processes often included are "heat transfer, morphological changes, expansion, shrinkage, char formation, chemical reactions and in-depth radiation" [13, p. 385]. Examples of comprehensive models are Gypro, ThermaKin, Pyropolis and FiresCones [13]. The incorporation of a pyrolysis model in the FDS and FireFOAM – two computational fluid dynamic software – allows

classification as a comprehensive model. The complexity of these models needs almost exclusively numerical solution methods either by finite difference methods or finite volume. As a consequence, a classification of the models by the solution approach is not very useful and hence, they are classified by their reaction scheme (table 4).

Table 4: Classification of comprehensive models

Type of model	Subclassification
Comprehensive models	One-step global reaction scheme
	One-step multi-reaction
	Multi-step semi-global schemes

The simplest of them is the *one-step global reaction scheme*. This only considers primary reaction; the conversion of virgin fuel into products. The products of the thermal degradation are considered as lumped materials either volatiles and char or gases, tar and char (equations 4 & 5).

$$virgin\ fuel \rightarrow volatiles + char \quad (4)$$

$$virgin\ fuel \rightarrow gases + tar + char \quad (5)$$

The pyrolysis rate r is calculated by an Arrhenius expression "proportional either to the weight residue or the weight loss of the fuel", [12, p. 9], as shown for example in equation 6.

$$r = A \exp\left(-\frac{E}{RT}\right) \quad (6)$$

Where:

- r Rate of reaction, [kg/(m^{3}s)]
- E Activation energy, [kJ/(mol.K)]
- R Gas constant, 8,314 [J/mol]
- T Temperature, [K]

The input parameters needed for that equation have to be defined experimentally. The main limitation of these group is that wood is an inhomogeneous material made out of different components. Each component has different thermal properties and they react to a diversity of products, each of them with different properties. Lumping it together can lead to erroneous simulation outcomes.

A more detailed reaction scheme is considered with the *one-step multi-reaction schemes*. Still each component undergoes only one independent reaction but this time wood is not modelled as a lumped material but made out of several components. Each of these components undergoes a separate reaction which takes place in parallel. An example for such a reaction scheme is shown in Rinta-Paavola and Hostikka [18] where wood is made out of cellulose, hemicellulose, lignin and extractives (equation 7):

$$\begin{gathered} cellulose \rightarrow char_c + volatiles \\ hemicellulose \rightarrow char_{hc} + volatiles \\ lignin \rightarrow char_l + volatiles \\ extractives \rightarrow char_e + volatiles \end{gathered} \quad (7)$$

The pyrolysis rate there is the sum of each component's reaction rate weighted by the percentage of each component.

The next step of complexity would be to consider the subsequent reaction some of these products can undergo. These reactions are called secondary reactions [9, p. 6] and an example would be char oxidation. Models which consider such reactions are called *multi-step semi-global schemes*. An example of such a complex reaction scheme is shown in figure 4 [19, Fig. 2]. This reaction scheme includes char oxidation and cellulose is converted in a smaller molecule called *active cellulose* which undergoes further chemical reactions.

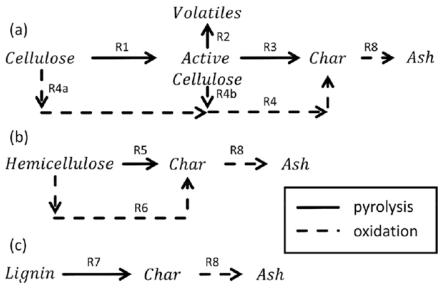

Figure 4: Example of a multi-step semi-global reaction scheme [19, Fig. 2]

Some models are also able to take into consideration the effect of moisture presence in the pyrolysis process. Moghtaderi [12] classifies these approaches in four classes:

1. "Simple energy balance on the drying front using an energy sink at 100°C to account for the heat vaporization
2. Additional chemical reaction
3. A boiling temperature criterion
4. Using local moisture-vapour equilibrium relations to track the movement of water vapour by a modified Darcy's law and liquid water by diffusion mass transfer expressions" [12, p. 14].

Classes 1-3 are only applicable to wood samples with moisture content below the FSP as they do not consider free water. However, *class 4* considers also free water.

A disadvantage of these comprehensive models is that even by using a model with a simple reaction scheme a lot of input parameters are needed. That number increases drastically if more detailed reaction schemes are used.

1.3.3 Input parameter for pyrolysis models

A challenge for the use of pyrolysis models is the required kinetic, thermal and material input parameters. The number of them increases drastically with the complexity of the model and depends to some extent on the type of wood and the model situation [5], [20]. Some of them are also temperature dependent leading to a further complication connecting material properties to environmental conditions [10].

Methods to define these input parameters are either on an experimental basis by direct measurements from thermal analysis or derived from analysis combined with optimization methods [13]. Examples for such experimental methods are thermo-gravimetric analysis (TGA), micro-combustion calorimetry (MCC) and fire propagation apparatus (FPA) or curve fitting for the analysis methods [13], [20]. As the experiments are small scale tests and many of their input data are also more experimental constants than physical properties and the optimization methods are often situation and optimization goal dependent [5], [20], the accuracy of such a pyrolysis model on a bigger scale and in other situations is not necessarily given. Therefore, tests should be run to study the appropriateness of the pyrolysis model [21].
A review of input parameters for the pyrolysis models can be found for example in Shi and Chew [10].

1.4 FDS – Fire Dynamic Simulator

FDS is a software which is mainly used for smoke handling systems, sprinkler/detector activation studies and residential and industrial fire reconstructions [21]. It is based on a computational fluid dynamic model and for situations which are fire-driven and with a focus on smoke and heat transfer. The software solves a set of Navier-Stoke equations and for that it assumes a flow with low Mach number ($Ma < 0.3$). The equations are solved on a rectilinear mesh and all objects have to align with this defined grid.

The main models in FDS are a hydrodynamic model, a combustion model and the radiation transport [21]. The core algorithm for the hydrodynamic model is an explicit predictor-corrector scheme with a second order accuracy in time and space. Depending on the grid resolution, turbulence is either treated by Large Eddy Simulations (LES) or by Direct Numerical Simulation (DNS). In most applications - and also in this work - the mesh is not fine enough to allow for a DNS simulation. The combustion model is mainly used as a single step, mixing-controlled chemical reaction. The combustion reaction includes air, fuel and products which are treated as lumped species. Furthermore, fuel and products are explicitly tracked in the simulations. In most of the cases, FDS approximates the radiative heat transfer by solving the radiation transport equation for a gray gas by a method called Finite Volume Method (FVM). By default, the resolution of the radiation transport is given by a number of 100 angles. The absorption coefficient for the radiative heat transfer is done by a narrow band model RADCAL which discretizes the spectral properties for a number of given species by wavelength and temperature [22]. For the interaction between fluid and solid surfaces, the software uses thermal boundary conditions. Additionally, the user can specify the burning behavior of materials. This work will focus on pyrolysis model in FDS which will be explained in detail under chapter 1.4.1 Pyrolysis model.

A material in FDS is defined by a geometrical obstruction to which material properties are attributed [21]. Each grid cell of that obstruction can consist of multiple layers and each layer can be made out of multiple material. Further, each of these materials can react in multiple thermal degradation reactions. Such reactions consist of reactants and multiple gaseous and solid products.

1.4.1 Pyrolysis model

FDS has the option to include different types of pyrolysis models, ranging from simple thermal ones to complex models based on kinetic modelisation [21], [22]. This study will use the *complex pyrolysis model* from FDS and therefore, the following description will focus on that type of model. As described for the comprehensive model, the pyrolysis model needs the definition of one or several chemical decomposition reactions and input data to calculate the reaction rate.
FDS's definition of the reaction rate $r_{\alpha\beta}$ is a combination of solid and gas phase conditions and defines the reaction rate depending on the temperature of the solid T_s. The definition in FDS contains the following sub-terms [22, p. 82]:

$$r_{\alpha\beta} = Reactant\ dependency * Arrhenius\ function * Oxidation\ function * Power\ function \quad (8)$$

The *reactant dependency* links the reaction rate with the amount of the reactant itself and is defined as [22, p. 82]:

$$Reaction\ dependency = \left(\frac{\rho_{s,\alpha}}{\rho_s(0)}\right)^{n_{s,\alpha\beta}} \quad (9)$$

Where:

α	Material component in material layer
β	Name of reaction
$\rho_{s,\alpha}$	Solid density of material component α in material layer, [kg/m³]
$\rho_s(0)$	Initial solid density of material layer, [kg/m³]
$n_{s,\alpha\beta}$	Partial reaction order for material component α in material layer and reaction β, [-]

The second term is the *Arrhenius function* which shows the dependency of the reaction rate on the temperature of the solid, therefore defining the reaction kinetics [22, p. 82]:

$$Arrhenius\ function = A_{\alpha\beta} exp\left(-\frac{E_{\alpha\beta}}{RT_s}\right) \quad (10)$$

Where:

α	Material component in material layer
β	Name of reaction
$A_{\alpha\beta}$	Pre-exponential factor, [1/s]
$E_{\alpha\beta}$	Activation energy, [J/mol]
R	Gas constant
T_s	Temperature of solid, [K]

The third term is the *oxidation function* and links the local oxygen concentration $X_{O_2}(x)$ and the heterogeneous reaction order $n_{O_2,\alpha\beta}$ to the reaction rate by [22, p. 82]:

$$Oxidation\ function = \left[X_{O_2}(x)\right]^{n_{O_2\alpha\beta}} \quad (11)$$

Where:

α	Material component in material layer
β	Name of reaction
$n_{O_2,\alpha\beta}$	Heterogeneous reaction order [-]
$X_{O_2}(x)$	Local oxygen concentration [-]

The last term is the *power function* which allows to turn on and off the reaction based on a threshold temperature, by [22, p. 82]:

$$Power\ function = max\left[0, S_{thr,\alpha,\beta}\left(T_s - T_{thr,\alpha\beta}\right)\right]^{n_{t,\alpha\beta}} \quad (12)$$

Where:

α	Material component in material layer
β	Name of reaction
$n_{t,\alpha\beta}$	Reaction order [-]
$T_{thr,\alpha\beta}$	Threshold temperature to dictate the occurrence or non-occurrence of reaction, [K]
$S_{thr,\alpha,\beta}$	Logical constant, either -1 or +1 depending on definition of threshold temperature

The described pyrolysis model in FDS is based on several assumptions [22, pp. 81–83]. One assumption is that the gaseous products from the thermal decomposition are instantaneously transported to the surface of the solid. Another assumption is that there is a local thermal equilibrium between the solid and gaseous component. With that, FDS ignores the convective heat transfer between the volatiles and the solid [12]. This is based on the argument that the time scale for the convective heat transfer is small and "the thermal capacity of the solid is much higher than the thermal capacity of the volatiles" [12, p. 13]. It is a reasonable assumption in cases where the convective effects are small compared to the ones for conduction [12]. In the inverse case, this simplification can lead to large errors in the final result. Other assumptions of FDS are that there is no condensation of gaseous products and that porosity is not included directly. As a consequence of the last assumption, there is no accumulation of gaseous products within the solid [12] and no pressure change. This is seen as a reasonable assumption except for cases where the longitudinal permeability of the wood sample varies [12].

1.4.2 Heat transfer to and into the solid

The transport of the heat into the solid is done by *conduction*. In this study, the heat conduction is only considered as one-dimensional, into the solid, defined as direction x [22, p. 75]. The solid phase temperature $T_s(x,t)$ can then be calculated by [22, p. 75]:

$$\rho_s c_s \frac{\partial T_s}{\partial t} = \frac{\partial}{\partial x}\left(k_s \frac{\partial T_s}{\partial x}\right) + \dot{q}_s''' \quad (13)$$

Where:

ρ_s	Solid density, [kg/m^3]
c_s	Specific heat capacity, [J/(kg.K)]
T_s	Solid phase temperature, [K]
x	Distance into the solid, [m], with surface at x=0 [m]
t	Time, [s]
k_s	Thermal conductivity of the solid, [W/(m.K)]
$\dot{q}_s'''$	Source term, net amount of energy released by the chemical reaction, [kW/m^3]

1.4.3 Gas combustion

The *combustion model* is a single-step, mixing controlled combustion based on Eddy Dissipation Concept where mixing is approximated as have being burnt [22] and where only one fuel can react [21]. The chemistry model relies on a reaction of the following form [21, p. 161]:

$$C_x H_y O_z N_v + v_{O_2} O_2 \rightarrow v_{CO_2} CO_2 + v_{H_2} H_2O + v_{CO} CO + v_s Soot + v_{N_2} N_2 \quad (14)$$

Therefore, the user needs to specify the chemical equation of the burning fuel along with the yield of CO, of soot and the volume fraction of hydrogen in the soot, X_H.

The model calculates the mean chemical mass production rate of species α per unit volume $\dot{m}_\alpha'''$ [22]. By summing up the chemical mass production rates multiplied by the corresponding enthalpy of formation, the heat release rate $\dot{q}'''$ can be calculated [22, p. 10]:

$$\dot{q}''' = -\sum_\alpha \dot{m}_\alpha''' \Delta h_{f,\alpha} \quad (15)$$

Where:

$\dot{m}_\alpha'''$	chemical mass production rate of species α per unit volume, [kg/s.m^3]
$\Delta h_{f,\alpha}$	Enthalpy of formation of species α, [kJ/mol]

The enthalpy of formation of the gaseous fuel can either be specified directly for each gas or can be calculated from the (specific) heat of combustion of the reaction if the enthalpy of formations of all the other molecules in the reactions are known [21]. This second approach will be chosen in this study for the definition of the enthalpy of formation.

2 Objectives

The goal of this study is to simulate the burning of timber with FDS including a complex pyrolysis model and analyse the results of the simulation in view of the charring properties. The burning includes the pyrolysis and gas combustion process and the heat transfer is limited to one dimension.

The evaluation of the results will be done by a comparison with experimental data from a non-standard burning situation with a high heat flux for ignition and with an air flow. The definition of the simulation environment will be as similar as possible to the experimental design and material used. The focus of the analysis will be on the charring rate and charring depth. As the pyrolysis model in FDS is only a framework and the exact pyrolysis model will depend on the input data of the user, some changes in the input parameters will be made and their influence on the charring properties assessed. Finally, possibilities and some limitations to study charring properties with FDS are also highlighted.

3 Methodology

This chapter defines the FDS simulation and describes how the charring properties will be analysed. It starts with the input parameters for the pyrolysis model, followed by the ones for the gas combustion model and then outlines the analysis method. Further, it defines the simulation environment where the burning happens, and how it is implemented in FDS. The last section is the assessment of the implementation of the simulation environment, the resulting modification in the FDS code and a description of the different test simulations.

3.1 Input parameters for the pyrolysis model

The pyrolysis model used in this study is limited to a one-dimensional heat transfer and uses a simple, *one-step global reaction scheme*. The type of wood is spruce in agreement with the experimental data described under section 3.4 “FDS simulation environment”. The chemical reaction is defined as the conversion of spruce into char and pyrolyzate (equation 16).

$$spruce \rightarrow char + pyrolyzate \qquad (16)$$

In the experimental setup, the spruce sample had a moisture content of 12 %. However, the simulation will start with dry spruce to keep the reaction scheme simple.

The reaction rate is only based on the reactant dependency and the Arrhenius function (equations 8 – 10). The two other terms of the reaction rate, the oxidation function and power function, will not be used in this study (equations 11 & 12).

The following table summarizes the input data for the decomposition process.

Table 5: Input parameter for decomposition process

Parameter	Code in FDS	Value	Source
Number of reactions	N_REACTIONS	1	Defined by reaction scheme
Yield of char	NU_MATL	0.16	[23]
Yield of pyrolyzate	NU_SPEC	0.84	[23]
Activation energy	E	190’500 [J/mol]	[23]
Pre-exponential factor	A	$4.691*10^{13}$ [1/s]	[23]
Absorptivity	ABSORPTION_COEFFICIENT	50’000 [1/m]	Default value FDS [21]
Reaction order	N_S	1	Default value FDS [21]
Heat of combustion	HEAT_OF_COMBUSTION	14’000 [kJ/kg]	[23]
Heat of reaction	HEAT_OF_REACTION	19 [kJ/kg]	[23]

For the estimation of the material and kinetic properties for spruce and char, the values are taken from an article by Rinta-Paavola and Hostikka [23]. This article defines input parameter for the pyrolysis of spruce for a simple and a parallel reaction scheme in FDS. The input parameters were validated and optimized against cone calorimeter experiments at different heat fluxes. The yield of char, and of pyrolyzate, the activation energy and the pre-exponential factor are estimated with the SCE algorithm from thermogravimetric analysis [23]. The value for the heat of combustion is per produced mass of gas and is coming from MCC experiments where the results are simulated by FDS [23]. The heat of combustion is the effective heat of combustion, which is also the default definition in FDS [21]. The heat of reaction for this simple reaction is defined as endothermic and is the optimized value by model fitting for a heat flux of 35 [kW/m2] in a cone calorimeter test from the publication of Rinta-Paavola and Hostikka [23].

Besides the pyrolysis parameters, other material properties for *spruce*, *char* and *pyrolyzate* need to be defined. These parameters for the for two materials are shown in the next table and in the following text. Information about the gaseous product "pyrolyzate" will be described in the next section (3.2 "Input parameters for the gas combustion model").

Table 6: Material properties for spruce and char

Parameter	**Code in FDS**	**Spruce**		**Char**	
		Value	**Source**	**Value**	**Source**
Density	DENSITY	408 [kg/m^3]	[23]	59 [kg/m^3]	[23]
Emissivity	EMISSIVITY	0.9	[23]	0.85	[24]
Conductivity	CONDUCTIVITY	0.09 [W/(m.K)]	[23]	0.22 [W/(m.K)]	[23]

The density for spruce is for dry spruce as defined above and measured in Rinta-Paavola and Hostikka [23]. The other two parameters for spruce are also from the same publication as well as the char density and the char conductivity. The conductivity for spruce is the optimized value by model fitting for a heat flux of 35 [kW/m^2] in a cone calorimeter test. The char density of 59 [kg/m^3] is in the same range as reported in the literature where the "initial char density is 10 – 20 % that of the dry wood [25]. The value for the emissivity of char is from Chaos [24].
The last input parameter needed is the specific heat for spruce and char. They are defined as temperature-dependent in the publication of Rinta-Paavola and Hostikka [23]. The specific heat capacity of spruce is defined with a linear growth starting at 30 [°C] with 920 [J/(kg.K)] until 230 [°C] with 1800 [J/(kg.K)]. Below and above that temperature, the specific heat capacity is assumed to be constant.

The specific heat of char is defined by the following equation [26] and shown in graph 1:

$$c_{p,char} = 1430 + 0.355 \cdot T - \frac{7.32 \cdot 10^7}{T^2} \quad (17)$$

Where:

T Temperature, [K]

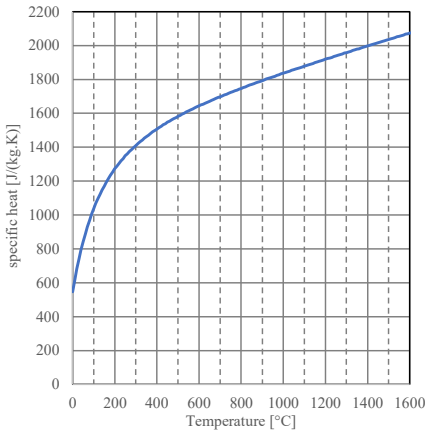

Graph 1: Values for specific heat of char from equation 17

3.2 Input parameters for the gas combustion model

The gaseous product *pyrolyzate* produced by the decomposition reaction (equation 16) is the main fuel for the gas combustion. The input values for the gas combustion in FDS can be seen in table 7.

Table 7: Input values for the gas combustion model

Parameter	Code in FDS	Value	Source
Number of carbons	C	1	[27]
Number of hydrogens	H	3.584	
Number of oxygens	O	1.55	
Number of nitrogens	N	0	
Soot yield for reaction	SOOT_YIELD	0.015	[27]
CO yield for reaction	CO_YIELD	0.0	Default value FDS [21]
Heat of combustion	HEAT_OF_COMBUSTION	14000[kJ/kg]	[23]
Fraction of atoms in the soot that are hydrogen	SOOT_H_FRACTION	0.1	Default value FDS [21]
Ambient mass fraction of oxygen	Y_O2_INFTY	0.232378	Default value FDS [21]
Ambient mass fraction of carbon dioxide	Y_CO2_INFTY	0.000595	Default value FDS [21]
Relative humidity of the air species	HUMIDITY	40 %	Default value FDS [21]
Surrogate molecule for thermal radiation	FUEL_RADCAL_ID*	'METHANE'	Default value FDS [21]

Most of the input parameters are default values from FDS [21], except for the chemical composition of the burning gas, the soot yield and the heat of combustion. The composition of the gas is for spruce [27, p. 494] and the soot yield for red oak [27, p. 3467]. Finally, the heat of combustion is again from the work of Rinta-Paavola and Hostikka [23].

Moreover, as the gaseous product is not a default molecule in FDS, table 8 defines that molecule for the simulations [21, pp. 154–157].

Table 8: Input parameters for the definition of a fuel in FDS

Parameter	Code in FDS	Value	Source
Chemical formula	FORMULA	'C1H3.584O1.55	[28]
Conductivity	CONDUCTIVITY	0.09	[23]
Diffusivity	DIFFUSIVITY	$4.3*10^{-7}$ [m^2/s]	[29]
Viscosity	VISCOSITY	0.00059 [kg/m.s]	[30]
Surrogate molecule for thermal radiation	RADCAL_ID*	'METHANOL'	[21]
Prandtl number	PR	0.5	Default value FDS [21]

*The defined "FUEL_RADCAL_ID" will be overridden by the one defined for the gaseous product "RADCAL_ID" if that one reacts as fuel [21, p. 163].

For the conductivity, the value for spruce is used [23], the diffusivity is the axial diffusivity for dry ash [28] and the viscosity is for wood [29]. For the surrogate molecule of the thermal radiation, FDS has a predefined list to chose from [21, p. 189]. From there, a chemical similar molecule to the gaseous product was chosen, which was 'METHANOL'.

3.3 Analysis method

As already explained, the analysis is focusing on the charring depth and rate. The position of the charring front in the simulations is derived from the temperature profile inside the wood sample. Its position is defined as being at 300 [°C] [7], [14]. The charring depth is then defined as the distance from the surface of the wood sample to the position of the charring front at the end of the simulation. The charring rate is calculated as the ratio of these charring depth divided by the simulation time at which the charring front reached that depth.

To study properties inside a solid, FDS has a special output recording option, called *&PROF* [21, pp. 283–284]. This provides in-depth profiles of physical properties like temperature, overall density or density of a type of solid material. The recording positions of these properties are defined by the spacing of the solid grid which is done automatically by FDS, unless changed manually [21, p. 93]. By default, the layers are smaller at the border and getting thicker towards the middle by doubling their size. At mid-depth, they start do shrink again. The user can change this solid grid to some extent, as making the node spacing more uniform or making the mesh cells smaller [21, pp. 93–94].

Adaption of the mesh size inside the wood sample is further explained under chapter 3.5.7 "Implementation of simulation with finer mesh in the wood sample".

3.4 FDS Simulation environment

The results of the simulations will be compared to experimental data from spruce burning tests to get an idea about the performance of the simulations. To be able to do that, the simulation environment will be defined as similar as possible to that experimental setup.

3.4.1 FANCI experiment description

The chosen experimental setup is called Fire Apparatus for Non-standard heating and Charring Investigation (FANCI) [3]. It allows to study amongst other the charring behavior, the char layer surface regression and the temperature distribution in a timber sample. The experimental environment is called non-standard as the application of an air flow from 1 to 6 [m/s] can be applied and a variable external heat flux up to 120 [kW/m^2] from a quick response heat panel can be used to ignite the sample (figure 5) [3].

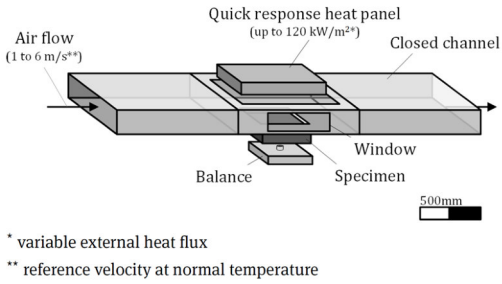

Figure 5: Schematic view of the FANCI test setup [3, Fig. 6]

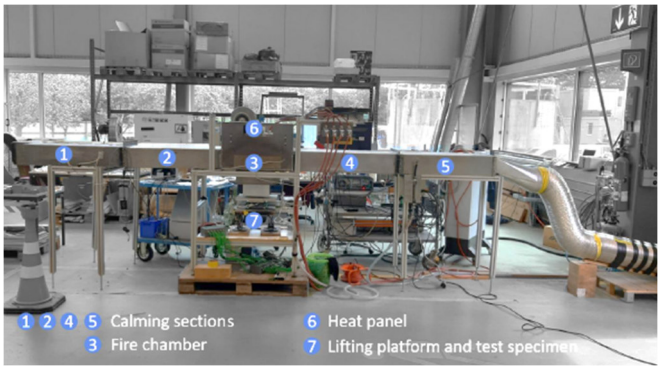

Figure 6: Photo of the FANCI-setup with the different components

The apparatus consists of a long tunnel made out of five sections, each section with a length of approximately 0.9 [m], a width of 0.5 [m] and a height of 0.15 [m] (figure 6) [31]. The total length is approximately 4.5 [m]. The sections are made out of steel plates of 1.5 or 3.0 [mm] thickness. The air flow is from left to the right in the figure 6. The wood sample is placed in section 3, called *fire chamber*, positioned on the floor, opposite to a heat panel on the ceiling. The samples have a length of 26 [cm], a width of 22.5 [cm] and a thickness of 12 [cm]. The wood type is spruce with a humidity of around 12 %.

3.4.2 Test JF00 with FANCI

For comparison with the simulation results, the test JF00 from the FANCI test series was chosen [31]. In this experiment, a timber sample was placed in the apparatus, where a velocity of around 2.5 [m/s] was prevailing and where the heat flux panel was calibrated to produce an incident

heat flux of 96.4 [kW/m^2] on the surface of the timber sample. The sample was heated by the heat panel for 20.1 [min]. Ignition occurred after ca. 0.42 [min]. The reported charring depth was 18 [mm], reached after 15.3 [min]. The plotted charring rate for this test was 1.28 [mm/min] and the surface recession 0.22 [min/mm] (graph 2).

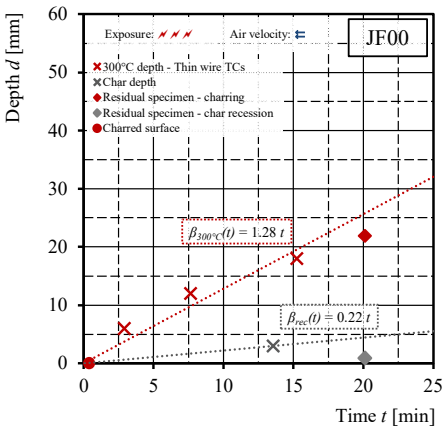

Graph 2: Charring rate for experiment JF00 [31, Fig. 5.2(b)]

The experimental environment of the air velocity of 2.5 [m/s] inside the tunnel was calculated from the negative pressure difference, recorded by the static pressure difference installed at the center of the timber sample and ca. 1.55 [m] from its sample center, as shown in figure 7 [31]. The air flow was produced by an induced draft fan at the exit of the tunnel.
The incident heat flux was measured during a heat flux test where no burning took place [31]. The heat flux was measured on the surface of a mock sample positioned at the position where the timber sample would be.
During the experiment, temperature measurements of the air, on the timber surface and inside the wood sample were performed (figure 7) [31]. The gas temperature measurements were installed at mid-height and in the center of the cross section of the tunnel, at both ends of the section with the timber sample (start and end of *fire chamber*) as well as another directly behind that section (figure 7). Two other thermocouples are positioned at the position where the inlet air velocity was measured (figure 7). The surface temperature was measured at two positions on the surface of the sample. The temperature measurements inside the wood sample were positioned at six different depths from the surface, starting at a depth of 6 [mm] until 36 [mm], with a spacing of 6 [mm]. For each depth, three measurements were placed and recorded.

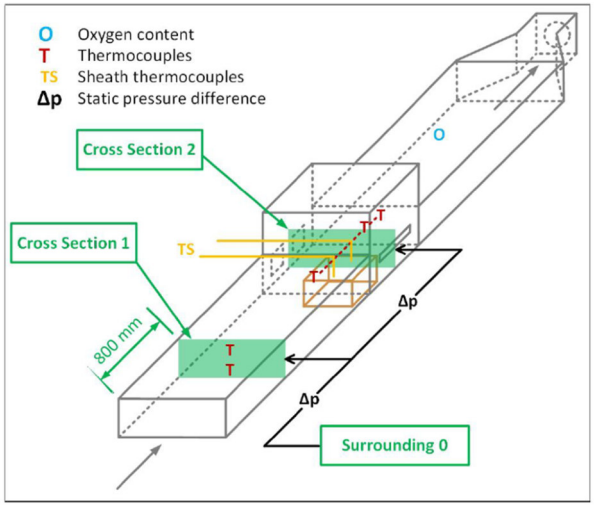

Figure 7: Schematic view of the different measurement points in the FANCI test JF00 [31, Fig. 4.3]

3.5 Implementation and assessment of the simulation environment in FDS

This section starts by explaining how the FANCI experiment was implemented in FDS and describing the different output recordings during the simulation. The following four subsections assess the simulation environment by comparing the simulation outputs with the experimental data. The findings are summarized in the subsequent subsection and the resulting changes in the FDS code are explained in the last subsection.

3.5.1 Implementation

This subsection presents the mesh size, the geometry, the implementation of the air velocity, the way of ignition, the output parameters and the simulation time.

Mesh size

The mesh size for the simulations is set to 1 [cm]. This is the result from a test series where the influence of mesh sizes 1.25 [cm], 1.0 [cm] and 0.625 [m] on the air flow are assessed together with the influence of a shortened tunnel. The shortened tunnel had a length of 1.8 [m] instead of 4.5 [m] by shortening each end of the tunnel by 1.5 sections. The simulation only considered the flow field without any burning. Recorded were air velocities at the surface of the timber sample, above it and at the outflow.
The detailed setup, FDS codes, presentation of the results and analysis are shown in Appendix B.

The qualitative analysis of the results of this test series showed similar flow fields for all simulations. As an example of that, figure 8 shows a still at 4.6 [min] of the simulation time for the situation with a mesh size of 1 [cm] and the whole length of the FANCI tunnel. The long tube shown is the tunnel with a vertical cut through. This cut recorded the air velocity during the

simulation. The two grey rectangles are enlarged in the two images below showing the flow field more in detail. The scale of the air velocity is from 0.0 – 3.83 [m/s].

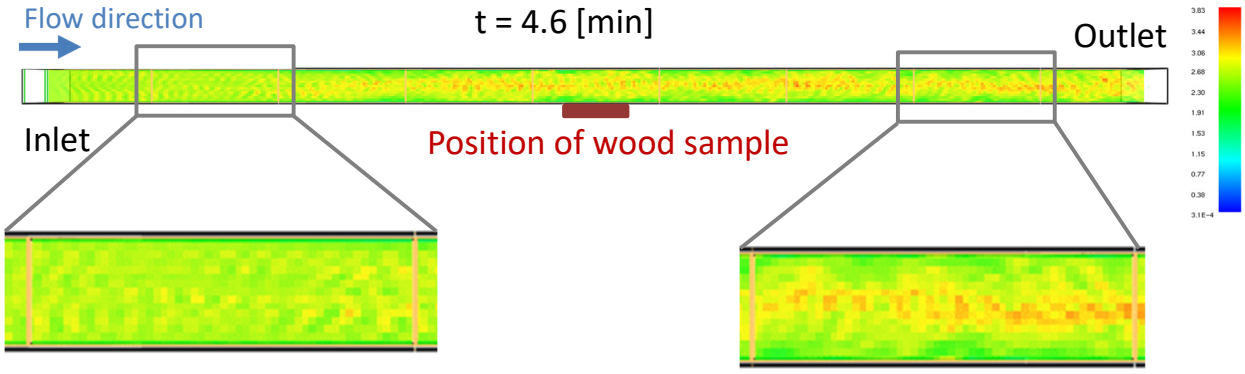

Figure 8: Result of the animated velocity output for the simulation with the whole FANCI geometry and a mesh size of 1.0 [cm]; with a velocity scale of 0.0 - 3.83 [m/s] and a simulation time of the still of 4.6 [min]

Figure 9 shows the same situation for the simulation with a shortened tunnel. The air velocity scale is from 0.0 – 3.63 [m/s].

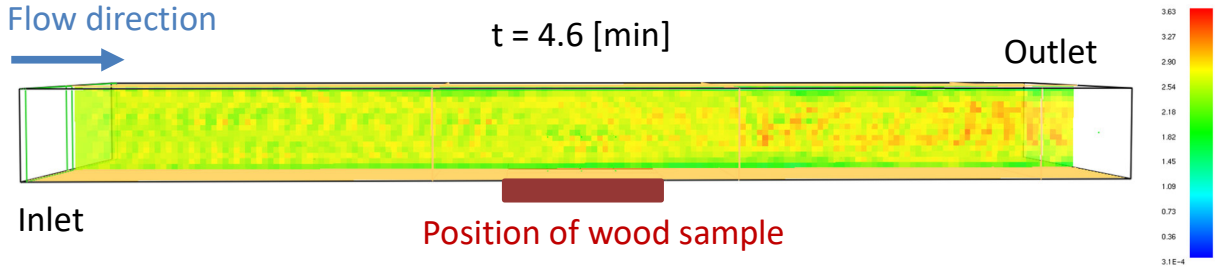

Figure 9: Result of the animated velocity output for simulation with the short FANCI geometry and a mesh size of 1.0 [cm]; with a velocity scale of 0.0 - 3.63 [m/s] and a simulation time of the still of 4.6 [min]

As there were no huge variations in the flow fields between the two geometries for all the simulations, a shortened geometry of the FANCI tunnel seems reasonable.

Quantitatively, the results are analysed by the comparison of the mean velocity at different locations. Graph 3 shows the comparison of the different mean velocities from the simulations with mesh sizes 1.25 [cm] (“T4-short-1.25”), 1.0 [cm] (“T5-short-1.0”) and 0.625 [cm] (“T6-short-0.625”) recorded in the shortened FANCI geometry (cf. Appendix B for the other results). The recordings were at the surface of the wood sample (“Surface”), above it (“Above”) and at the outflow (“Outflow”).

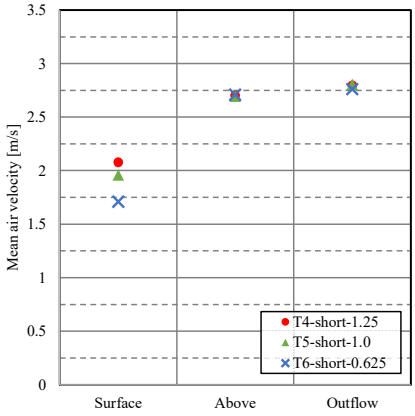

Graph 3: Comparison of the different mean air velocities recorded at the surface of the wood sample ("Surface"), above it ("Above") and at the outlet ("Outlet") for a shortened FANCI-tunnel geometry and for mesh sizes of 1.25 [cm] ("T4-short-1.25"), 1.0 [cm] ("T5-short-1.0") and 0.625 [cm] ("T6-short-0.625") (cf. Appendix B)

The graph 3 shows very similar results, except for the measurements at the border of the tunnel, measured at the surface of the wood sample ("Surface"). Given that, choosing the mesh size of 1.0 [cm] seems a reasonable compromise between simulation time and accuracy. However, it has the disadvantage of only giving 15 cells along the height of the tunnel, which may not be enough for the flaming combustion (cf. 5.6.2 "Simulation parameters").

Geometry

For the final simulation geometry, the tunnel length of 1.8 [m] from the previous paragraph was extended to a length of ca. 2.2 [m], to be able to incorporate all the measurements that were present in the experimental setup of the FANCI-test (figure 7). Therefore, the simulated tunnel ranges from the first air velocity measurement point until a little bit further than the fire chamber, with a total length of ca. 2.2 [m] (figure 8).

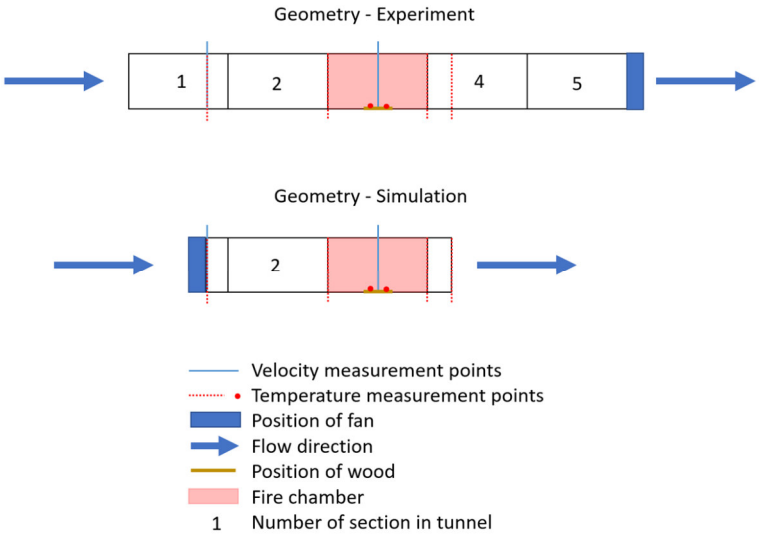

Figure 10: Comparison of the geometry of the experiment and the simulation

Air flow

The air flow in the simulation is done by an inlet air flow positioned at the beginning of the shortened tunnel; the air is therefore pushed through the tunnel instead of pulled as in the experiment. The estimation of the air velocity in the experiment showed a drop from 2.5 [m/s] to around 2.0 [m/s] after the start of the experiment [31, modified Fig. E.1] (graph 4).

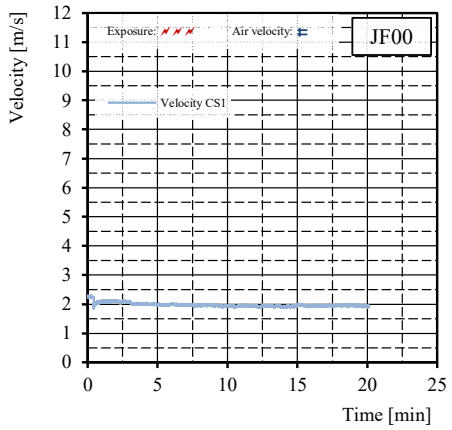

Graph 4: Experimental air velocity measurements in section 1 in experiment JF00 [31, modified Fig. E.1]

Because of this, the inlet velocity in the simulation was set to 2.0 [m/s]. The reason for this drop in the experiment is not known, but could be due to the flow resistance produced by the fire.
The given geometry and air velocity in the tunnel lead to a Reynolds number of higher than 5000 and therefore, to a turbulent flow pattern (cf. Appendix C).

Way of ignition

For the heating of the wood sample, the available information from the experiment is an estimation of the incident heat flux on the surface of the wood sample. For the FDS simulations, two ways to heat the wood sample are tested. **S**imulation option **1** is by an **ex**ternal **H**eat **F**lux applied over the wood sample with the same intensity as the incident heat flux. This simulation is named “S1-exHF”. This heat flux acts like a “perfect radiant panel or a conical heating unit” [21, p. 114]. **S**imulation option **2** is by defining a **H**eat **P**anel on the ceiling of the tunnel, above the wood sample, and calibrate in a way, that the amount of incident heat flux measured on the wood sample surface has the same intensity as the one estimated in the experiment. This simulation is named “S2-HP”. Details on this calibration can be found in Appendix D.

Output recordings

To check the air velocity in the simulation, different recording points are positioned at mid-height of the tunnel along the whole tunnel (table 9, figure 10). More precisely, one above the center of the timber sample, seven between inlet and timber sample and three between timber sample and outlet.

Table 9: Position of the air velocity measurement points in the tunnel

Area	Distance between center of the timber sample and measurement point [m]						
Inlet – timber sample (I)	1.45	1.25	1.05	0.85	0.65	0.45	0.25
Timber sample (W)	0.0*						
Timber sample – outlet (O)	0.25	0.45	0.65				

* indicates that at this position also a velocity recording in the experiment was placed

As in the experimental setup, gas temperature measurements are done on the center line in the tunnel. In the simulation, they are distributed between the start of the fire chamber and the outlet. Two were between the start of the fire chamber and the timber sample, one above the timber sample, and four between timber sample and outlet (table 10, figure 10).

Table 10: Position of temperature measurement points in the tunnel

Area	Distance between center of the timber sample and measurement point [m]			
Inlet – timber sample (I)	0.45* (=start fire chamber)	0.25		
Timber sample (W)	0.0			
Timber sample – outlet (O)	0.25	0.45* (=end fire chamber)	0.55 (=right behind fire chamber)	0.65* (=after fire chamber)

* indicates that at this position also a temperature recording in the experiment was placed

Additional temperature measurements are done on the surface of the timber sample and inside the solid, similar to the experimental setup.
For future analysis, additional outputs have been incorporated: another way of measuring the surface temperature, measurements of the thickness of the wood sample, the density of the sample and its components recorded with different modes.

Simulation time
The simulation time is the same as the duration of the experiment, 20.1 [min].

All the simulations were run on Ghent's HPC and all on the same cluster ("doduo") with FDS version 6.7.7. Visualisations are done with Smokeview version 6.7.14.
The two FDS codes, one for each mode of ignition ("S1-exHF" & "S2-HP"), are displayed in Appendix E. They were run and their results compared with the experimental data from JF00 (cf. following subsections). This allows to assess the similarity between the two environments and if needed to modify the FDS codes.

3.5.2 Gas temperatures measurements in the tunnel
The following images (figures 11-14) show the simulation results for the temperature recordings at t = 0 [min], at t = 6.0 [min] and at t = 10.0 [min]. The figures show the section 3 (*fire chamber*) and 4 of the tunnel (black lines) with the air flow from the left to the right side. The timber sample is outlined on the floor by a brown rectangular. The green dots indicate positions of temperature measurements, the dark green ones are the positions at the start and at the end of the fire chamber, as well as after the fire chamber (from left to right).

In figure 12 and 14, temperatures above 150 [°C] are colored in orange which is around the mean value of the experimental measurements at the position “end of the fire chamber” and “behind the fire chamber”. Figure 13 shows the temperature distribution as a vertical cut through the length of the tunnel. The temperature scale is from 0 – 1500 [°C] and colored in black are temperatures at around 150 [°C]

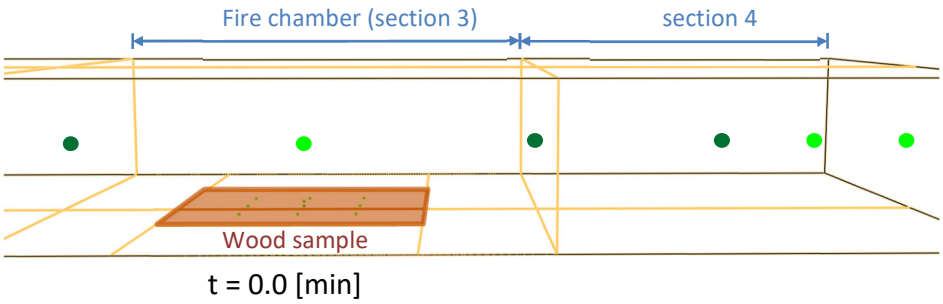

Figure 11: Simulation result at t = 0 [min] for simulation "S1-exHF"

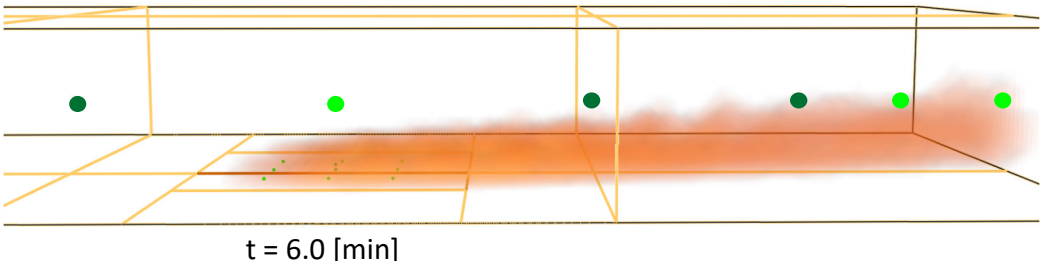

Figure 12: Simulation result at t = 6.0 [min] for simulation "S1-exHF"

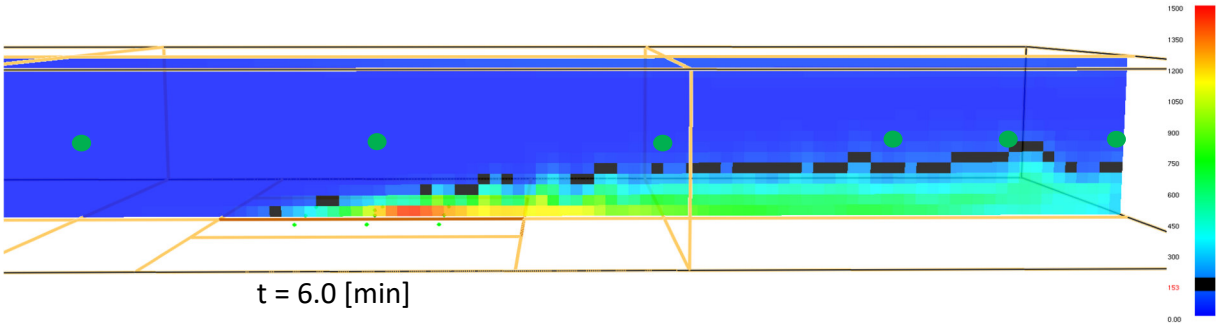

Figure 13: Simulation result at t = 6.0 [min] for simulation "S1-exHF"

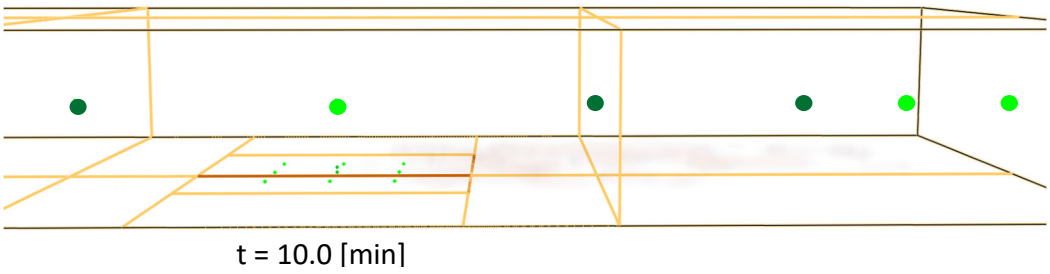

Figure 14: Simulation result at t = 10.0 [min] for simulation "S1-exHF"

The images show that the heat is rarely reaching the three dark green measuring points. The heat is not reaching the measuring point at the start of the fire chamber, as the heat is pushed away towards the exit, and therefore, the temperature stays low. For the other two positions, the simulation also showed that the bulk of heat does not reach these two measuring points, resulting in relatively low temperature measurements. But figure 13 however shows that below the measuring points, the heat production is not low.

From the FANCI-experiment JF00, no information about the presence and behaviour of the flames was available. However, for another FANCI-experiment, called FH03, there was a movie showing the burning. This experiment also used the same air velocity as JF00, and had the same incident heat flux of 96.4 [kw/m^2] in the first 5 [min] of the experiment before it was lowered down to 8.4 [kW/m^2]. In this movie (figure 15), it can be seen that the flames are pushed into the direction of the air flow. This is in agreement with what was seen in the simulation. But it also seems that the flames are less pushed than in the simulation and that the flames are higher than in the simulation.

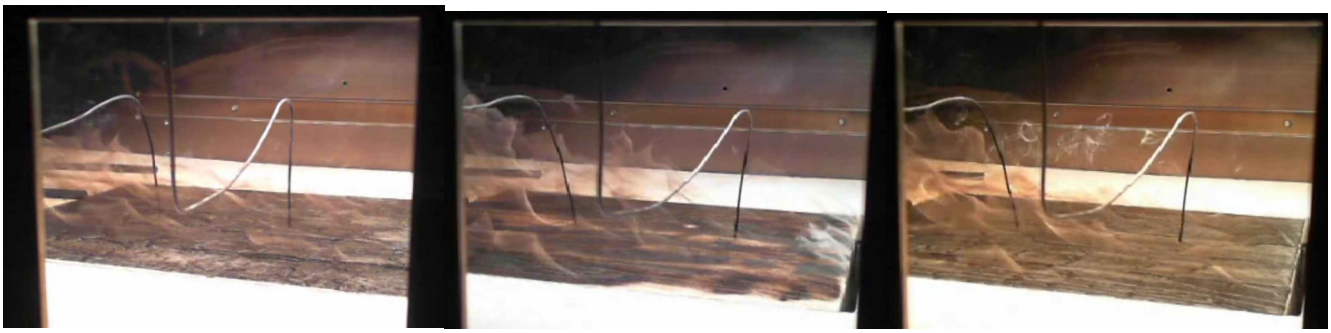

Figure 15: Stills from the movie from experiment FH06; air flow is from right to left; time increases from image at the left to the right

Moreover, the burning was not constant in the simulation but showed a “flickering”. This can also be seen in the heat release graph over the whole simulation time (graph 5).

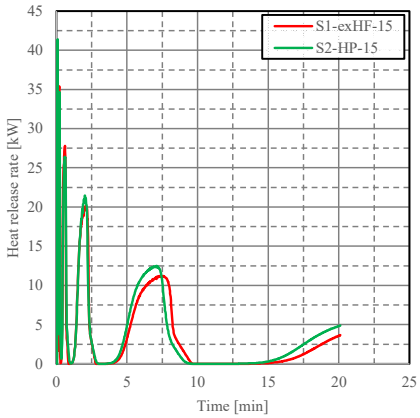

Graph 5: HRR over the whole simulation time for "S1-exHF" & "S2-HP"

This flickering was not seen in the above-mentioned movie.

The following three graphs show the gas temperature in the tunnel, once at the start of the fire chamber, once at the end of the fire chamber and once behind the fire chamber ("exhaust").

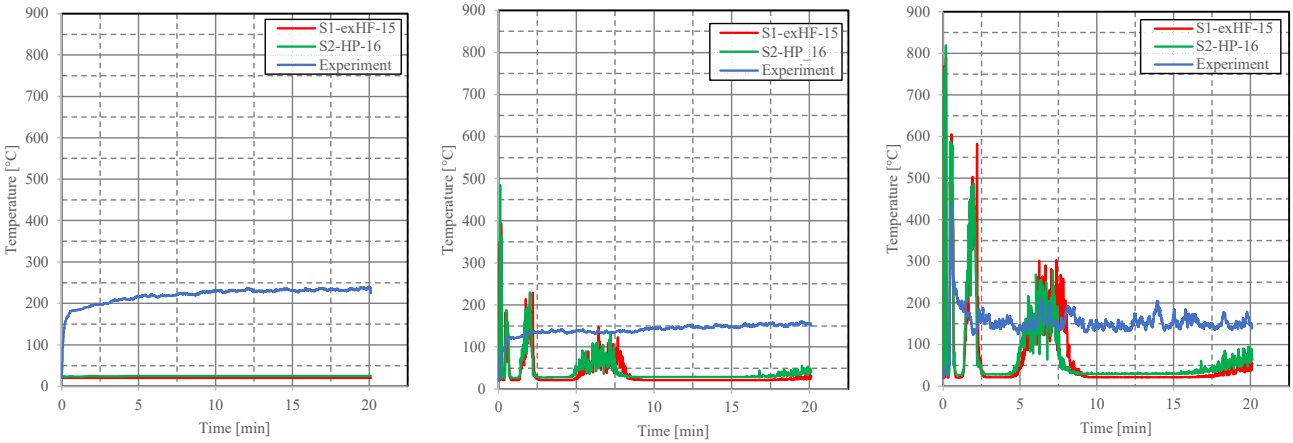

Graph 6: Gas temperatures at the start of the fire chamber (left), at the end of the fire chamber (middle) and behind the fire chamber (right) for the two simulations and the experiment

First of all, the simulation temperatures are much lower than the experimental ones, as can also be seen in the mean gas temperatures in table 11. The reason for that was shown in figure 11 – 14. Additionally, the "flickering" in the HRR from graph 5 is also reflected in these temperature measurements from the simulation. However, the experimental data show a steady temperature recording. This seems to support the fact, that the burning in the experiment was constant and not flickering, and would correspond to what was seen in the movie from experiment FH06.

Table 11: Mean gas temperatures for the simulations and the experiment

Mean gas temperature [°C]	***Start of fire chamber***	***End of fire chamber***	***Behind fire chamber***
S1-exHF	20.0	35.8	68.1
S2-HP	20.4	42.2	72.4
Experiment	219.8	141.1	180.4

3.5.3 Surface temperature measurements on the timber sample

The following graph shows the temperature measurements on the timber sample surfaces for the two simulations and the experiment. The experiment recorded at two positions surface temperature as described under chapter 3.4.2 “Test JF00 with FANCI”. As there was a problem with the temperature recordings of one of them (cf. Appendix F), the comparison is only done with the other temperature recording.

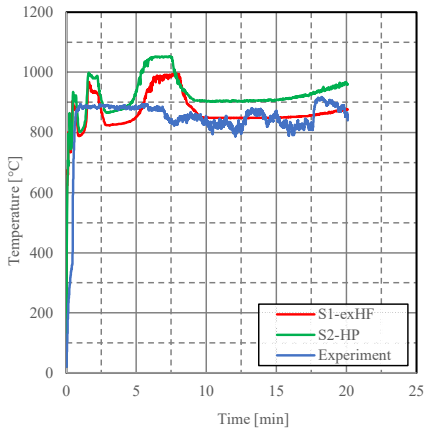

Graph 7: Surface temperature measurements on the timber sample for the two simulations and the experiment

Table 12: Mean surface temperatures on the timber sample for the simulations and experiment

	Mean surface temperature on timber sample [°C]
S1-exHF	868.6
S2-HP	924.6
Experiment	843.7

The qualitative behaviour of the temperature recordings for the simulation reflects again the inconsistence seen in the HRR and the gas temperature measurements.

The comparison of the mean surface temperatures shows temperature measurement very close to the experimental measurements. Taking into account that the measurements in the simulation were done by direct temperature measurements where higher measurements are expected than for the ones in the experiment where thermocouples have been used, the temperature measurements in the simulation are in a good range.

3.5.4 Air velocity measurements over the timber sample

A qualitative analysis of the air velocity during the simulation showed that the velocity for both simulations was relatively homogenous during the simulation and stayed in the range between 2.0 and 2.5 [m/s] (green colors, figures 16 & 17). Figures 16 and 17 show stills from the air velocity results at 6.0 and 10.0 [min], again by a vertical cut through the tunnel in section 3 and 4. The scale is from 0.0 – 4.5 [m/s] and the black color would correspond to the mean velocity in the experiment which was around 3.7 [m/s] (table 13).

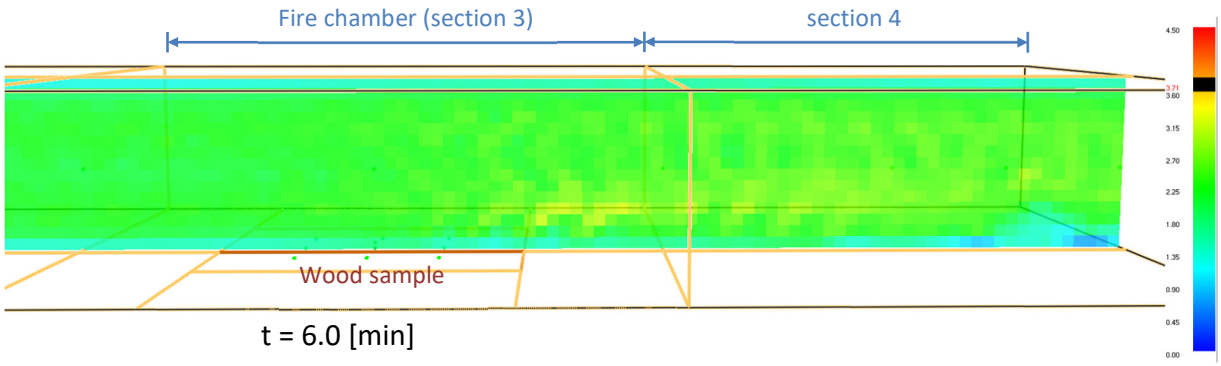

Figure 16: Simulation result of air velocity at t = 6.0 [min] for simulation "S1-exHF"

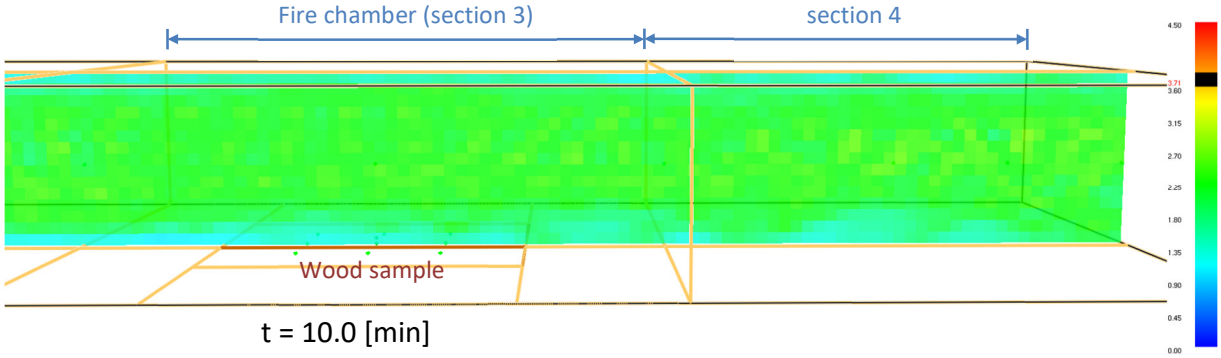

Figure 17: Simulation result at t = 10.0 [min] for simulation "S1-exHF"

The experimental value above the wood sample had a mean velocity of 3.7 [m/s]. Both types of simulations very rarely reached values of 3.7 [m/s] and above during the simulation.

There are two measurements of the air velocity in the tunnel during the experiment, one 1.55 [m] upstream from the timber sample center and one above the center of it. In the simulations, the first measurement point was used to define the air velocity in the tunnel. Therefore, only the last measuring point can be use for comparison between experimental and simulation result (graph 8 and table 13).

The following graph shows the measured air velocity over the timber sample for the simulation where the ignition is done with an external heat flux (“S1-exHF-15”) and the one with the heat panel (“S2-HP-16”) together with the air velocity measured during the experiment (“Experiment”). The mean values of the air velocities are shown in table 13.

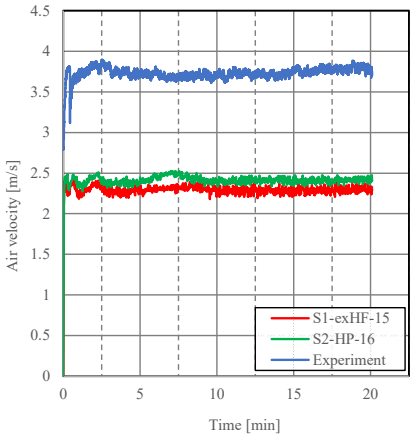

Graph 8: Air velocity measurements over the timber sample for the two simulations and the experiment

Table 13: Mean air velocities over the timber sample for the simulations and experiment

	Mean air velocity [m/s]
S1-exHF	2.3
S2-HP	2.4
Experiment	3.7

Both simulations show lower air velocity measurements than in the experiment.

3.5.5 Temperature recordings inside the timber sample

The following graph shows the temperature recordings inside the timber sample during the whole simulation for the simulation with ignition by the external heat flux ("S1-exHF"). Every line stands for a temperature distribution in time for a given depth from the surface. The higher the value the deeper inside the solid the recording is. The blue line named "0 mm" is on the surface of the timber sample. The positions and spacing of the recordings are the default ones from FDS. In total, FDS positioned 15 layers in the timber sample with a starting spacing of 0.48 [mm], which is increased until the middle of the sample until a maximum spacing of 30.6 [mm] is reached, before the spacing is halved again. This is visible in the legend of graph 9.
By setting the decomposition of wood into char at 300 [°C], the final position of the charring front for that simulation is at a depth of 14.8 [mm] from the timber sample surface (green line).

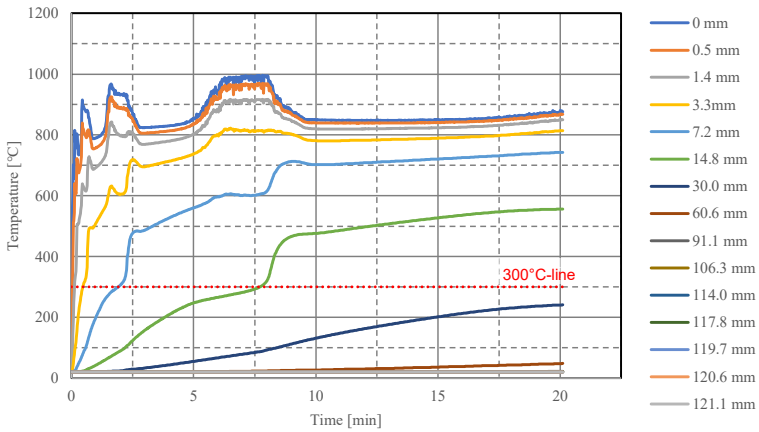

Graph 9: Temperature measurements inside the timber sample for "S1-exHF"

For the layers closer to the surface, the temperature recordings reflect again the inconsistency of the HRR and of the gas temperature measurements.
From the previous presented results, a graph showing the progression of the charring front can be established by using the criteria of 300 [°C] (300°C-ISO profile, graph 10).

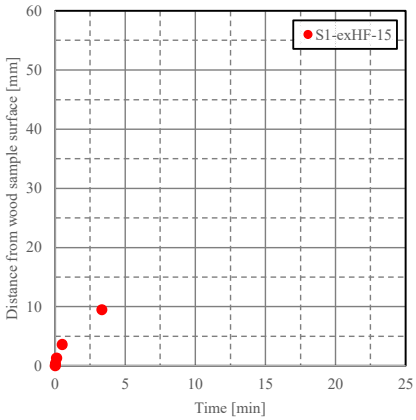

Graph 10: 300°C-ISO profile for "S1-exHF"

The following table summarizes the charring depth and rate based on the time when the last temperature recording position reached 300 [°C].

Table 14: Char properties for simulation "S1-exHF" and experiment

Charring depth – 300°C-ISO line	***Depth [mm]***	***Time [min]***	***Charring rate [mm/min]***
S1-exHF	14.8	7.7	1.92
Experiment	18.0	14.5	1.28

From the presented results and especially from the distance between the green and dark blue line in graph 9, it can be seen that more temperature recordings inside the timber would be beneficial. The default one is too coarse for a reliable estimation of char properties and need to be changed for the subsequent simulations.

3.5.6 Conclusion of the assessment

The main finding of this assessment is that the default position for the recordings inside the timber sample is not adapted for a detailed study of the char properties. A more even spacing of the recordings is needed and will be implemented for further simulations (cf. Chapter. 3.5.7 “Implementation of simulation with finer mesh inside the solid”).
Another difference between the simulation and the experiment is the “flickering” of the flames. As pyrolysis and gas phase combustion are linked, there is a chance that this is due to the not detailed enough mesh resolution inside the timber sample. Once the resolution is better, this problem may be solved as well as the irregularities in the surface temperature measurements and in the temperature measurements inside the timber sample.

There are also lower gas temperature measurements in the simulation but higher temperatures are present if the recording positions have been positioned closer to the floor of the tunnel. However, the measured surface temperatures are very similar.
The assessment showed also that the simulation led to lower air velocity measurements over the timber sample. This may also be linked to some extent to the smaller flames and lower position of the heat flow in the simulation.
The two ways to ignite the timber sample, once by a constant external heat flux over the sample ("S1-exHF") and once by a heat panel ("S2-HP") showed similar results. The measurements are slightly higher for the second situation.

3.5.7 Implementation of simulation with finer mesh inside the timber sample ("fine")

The spacing of the recording for the properties as temperature or density is done automatically by FDS. The size of a cell or – in case of a one-dimensional heat transfer – the thickness of one layer is given by the following equation [21, p. 93] and is equal or less in the simulations.

$$\sqrt{\tau k/\rho c} \qquad (18)$$

Where:

- τ Time constant, 1 [s]
- k Thermal conductivity, [W/m.K]
- ρ Density, [kg/m^3]
- c Specific heat, [J/kg.K]

To save computational resources, FDS does not use that spacing through the whole solid but only on the outermost positions. When moving into the solid, the spacing is doubled in every step until the middle is reached. This leads to the 15 layers shown in chapter 3.5.5 "Temperature recordings inside the timber sample". This non-uniform spacing is done by the code line STRETCH_FACTOR which by default is 2. For all further simulation, this STRETCH_FACTOR is set at 1 to get a uniform spacing. For the simulation "S1-exHF" and "S2-HP" this results in around 248 layers inside the solid with a maximum thickness of 0.5 [mm]. All subsequent simulations are run with this finer mesh. To distinguish these simulations from the ones with the default value 2, the word "fine" is added at the end of the simulation name, for example "S1-exHF-fine". The simulations with the default mesh size inside the solid get the word "coarse" added.

It should be noted that equation 18 for the spacing is dependent on the thermal properties of the materials, when one of those are changing, the number of layers is also changing. Moreover, if the burning results in a shrinking or swelling of the material, and therefore in a change of material thickness, FDS rechecks the total number of layers and either adds or removes layers.
The FDS codes "S1-exHF-fine" and "S2-HP-fine" can be found in Appendix E.

3.6 Test situations

Apart from the previously described simulation situations, other simulations with modified input parameters were run. The previously described simulation situations “S1-exHF-fine” (ignition mode by external heat flux) and “S2-HP-fine” (ignition mode by heat panel) act as standard cases. Modifications where only made to this standard cases.

The first modification is to use a moderate fine mesh resolution for the timber sample. This modification is done in the standard case with ignition by an external heat flux (“S1-exHF-medium”). The results of that simulation, together with the ones from the standard case (fine mesh resolution, “S1-exHF-fine”) and the simulation from the assessment of the simulation environment (coarse mesh resolution, “S1-exHF-coarse”) will be used to assess the influence of the mesh resolution in the wood sample on the HRR, on the charring depth and on the charring rate.

The second modification is the introduction of the moisture content from the timber sample into the standard simulation situations (“S1-exHF-moisture-fine” & “S2-HP-moisture-fine”). This change is also in agreement with the experimental information, where the spruce had a moisture content of 12%. The goal is to test if a more complicated pyrolysis model adds any additional value to the output.

The final modification is to test the influence of temperature dependent input parameters against constant input parameters. This was done by changing the temperature dependent specific heat input parameters for spruce and char in the simulation “S1-exHF-fine” to constant values (“S1-exHF-cp-fine”).

The next subsection gives an overview of all performed simulations and the following three subsection explain the changes in the standard simulations more in detail.

3.6.1 Overview of all performed simulations

The following two tables (table 15 and 16) give an overview of all the performed simulations. The first one is for simulations where ignition is done by an **ex**ternal **H**eat **F**lux over the timber sample (simulation name starting by “S1-exHF”) and the other one about the ignition by a **H**eat **P**anel on the ceiling (“S2-HP”). The words “fine”, “medium”, “coarse” indicate the mesh resolution inside the timber sample.

Table 15: Summary of simulations with ignition by an external heat flux

Name	Description
S1-exHF-fine	Ignition by external heat flux over timber sample, 247-249 layers through the timber sample
S1-exHF-medium	Ignition by external heat flux over timber sample, 82-83 layers through the timber sample
S1-exHF-coarse	Ignition by external heat flux over timber sample, 15 layers in timber sample
S1-exHF-moisture-fine	Ignition by external heat flux over timber sample, Moisture percentage added into timber sample, 319 layers through the timber sample
S1-exHF-cp-fine	Ignition by external heat flux over timber sample, Constant specific heat for spruce and char, 344-348 layers through the timber sample

Table 16: Summary of simulations with ignition by a heat panel

Name	Description
S2-HP-fine	Ignition by heat panel on ceiling, 247-249 layers through the timber sample
S2-HP-moisture-fine	Ignition by heat panel on ceiling, Moisture percentage added into timber sample, 319 layers through the timber sample

3.6.2 Implementation of a moderate fine mesh resolution inside the timber sample ("medium")

The mesh resolution inside the timber sample for the standard simulation with ignition by an external heat flux ("S1-exHF-fine") was changed to a moderate fine mesh resolution. This is done by using a STRETCH_FACTOR(1)=1.05 instead of 2. This simulation will be named "S1-exHF-medium".

The code can be seen in Appendix E.

3.6.3 Implementation of simulations with moisture content ("moisture")

In both standard simulations, the one with ignition by an external heat flux ("S1-exHF-fine") and the one with ignition by a heat panel ("S2-HP-fine"), moisture content of the timber sample was added. This is done by a second parallel reaction where water is evaporated (*class 2*, cf. subsection 1.3.2 "Comprehensive models"). This is in agreement with Bartlett and al. [14], that at high heat fluxes, the evaporation of water and the pyrolysis are taking place at the same time.

$$moisture \rightarrow water\ vapor \qquad (19)$$

The evaporation reaction parameters are presented in the next table (table 17).

Table 17: Parameters and values for the evaporation reaction

Parameter	Code in FDS	Value	Source
Number of reactions	N_REACTIONS	1	Defined by reaction scheme
Yield	NU_SPEC	1	Defined by reaction scheme
Activation energy	E	100'000 [J/mol]	[32]
Pre-exponential factor	A	10^{13} [1/s]	[32]
Absorptivity	ABSORPTION_COEFFICIENT	50'000 [1/m]	Default value FDS [21]
Reaction order	N_S	1	Default value FDS [21]
Heat of reaction	HEAT_OF_REACTION	2260 [kJ/kg]	[32]

The following table shows material properties for water for the simulation in FDS (table 18).

Table 18: Material properties for water

Parameter	Code in FDS	Value	Source
Density	DENSITY	1000 [kg/m^3]	[32]
Emissivity	EMISSIVITY	1.0	[32]
Conductivity	CONDUCTIVITY	0.06 [W/(m.K)]	[32]

The density, the conductivity, the specific heat and the heat of combustion for spruce change with moisture content. Table 19 shows the changed values for density and conductivity.

Table 19: Density and conductivity for wood with a moisture content of 12%

Parameter	Code in FDS	Value	Source
Density	DENSITY	371.8 [kg/m^3]	[31]
Conductivity	CONDUCTIVITY	0.2 [W/(m.K)]	[10]

The conductivity in Shi and Chew [10] is given as interval of 0.19 – 0.22 [W/(m.K)].

The following equation allows to calculate the specific heat with moisture content C_p [kJ/kg.K] [10, p. 10]:

$$C_p = \frac{C_p^D + 0.01 M C_p^W}{1 + 0.01M + (0.0002355T - 0.0001326M - 0.06191)M} \quad (20)$$

Where:

C_p^D Specific heat of dry wood, [kJ/(kg.K)]
C_p^W Specific heat of water, 4.186 [kJ/(kg.K)]
M Moisture content of timber, 12 % [31]

The input data for the specific heat for dry wood was equation 17 under 3.1 "Input parameters for the pyrolysis model". By applying the above equation, the specific heat for wood with a moisture content of 12 % becomes as shown in the following graph 9.

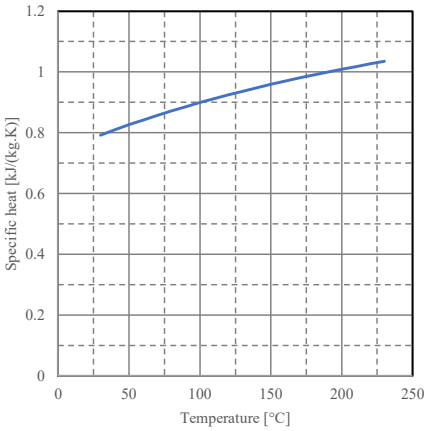

Graph 11: Specific heat for wood with a moisture content of 12%

The heat of combustion for the moisture can be adapted by the following equation [33, p. 652]:

$$LHV = HHV - 2.535\ (9H + W) \qquad (21)$$

Where:

LHV	Lower heating value or heat of combustion without condensed water, [kJ/kg]
HHV	Higher heating value or heat of combustion with condensed water, [kJ/kg]
H	Hydrogen contents of fuel, [%]
W	Water (hygroscopic moisture) contents of fuel ,[%]

The heat of combustion without condensed water used in the standard simulations was 14'000 [kJ/kg], the hydrogen content is 5.8 % [33, p. 652] and the water content is 12 % [31]. This results in a heat of combustion with condensed water of 14'163 [kJ/kg].
Simulations with a moisture content will have the word "moisture" in the simulation name. The FDS codes are shown in Appendix E.

3.6.4 Implementation of the simulation with constant specific heat values ("cp")

In the standard simulation with ignition by an external heat flux, the input parameter for specific heat for spruce and char was changed to a constant value (table 20).

Table 20: Constant specific heat for spruce and char

	Specific heat [kJ/(kg.K)]
Spruce	1.8
Char	1.5

The value for spruce is the specific heat value for a temperature of 230 [°C] and onwards introduced in the linear equation explained under 3.1 "Input parameters for the pyrolysis model" and the one for char correspond to a specific heat value for a temperature of 390 [°C] from equation 17. These numbers are chosen under the assumption that the gas temperature at the solid surface is higher than ambient which could also be seen in the first results shown in the previous section.

The simulation with a constant specific heat for spruce and char will be named “S1-exHF-moisture-fine”. The FDS code is shown in Appendix E.

4 Results

This chapter summarizes the main results from all the simulations. The first section presents the information from the simulations where ignition was done by an external heat flux (“S1-exHF-fine” and all the modifications). The second section shows the results from the simulations where ignition happened with a heat panel (“S2-HP-fine” and the modified simulations). In each subsection, the heat release rate over the whole simulation is presented followed by the surface temperature measurements, the temperature profile inside the timber sample, the charring depth and the charring rate. The last result is a graph showing the way the charring front moved through the timber sample over the simulation time (300°C-ISO profile). For the simulations “S1-exHF-fine” and “S2-HP-fine” also the air velocity measurements above the timber sample as well as the gas temperature recordings at the start, the end and behind the fire chamber are presented. For the other simulations, these results are displayed in Appendix G.
For the raw data from all the simulations and some additional material, it is referred to appendix J.

4.1 Simulations with ignition by an external heat flux

This section presents the five simulations “S1-exHF-fine”, “S1-exHF-medium”, “S1-exHF-coarse”, “S1-exHF-moisture-fine” and “S1-exHF-cp-fine”.

4.1.1 Standard case (“S1-exHF-fine”)

The following graph shows the heat release rate over the whole simulation time.

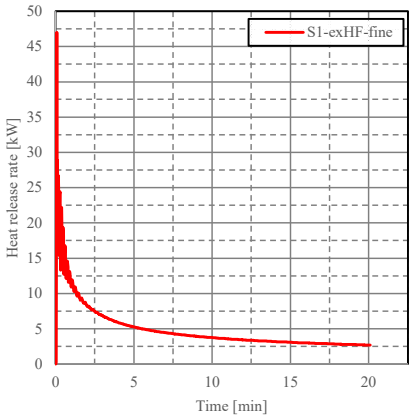

Graph 12: HRR over the simulation time for simulation "S1-exHF-fine"

Graph 13 shows the air velocity measurements above the timber sample.

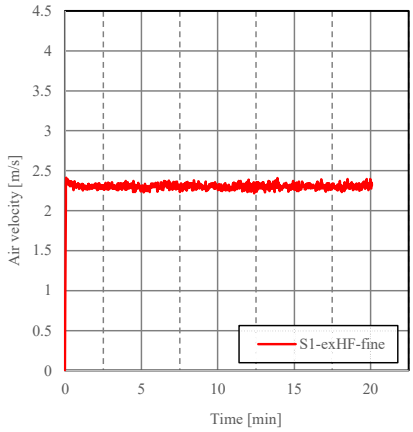

Graph 13: Air velocity measurements above the wood sample for simulation "S1-exHF-fine"

The next three graphs show the gas temperatures at the start, the end and behind the fire chamber.

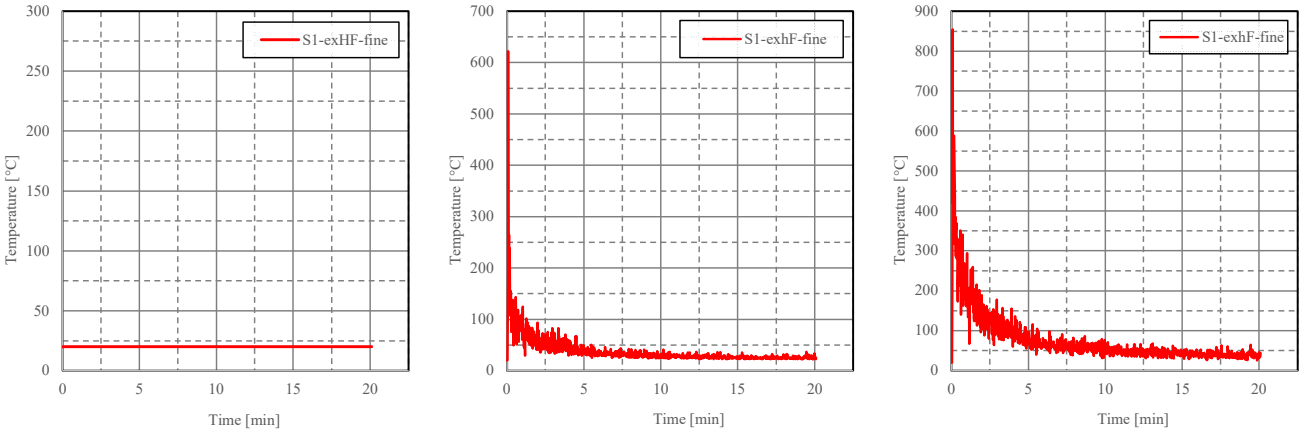

Graph 14: Gas temperature measurements at the start (left), at the end (middle) and behind the fire chamber (left) for the simulation "S1-exHF-fine"

The next graph shows the temperature recordings on the timber sample surface.

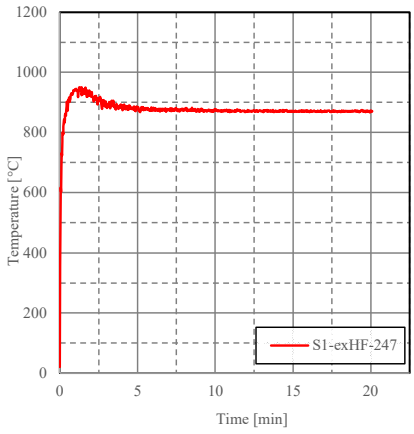

Graph 15: Surface temperature measurements for simulation "S1-exHF-fine"

Graph 16 shows the temperature recordings inside the timber sample. Every line stands for a temperature distribution in time for a given depth from the surface. From the 249 layers of recordings, only six layers at a position close to the experimental recording depths which are 6 [mm], 12 [mm], 18 [mm], 24 [mm], 30 [mm] and 36 [mm], are selected and presented in the graph.

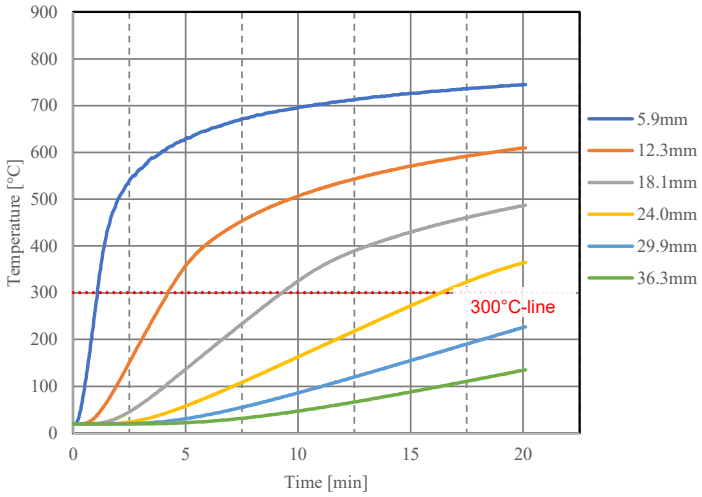

Graph 16: Temperature recordings inside the timber sample for the simulation "S1-exHF-fine"

The charring depth at the end of the simulation is 26.5 [mm]. This results in a charring rate of 1.33 [mm/min] (table 21).

Table 21: Charring properties for simulation "S1-exHF-fine"

	Charring depth [mm]	***Time to reach depth [min]***	***Charring rate [mm/min]***
S1-exHF-fine	26.5	19.9	1.33

The next graph shows the progression of the charring front through the timber sample by the 300°C-ISO profile. It is done with all the 249 measuring points through the solid where 54 reached 300 [°C].

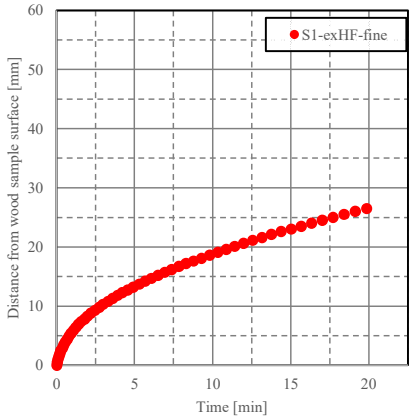

Graph 17: 300°C-ISO profile for the simulation "S1-exHF-fine"

The charring front progression over time shows a logarithmic behavior.

The analysis of the data also showed that the timber sample swells; the thickness increases by 2.2 [mm].

4.1.2 Simulation with moderate fine mesh size inside the timber sample (“S1-exHF-medium”)

The following graph shows the heat release rate over the whole simulation time.

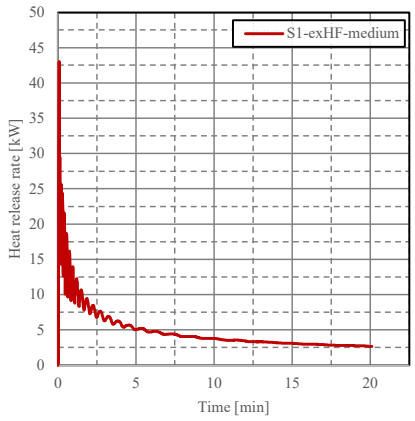

Graph 18: HRR over the simulation time for simulation "S1-exHF-medium"

Graph 19 shows the temperature recordings on the timber sample surface.

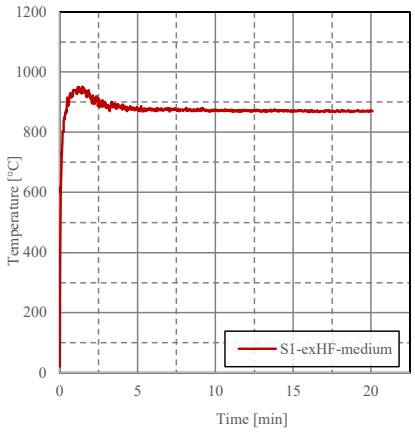

Graph 19: Surface temperatures on timber sample for simulation "S1-exHF-medium"

The following graph shows the temperature recordings inside the timber sample. Again, each line stands for a temperature distribution in time for a given depth from the surface.

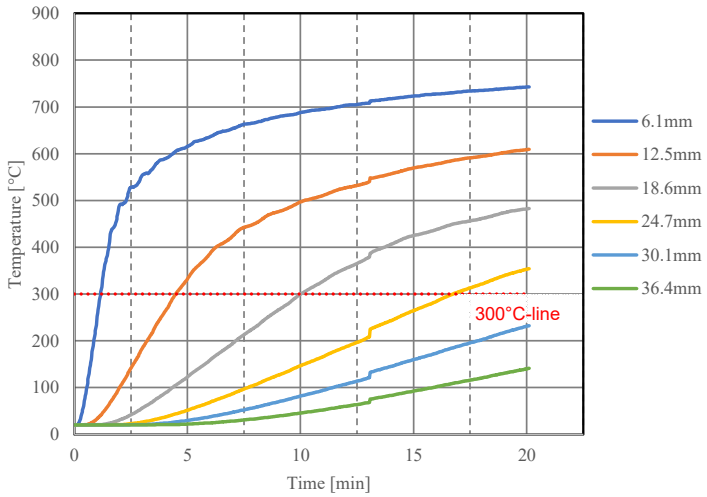

Graph 20: Temperature recordings inside the timber sample for the simulation "S1-exHF-medium"

The charring depth at the end of the simulation is 26.4 [mm]. This results in a charring rate of 1.38 [mm/min] (table 22).

Table 22: Charring properties for simulation "S1-exHF-medium"

	Charring depth [mm]	***Time to reach depth [min]***	***Charring rate [mm/min]***
S1-exHF-medium	26.4	19.2	1.38

The next graph shows the progression of the charring front through the timber sample by the 300°C-ISO profile. It is done with all the 83 measuring points through the solid where 27 reached 300 [°C].

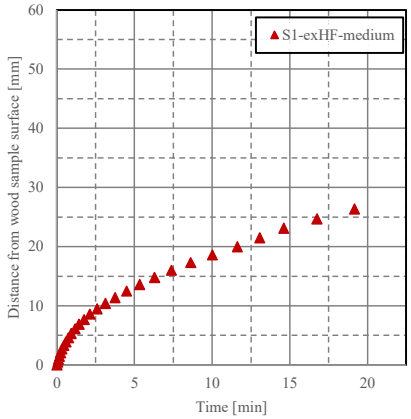

Graph 21: 300°C-ISO profile for the simulation "S1-exHF-medium"

The charring front progression over time shows a logarithmic behavior.

The analysis of the data also showed that the timber sample swells; the thickness increases by 2.2 [mm].

4.1.3 Simulation with coarse mesh size inside the timber sample (“S1-exHF-coarse”)

The following graph shows the heat release rate over the whole simulation time.

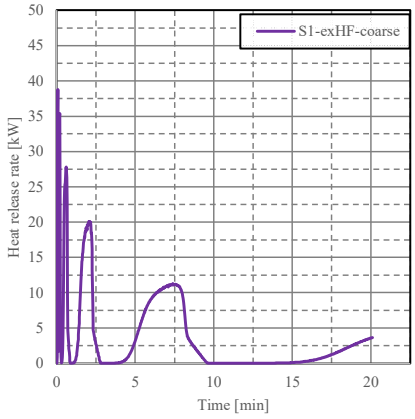

Graph 22: HRR over the simulation time for simulation "S1-exHF-coarse"

Graph 23 shows the temperature recordings on the timber sample surface.

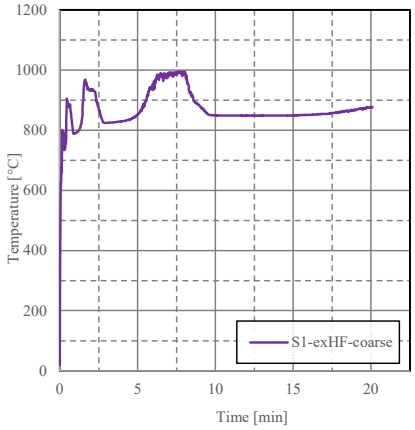

Graph 23: Surface temperatures on wood sample for simulation "S1-exHF-coarse"

The following graph shows the temperature recordings inside the timber sample. Again, each line stands for a temperature distribution in time for a given depth from the surface. This time, only three lines are shown, as only three layers correspond to the position of the experimental values.

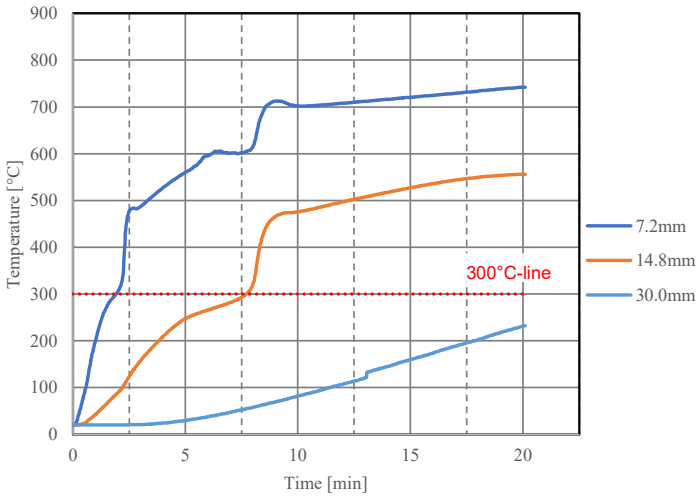

Graph 24: Temperature recordings inside the timber sample for the simulation "S1-exHF-coarse"

The charring depth at the end of the simulation is 14.8 [mm]. This results in a charring rate of 1.92 [mm/min] (table 23).

Table 23: Charring properties for simulation "S1-exHF-coarse"

	Charring depth [mm]	***Time to depth [min]***	***Charring rate [mm/min]***
S1-exHF-coarse	14.8	7.7	1.92

The next graph shows the progression of the charring front through the timber sample by the 300°C-ISO profile. It is done with all the 15 measuring points through the solid where 5 reached 300 [°C].

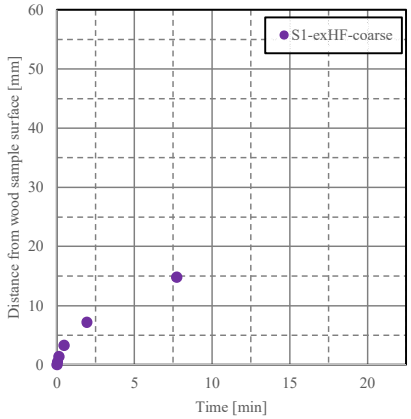

Graph 25: 300°C-ISO profile for the simulation "S1-exHF-coarse"

There are not enough points to clearly identify a charring front progression shape, either a logarithmic or a linear behaviour could be assumed.

The analysis of the data also showed that the timber sample swells; the thickness increases by 1.5 [mm].

4.1.4 Simulation with moisture content (“S1-exHF-moisture-fine”)

The following graph shows the heat release rate over the whole simulation time.

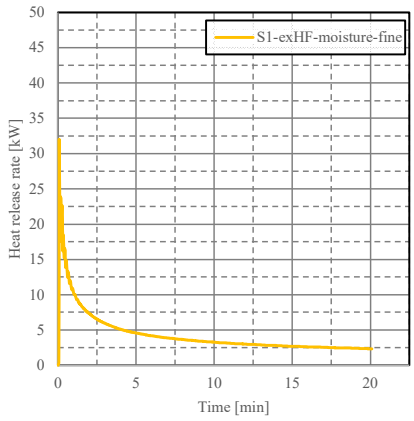

Graph 26: HRR over the simulation time for simulation "S1-exHF-moisture-fine"

Graph 27 shows the temperature recordings on the timber sample surface.

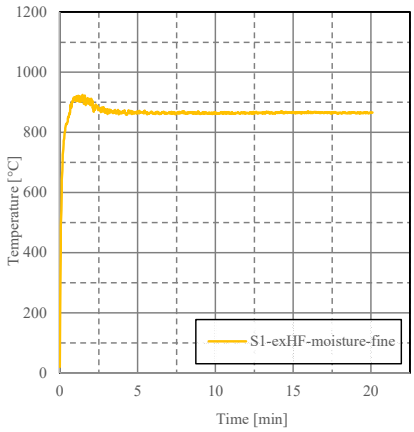

Graph 27: Surface temperature measurements on the timber sample for simulation "S1-exHF-moisture-fine"

The next graph shows the temperature recordings inside the timber sample. Again, each line stands for a temperature distribution in time for a given depth from the surface.

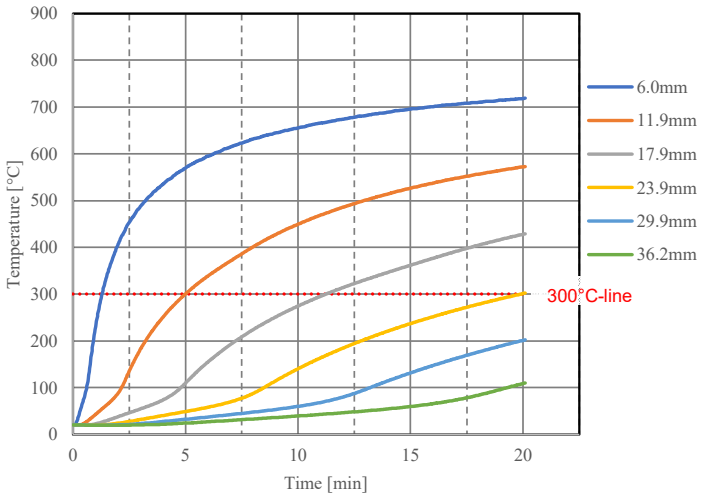

Graph 28: Temperature recordings inside the timber sample for the simulation "S1-exHF-moisture-fine"

The charring depth at the end of the simulation is 23.9 [mm]. This results in a charring rate of 1.20 [mm/min] (table 24).

Table 24: Charring properties for simulation "S1-exHF-moisture-fine"

	Charring depth [mm]	***Time to reach depth [min]***	***Charring rate [mm/min]***
S1-exHF-moisture-fine	23.9	19.9	1.20

The next graph shows the progression of the charring front through the wood sample by the 300°C-ISO profile. It is done with all the 319 measuring points through the solid where 64 reached 300 [°C].

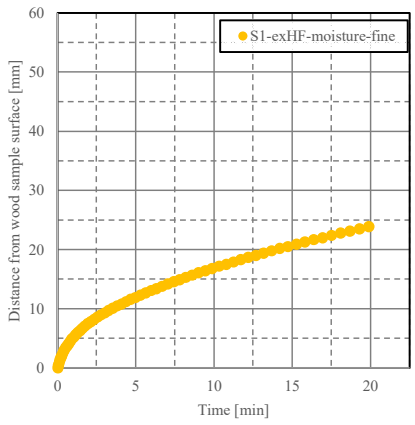

Graph 29: 300°C-ISO profile for the simulation "S1-exHF-moisture-fine"

The charring front progression over time shows a logarithmic behavior.

The analysis of the data also showed that the timber sample shrinks; the thickness decreases by 1.9 [mm].

4.1.5 Simulation with constant specific heat parameters (“S1-exHF-cp-fine”)

The following graph shows the heat release rate over the whole simulation time.

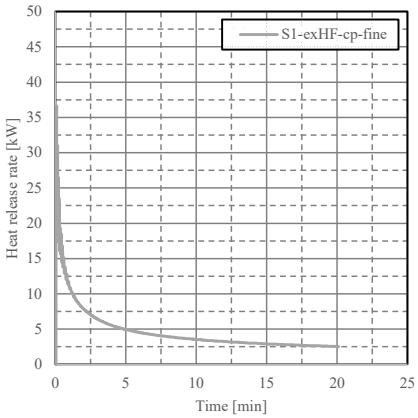

Graph 30: HRR over the simulation time for simulation "S1-exHF-cp-fine"

Graph 31 shows the temperature recordings on the timber sample surface.

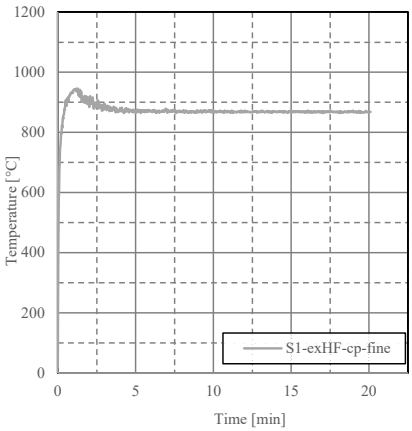

Graph 31: Surface temperature measurements on the timber sample for simulation "S1-exHF-cp-fine"

The next graph shows the temperature recordings inside the timber sample. Again, each line stands for a temperature distribution in time for a given depth from the surface.

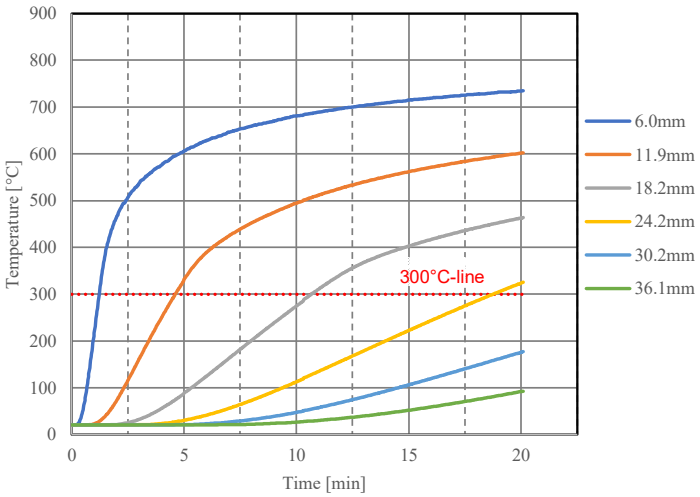

Graph 32: Temperature recordings inside the timber sample for the simulation "S1-exHF-cp-fine"

The charring depth at the end of the simulation is 24.9 [mm]. This results in a charring rate of 1.25 [mm/min] (table 25).

Table 25: Charring properties for simulation "S1-exHF-cp-fine"

	Charring depth [mm]	***Time to reach depth [min]***	***Charring rate [mm/min]***
S1-exHF-cp-fine	24.9	19.9	1.25

The next graph shows the progression of the charring front through the timber sample by the 300°C-ISO profile. It is done with all the 348 measuring points through the solid where 71 reached 300 [°C].

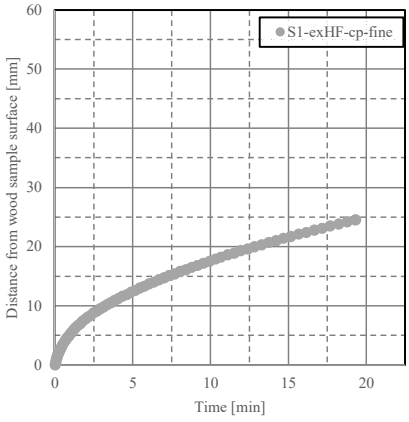

Graph 33: 300°C-ISO profile for the simulation "S1-exHF-cp-fine"

The charring front progression over time shows a logarithmic behavior.

The analysis of the data also showed that the timber sample swells; the thickness increases by 2.1 [mm].

4.2 Simulations with ignition by a heat panel

This section presents the results for the simulations “S2-HP-fine” and “S2-HP-moisture-fine”.

4.2.1 Standard simulation (“S2-HP-fine”)

The following graph shows the heat release rate over the whole simulation time.

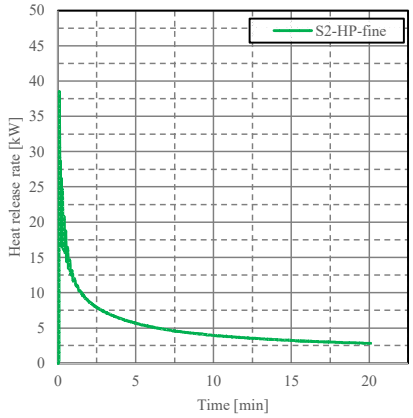

Graph 34: HRR over the simulation time for simulation "S1-HP-fine"

Graph 35 shows the air velocity measurements above the timber sample.

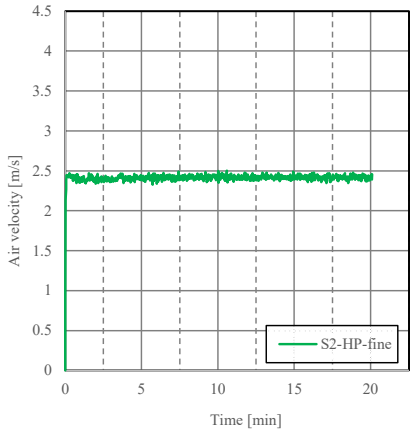

Graph 35: Air velocity measurements above the timber sample for simulation "S2-HP-fine"

The next three graphs show the gas temperatures at the start, the end and behind the fire chamber.

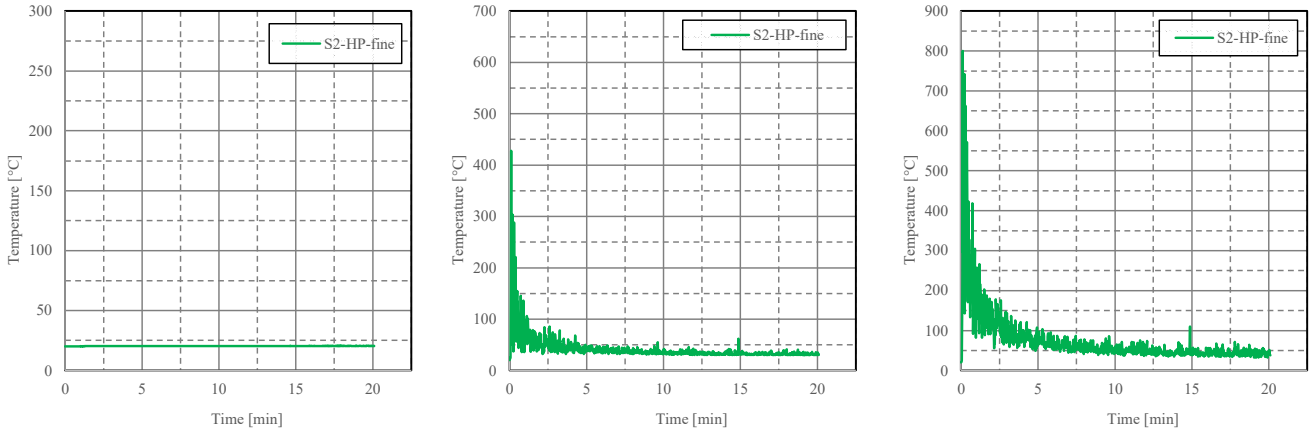

Graph 36: Gas temperature measurements at the start (left), at the end (middle) and behind the fire chamber (left) for the simulation "S2-HP-fine"

The next graph shows the temperature recordings on the timber sample surface.

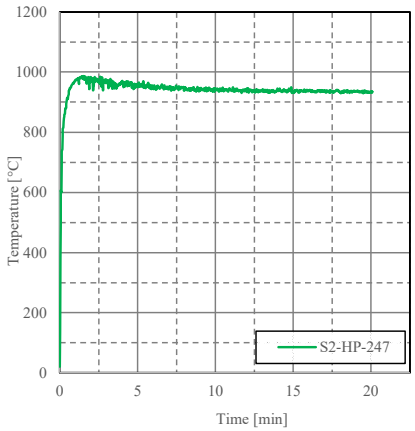

Graph 37: Surface temperature measurements on the timber sample for simulation "S2-HP-fine"

Graph 38 shows the temperature recordings inside the timber sample. Again, each line stands for a temperature distribution in time for a given depth from the surface.

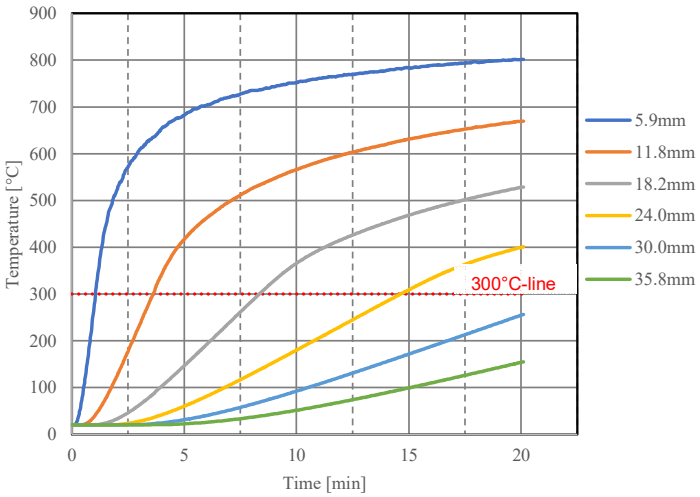

Graph 38: Temperature recordings inside the timber sample for the simulation "S1-HP-fine"

The charring depth at the end of the simulation is 28.0 [mm]. This results in a charring rate of 1.41 [mm/min] (table 26).

Table 26: Charring properties for simulation "S1-HP-fine"

	Charring depth [mm]	***Time to reach depth [min]***	***Charring rate [mm/min]***
S2-HP-fine	28.0	19.8	1.41

The next graph shows the progression of the charring front through the timber sample by the 300°C-ISO profile. It is done with all the 249 measuring points through the solid where 57 reached 300 [°C].

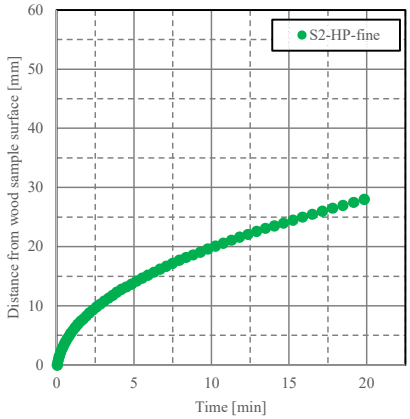

Graph 39: 300°C-ISO profile for the simulation "S1-HP-fine"

The charring front progression over time shows a logarithmic behavior.

The analysis of the data also showed that the timber sample swells; the thickness increases by 2.4 [mm].

4.2.2 Simulation with moisture content (“S2-HP-moisture-fine”)

The following graph shows the heat release rate over the whole simulation time.

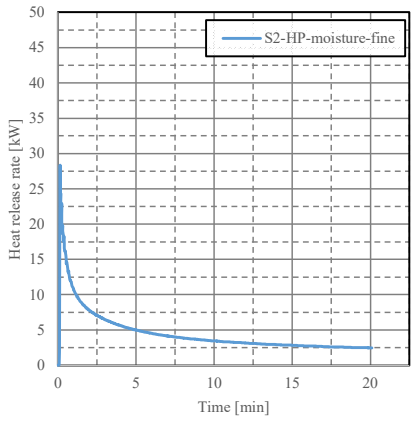

Graph 40: HRR over the simulation time for simulation "S1-HP-moisture-fine"

Graph 41 shows the temperature recordings on the timber sample surface.

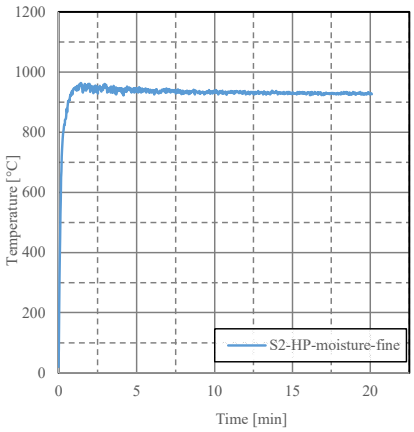

Graph 41: Surface temperature measurements on the timber sample for simulation "S2-HP-moisture-fine"

The next graph shows the temperature recordings inside the timber sample. Again, each line stands for a temperature distribution in time for a given depth from the surface.

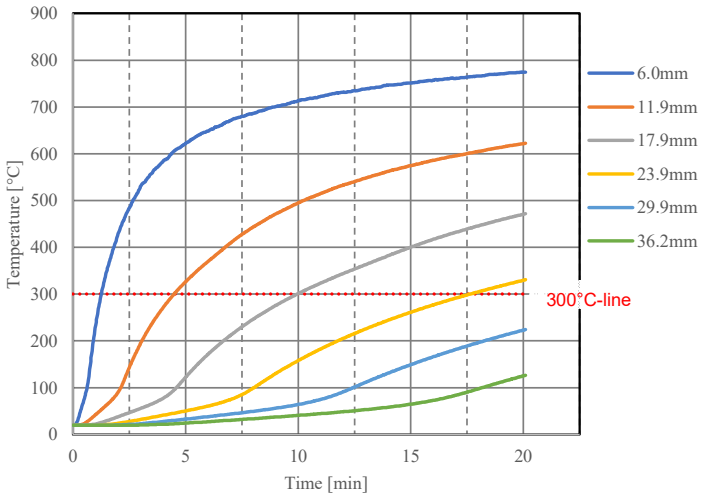

Graph 42: Temperature recordings inside the timber sample for the simulation "S1-HP-moisture-fine"

The charring depth at the end of the simulation is 25.4 [mm]. This results in a charring rate of 1.28 [mm/min] (table 27).

Table 27: Charring properties for simulation "S1-HP-moisture-fine"

	Charring depth [mm]	***Time to reach depth [min]***	***Charring rate [mm/min]***
S2-HP-moisture-fine	25.4	19.9	1.28

The next graph shows the progression of the charring front through the timber sample by the 300°C-ISO profile. It is done with all the 319 measuring points through the solid where 68 reached 300 [°C].

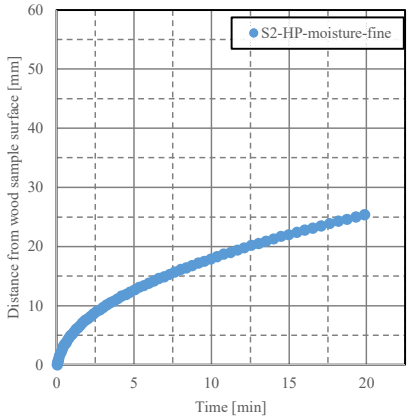

Graph 43: 300°C-ISO profile for the simulation "S1-HP-moisture-fine"

The charring front progression over time shows a logarithmic behavior.

The analysis of the data also showed that the timber sample shrinks; the thickness decreases by 2.0 [mm].

5 Discussion

This chapter starts with a discussion of the influence of several parameters on the results of the simulations, namely:

- the ignition mode
- the mesh resolution inside the timber sample
- the addition of moisture content to the timber sample
- temperature dependent specific heat against a constant value

Each of this discussion sections starts with the comparison of the HRR, followed by the charring depth, the charring rate and the propagation of the 300°C-ISO curve inside the timber sample. The last section discusses the limitation of the study and gives some ideas for further tests.

5.1 Influence of the ignition mode on the results

This section compares the two standard simulations (“S1-exHF-fine” & “S2-HP-fine”) to assess the influence of the ignition way on the simulation results.

5.1.1 HRR

Graph 44 compares the HRR for the two simulations. The two adjacent tables show some key quantities from this graph (table 28 & 29).

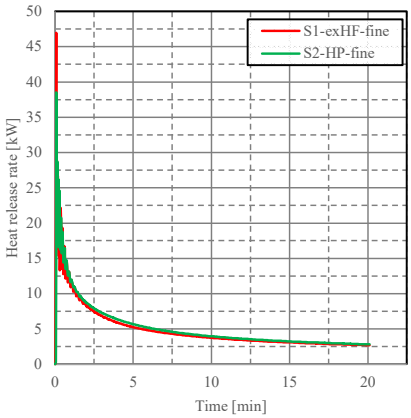

Graph 44: HRR for the simulations "S1-exHF-fine" & "S2-HP-fine"

Table 28: Released heat over the simulation time for "S1-exHF-fine" & "S2-HP-fine"

	Released heat over simulation time [MJ]
S1-exHF-fine	5.9
S2-HP-fine	6.2

Table 29: Key quantities from graph 44

	Peak [kW]	***Time to peak [s]***	***HHR at simulation end [kW]***	***Mean [kW]***
S1-exHF-fine	47.0	4.8	2.7	4.9
S2-HP-fine	38.5	6.0	2.8	5.1

The ignition mode with an external heat flux leads to a high peak in shorter time than the ignition by heat panel, but shows a faster decrease of the heat release rate then the other one. The overall release of energy is similar.

5.1.2 Temperature measurements inside the timber sample

The next six graphs show the comparison of the temperature inside the timber sample. The depths are ca. 6 [mm], 12 [mm], 18 [mm], 24 [mm], 30 [mm] and 36 [mm].

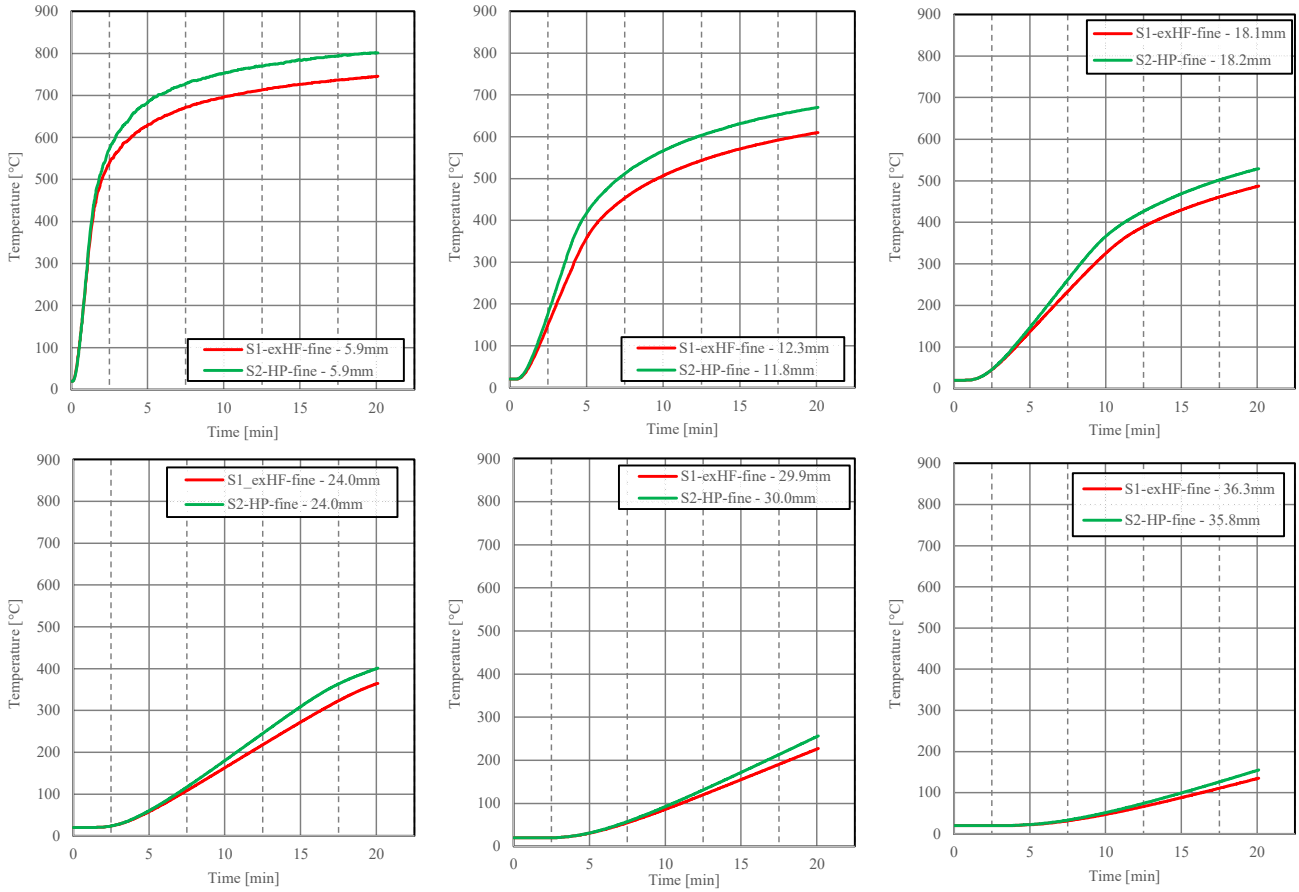

Graph 45: Comparison of temperature recordings inside the timber sample for "S1-exHF-fine" & "S2-HP-fine"

The temperature recordings are slightly higher for the ignition mode by a heat panel than for the external heat flux. Both types of simulations show a similar temperature behaviour through the whole simulation time.

This also corresponds to the finding in the assessment of the simulation environment (3.5.5 “Temperature recordings inside the timber sample”).

5.1.3 Char properties

Table 30 compares the charring depth and the charring rate for the two types of simulations.

Table 30: Charring depth and rate for simulations "S1-exHF-fine" & "S2-HP-fine"

	Charring depth [mm]	***Charring rate [mm/min]***
S1-exHF-fine	26.5	1.33
S2-HP-fine	28.0	1.41

The charring depth and rate are slightly higher for the ignition mode by the heat panel than for the one with an external heat flux. This is in agreement with the slightly higher temperatures inside the timber sample.

The next graph compares the progression of the charring front through the timber sample by the 300°C-ISO profile for both simulations.

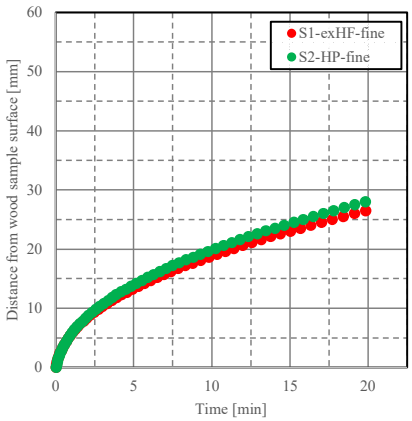

Graph 46: 300°C-ISO profile for the simulations "S1-exHF-fine" & "S2-HP-fine"

Both show a similar charring front behaviour, there is only a slight difference in the charring speed. Again, the simulation with ignition by a heat panel shows a slightly faster rate, in agreement with the findings above.

5.1.4 Simulation time

The next table compares the simulation times. Both simulations were run on the same HPC cluster and with the same number of meshes.

Table 31: Simulation time for the simulations "S1-exHF-fine" & "S2-HP-fine"

	Simulation time
S1-exHF-fine	24 [h] 38 [min]
S2-HP-fine	35 [h] 33 [min]

The simulation with the ignition mode by a heat panel had a much longer simulation time, around 1.4 times higher, than the one with the external heat flux.

5.1.5 Summary

Both simulations result in similar outputs. The main difference was the effort to define the input values; for the simulation with a heat panel, additional calibration simulations had to be run. Therefore, the simulation with ignition by the external heat flux allows the user to more easily change simulation environment parameters as incident heat flux for future comparison with other experimental results from the FANCI setup, than the simulation with ignition by a heat panel. It also seems that the simulation time is shorter for the simulations with ignition by an external heat flux.

5.2 Influence of the mesh resolution inside the timber sample on the results

This section compares the simulations with a fine mesh inside the timber sample (“S1-exHF-fine”) with the moderate fine one (“S1-exHF-medium”) and the coarse one (“S1-exHF-coarse”). All the simulations are performed with the standard case and ignition by an external heat flux. This section has an additional output comparison which is the surface temperature measurements, making a direct connection between the HRR and the temperature profile inside the timber sample.

5.2.1 HRR

Graph 47 compares the HRR for the three simulations. The two tables adjacent to it show some key quantities from this graph (table 32 & 33). Simulation “S1-exHF-coarse” is not present in table 33 because its shape of the HRR curve is different then for the other two, not allowing the same type of quantification.

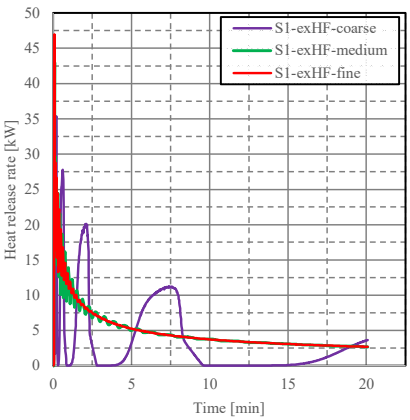

Graph 47: HRR for the simulations "S1-exHF-fine", "S1-exHF-medium" & "S1-exHF-coarse"

Table 32: Released heat over the simulation time for "S1-exHF-fine", "S1-exHF-medium" & "S1-exHF-coarse"

	Released heat over simulation [MJ]
S1-exHF-fine	5.9
S1-exHF-medium	5.9
S1-exHF-coarse	4.0

Table 33: Key quantities from graph 47

	Peak [kW]	***Time to peak [s]***	***HHR at simulation end [kW]***	***Mean [kW]***
S1-exHF-fine	47.0	4.8	2.7	4.9
S1-exHF-medium	43.0	4.8	2.7	4.9

The analysis of the simulations and of the graph both show that the finer mesh resolution and a moderate fine mesh resolution got rid of the flickering in the burning behaviour of the timber. Both simulations show what would be expected as burning behaviour, a peak followed by a decrease in HRR and ending in a relatively steady heat release rate before burn out happens [1], [11]. The quantification of the HRR behaviour is very similar in the simulation with the fine mesh resolution and the moderate fine.

5.2.2 Surface temperature measurements

The next graph shows the comparison of the surface temperature of the timber sample for the three different mesh resolution simulations.

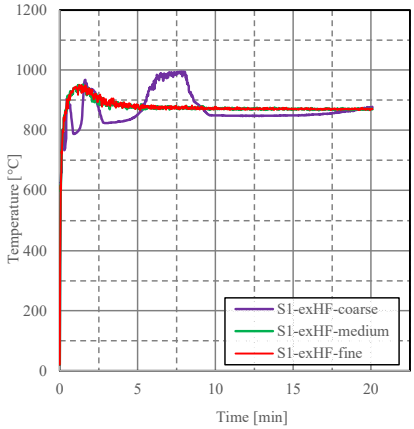

Graph 48: Surface temperature measurements for the simulations "S1-exHF-fine", "S1-exHF-medium" & "S1-exHF-coarse"

The simulation with the coarse mesh shows again a different behaviour in comparison to the other two. The first one reflects the shape of the flickering from the HRR as already seen under 3.5.3 “Surface temperature measurements on the timber sample”. However, the simulations with the fine mesh and the moderate fine mesh show similar behavior which is also reflecting the HRR behaviour from the previous subsection. The difference between these two simulations is that the temperature behavior of the fine mesh resolution is smoother than for the moderate one.

5.2.3 Temperature measurements inside the timber sample

The next four graphs show the comparison of the temperature inside the timber sample between the three simulations at depths of around 3.4 [mm], 7.4 [mm], 14.7 [mm], and 30.0 [mm].

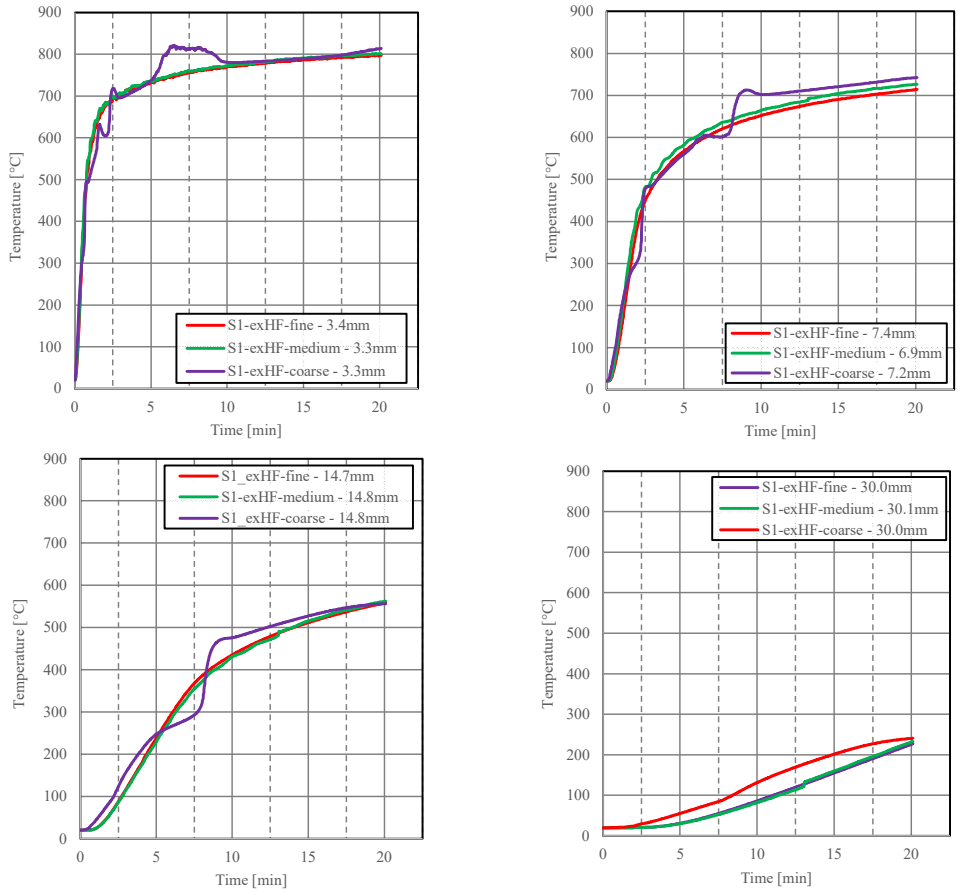

Graph 49: Temperature measurements inside the timber sample for simulations "S1-exHF-fine", "S1-exHF-medium" & "S1-exHF-coarse"

The simulations with a fine and a moderate fine mesh results in very similar findings as can be seen by the almost overlapping lines. As with the graph of the surface temperature measurements from the previous section (graph 48), the fine mesh shows a slightly smoother line than the other one. The results for the coarse mesh show a much more unsteady behaviour than the other two simulations reflecting again to some extent the unsteadiness in the HRR (graph 47).

A note for the temperature recordings inside the wood sample for the simulation with the moderate fine mesh resolution inside the timber sample (“S1-exHF-medium”): At the time of about 13.1 [min], a small jump is visible in graph 48 and more clearly in graph 20 (4.1.2 “Simulation with moderate fine mesh size inside the timber sample (“S1-exHF-medium”)”). This happens when FDS adds another layer of temperature recording inside the timber sample as the material thickness has increased so much, that another layer is needed. This also happens in the simulations with the fine mesh resolution inside the timber sample (“S1-exHF-fine” and “S1-exHF-cp-fine”) but without any visible consequences in the temperature recordings. The actual reason for this small jump could not be determined. It should also be noted, that this steep

increase is only visible in the output recorded inside the timber sample and not in the surface temperature measurements.

5.2.4 Char properties

Table 34 compares the charring depth and the charring rate for the three simulations.

Table 34: Charring depth and rate for the simulations "S1-exHF-fine", "S1-exHF-medium" & "S1-exHF-coarse"

	Charring depth [mm]	***Charring rate [mm/min]***
S1-exHF-fine	26.5	1.33
S1-exHF-medium	26.4	1.38
S1-exHF-coarse	14.8	1.92

The charring depth and rate is almost the same for the two cases with the fine and the moderate fine mesh. Again, there is a bigger difference compared to the coarse mesh simulation.

The next graph compares the progression of the charring front through the timber sample by the 300°C-ISO profile for the three simulations.

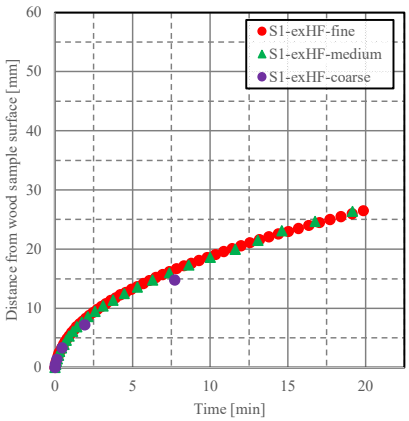

Graph 50: 300°C-ISO profile for the simulations "S1-exHF-fine", "S1-exHF-medium" & "S1-exHF-coarse

The two simulations with the finer mesh resolutions demonstrate the same behaviour of the charring front with a logarithmic shape. The values of both simulations are almost the same, the results for the simulations with a moderate fine mesh resolution inside the timber sample show only slightly lower values. The data for the simulation with the coarse mesh resolution inside the timber sample show again lower values. This graph demonstrates that there is a grid dependency of the simulations results and therefore, it is important to have an appropriate mesh resolution inside the timber sample to get accurate results.

5.2.5 Simulation time

Table 35 compares the simulation times. All simulations were run on the same HPC cluster and with the same number of meshes.

Table 35: Simulation times for the simulations "S1-exHF-fine", "S1-exHF-medium" & "S1-exHF-coarse

	Simulation time
S1-exHF-fine	24 [h] 38 [min]
S1-exHF-medium	16 [h] 08 [min]
S1-exHF-coarse	16 [h] 23 [min]

This time, the simulation with the coarse and the moderate fine mesh show very similar results. The simulation with the fine mesh resolution results in around 1.5 times higher simulation time than the other two.

5.2.6 Summary

Summarizing the discussed results, the simulation with the coarse mesh resolution inside the timber sample does not give satisfying results. First of all, the few numbers of recordings inside the solid do not allow a detailed analysis of the charring properties. There is a solid grid dependency of the results showing that an appropriate mesh resolution inside the timber sample is important. The moderate fine mesh resolution tested in this study could be a good compromise between accuracy and simulation time. However, due to the mentioned irregularity in the temperature recordings inside the timber sample, further studies should be carried out, to understand that phenomena.

The importance to have a good mesh resolution inside the solid material was also mentioned by Šálek et al. [5]. Also, in the simulations from Moinuddin et al. [34], the default mesh size inside the solid was changed to end up with perfectly uniform cells. Changes were made on the CELL_SIZE_FACTOR and the time interval for the solid-phase solution.

5.3 Influence of the moisture content on the results

This section compares the simulation between a dry timber sample and timber sample with a moisture content of 12%. The comparison includes four simulations, two simulations with ignition by an external heat flux (“S1-exHF-fine” & “S1-exHF-moisture-fine”) and two simulations with ignition by a heat panel (“S2-HP-fine” & “S2-HP-moisture-fine”).

5.3.1 HRR

The next two graphs compare the HRR for the two simulations with ignition by an external heat flux and for the two simulations with ignition by a heat panel. The two tables show some key quantities from these two graphs (table 36 & 37).

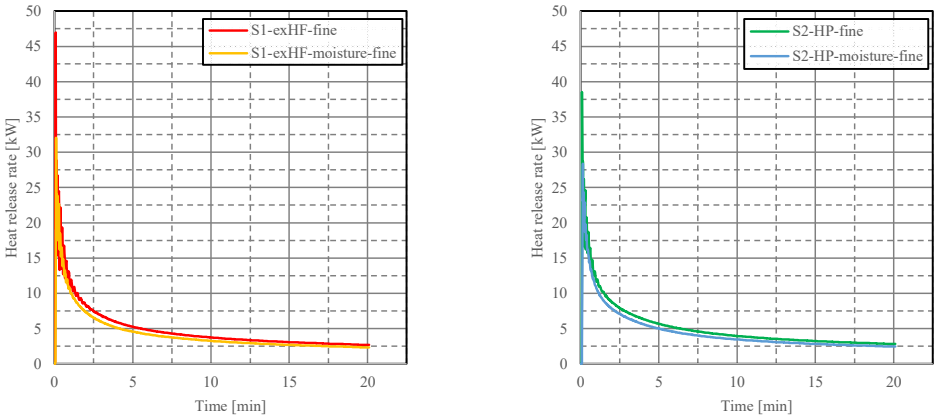

Graph 51: HRR for simulations "S1-exHF-fine" & "S1-exHF-moisture-fine" (left) and for "S2-HP-fine" & "S2-HP-moisture-fine" (right)

Table 36: Released heat over simulation time for the simulations "S1-exHF-fine", "S1-exHF-moisture-fine”, "S2-HP-fine" & "S2-HP-moisture-fine"

	Released heat over simulation time [MJ]
S1-exHF-fine	5.9
S1-exHF-moisture- fine	5.2
S2-HP-fine	6.2
S2-HP-moisture-fine	5.5

Table 37: Key quantities from graph 51

	Peak [kW]	***Time to peak [s]***	***HHR at simulation end [kW]***	***Mean [kW]***
S1-exHF-fine	47.0	4.8	2.7	4.9
S1-exHF-moisture- fine	32.0	6.0	2.3	4.3
S2-HP-fine	38.5	6.0	2.8	5.1
S2-HP-moisture-fine	28.3	8.4	2.5	4.5

The comparison shows that the simulation with wood including moisture content leads to less heat released over the simulation time. This is in agreement with what is expected to happen as

water needs also energy to evaporate and with what was previously explained in subsection 1.2.1 “Pyrolysis of timber”.

5.3.2 Temperature measurements inside the timber sample

The next six graphs show the comparison of the temperature inside the timber sample for the simulation with dry timber and with moisture content, for the simulation situation with ignition by an external heat flux (“S1-exHF-fine” & “S1-exHF-fine-moisture”). The depths are ca. 6 [mm], 12 [mm], 18 [mm], 24 [mm], 30 [mm] and 36 [mm].

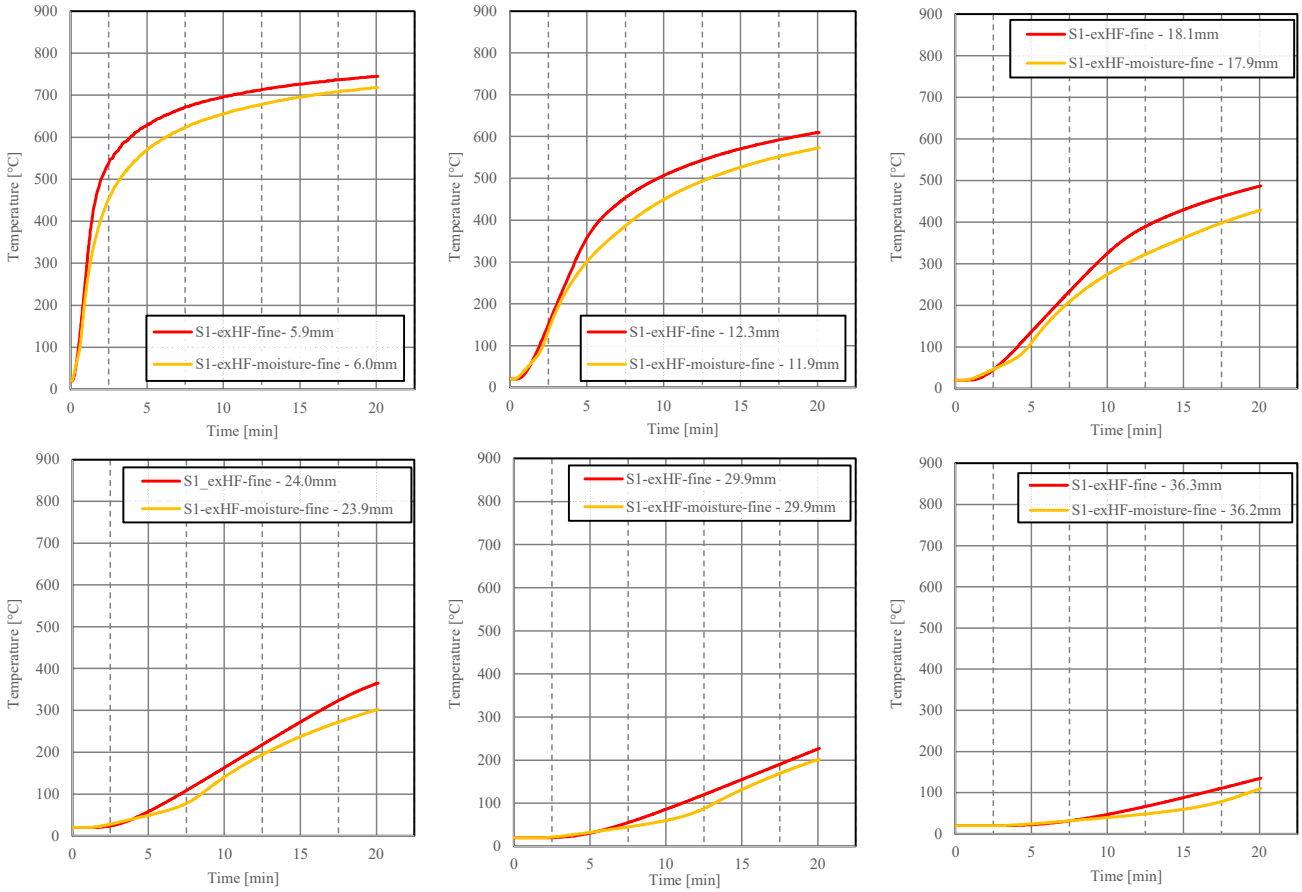

Graph 52: Comparison of temperature recordings inside the wood sample for "S1-exHF-fine" & "S1-exHF-moisture-fine"

As expected, the comparison shows higher values for the case with dry timber than for the one with moisture content.

The comparison for the simulations with ignition by a heat panel show similar results and lead to the same conclusion. The comparison is shown in Appendix H.

5.3.3 Char properties

The following table compares the charring depth and the charring rate for the four simulations.

Table 38: Charring depth and rate for simulations "S1-exHF-fine", "S1-exHF-moisture-fine", "S2-HP-fine" & "S2-HP-moisture-fine"

	Charring depth [mm]	***Charring rate [mm/min]***
S1-exHF-fine	26.5	1.33
S1-exHF-moisture-fine	23.9	1.20
S2-HP-fine	28.0	1.41
S2-HP-moisture-fine	25.4	1.28

In agreement with the lower temperatures for the simulation with moisture content, the charring depth and rate are also lower for the simulation with moisture.

The next graphs compare the progression of the charring front through the timber sample by the 300°C-ISO profile for the four simulations.

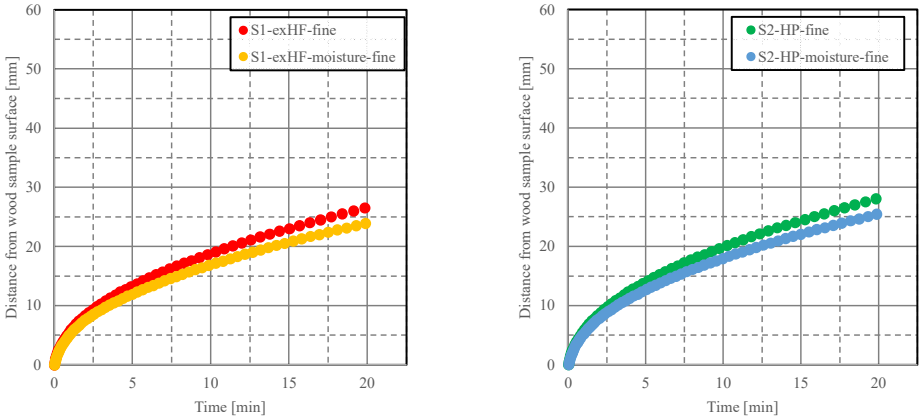

Graph 53: 300°C-ISO profile for simulations "S1-exHF-fine" & "S1-exHF-moisture-fine" (left) and for "S2-HP-fine" & "S2-HP-moisture-fine" (right)

The behaviour for the charring front is logarithmic for all four simulations and in agreement with the other previous comparisons: timber with moisture content shows a slower charring progression than dry timber.

5.3.4 Simulation time

Table 39 compares the simulation times. All simulations were run on the same HPC cluster and with the same number of meshes.

Table 39: Simulation time for "S1-exHF-fine", "S1-exHF-moisture-fine", "S2-HP-fine" and "S1-HP-moisture-fine"

	Simulation time
S1-exHF-fine	24 [h] 38 [min]
S1-exHF-moisture- fine	38 [h] 31 [min]
S2-HP-fine	35 [h] 33 [min]
S2-HP-moisture-fine	37 [h] 17 [min]

The simulation with the included moisture content had around 1.6 times longer simulation time than the simulation with ignition by an external heat flux. For the simulation type with ignition by a heat panel the difference is very small. Also, the comparison between both simulations with moisture content shows only a small difference.
As a summary, it seems that in simulations with relatively simple heat transfers, the addition of moisture content remarkably increases the simulation time but if the simulation without water has already more time-consuming heat transfers included, the addition of the moisture content does not lead to a huge increase of the simulation time.

5.3.5 Summary

As was to be expected, the simulation with a timber sample containing some moisture leads to slower HRR, a lower temperature profile inside the solid, a shorter charring depth and a slower charring rate, because of the presence of water.
Adding moisture into the timber also leads to a decrease in the sample thickness instead of a swelling of the material seen in the other simulations. The results from the simulations with moisture includes is closer to what would be expected in reality.
The usefulness of the addition of a moisture content into the simulation will be assessed in the comparison with the experimental data (5.5 “Comparison with the experimental results”).

5.4 Influence of temperature dependent specific heat against a constant on the results

This section compares the simulation with a temperature dependent specific heat ("S1-exHP-fine") with the simulation where constant specific heat values were defined ("S1-exHP-cp-fine"). The simulation situation used an ignition by an external heat flux.

5.4.1 HRR

Graph 54 compares the HRR for the two simulations. The two adjacent tables show some key quantities from this graph (table 40 & 41).

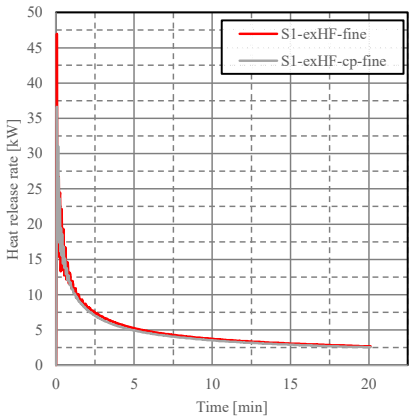

Graph 54: HRR for the simulations "S1-exHF-fine" & "S1-exHF-cp-fine"

Table 40: Release heat over simulation time for "S1-exHF-fine" & "S1-exHF-cp-fine"

	Released heat over simulation time [MJ]
S1-exHF-fine	5.9
S2-HP-cp-fine	5.6

Table 41: Key quantities from graph 54

	Peak [kW]	***Time to peak [s]***	***HHR at simulation end [kW]***	***Mean [kW]***
S1-exHF-fine	47.0	4.8	2.7	4.9
S2-HP-cp-fine	32.0	6.0	2.3	4.3

The simulation with constant specific heat for spruce and char leads to less heat being released and to a lower peak with a faster decrease afterwards than the simulation with temperature-dependent values. This seems reasonable, as the constant specific heats were values for higher temperatures.

5.4.2 Temperature measurements inside the timber sample

The next six graphs show the comparison of the temperature inside the timber sample for the two simulations. The depths are ca. 6 [mm], 12 [mm], 18 [mm], 24 [mm], 30 [mm] and 36 [mm].

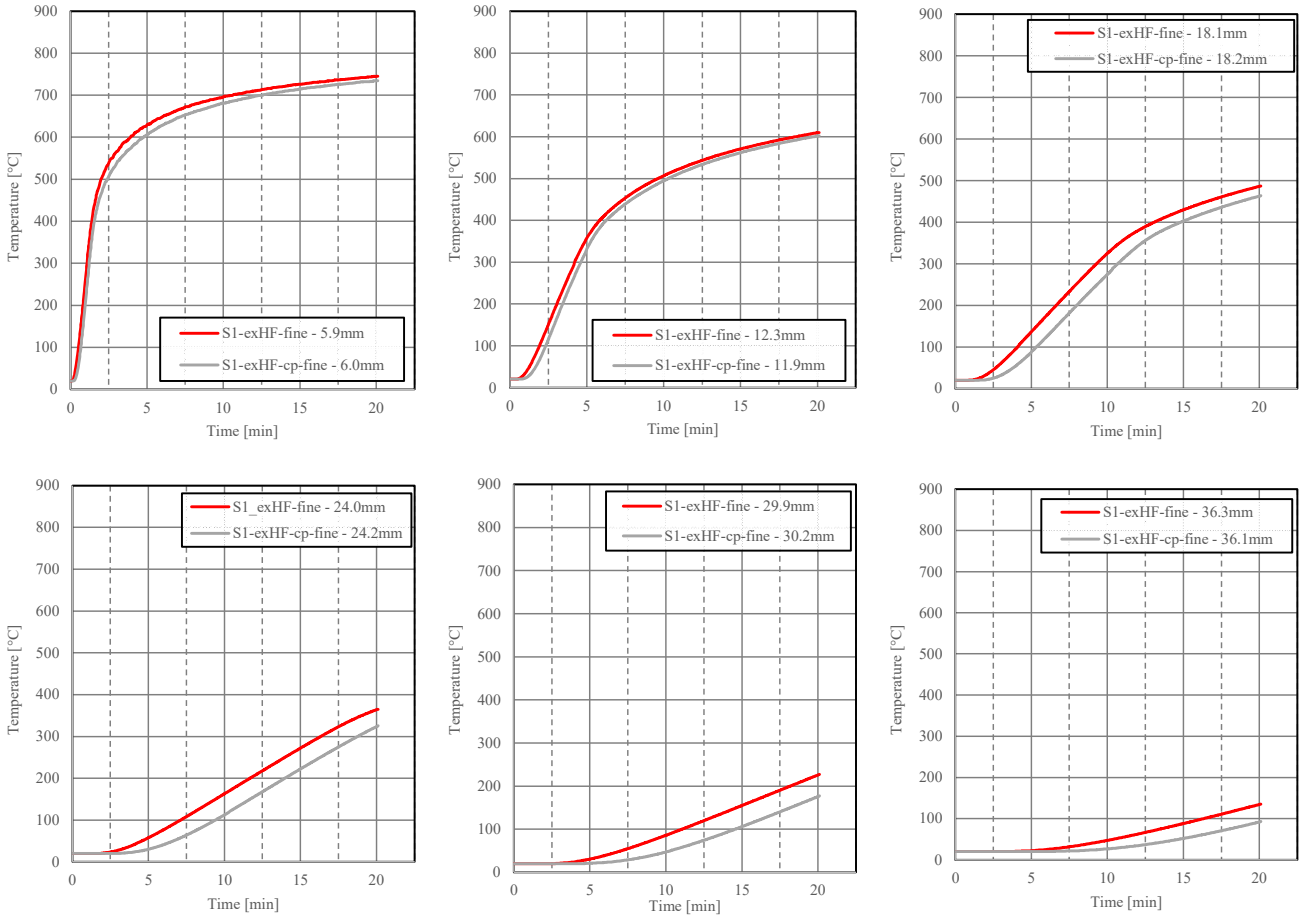

Graph 55: Comparison of temperature recordings inside the timber sample for "S1-exHF-fine" & "S1-exHF-cp-fine"

Both simulations show the same behaviour of the temperature evolution but the simulation with constant specific heat values shows lower temperature values than the other one. This is also in agreement with what have been observed in the HRR profiles.

5.4.3 Char properties

The following table compares the charring depth and the charring rate for the two simulations.

Table 42: Charring depth and rate for "S1-exHF-fine" & "S1-exHF-cp-fine"

	Charring depth [mm]	***Charring rate [mm/min]***
S1-exHF-fine	26.5	1.33
S1-exHF-cp-fine	24.9	1.25

The charring depth and rate for the simulation with constant specific heat is smaller than for the other simulation as would be expected from the previous results.

The next graph compares the progression of the charring front through the wood sample by the 300°C-ISO profile for the four simulations.

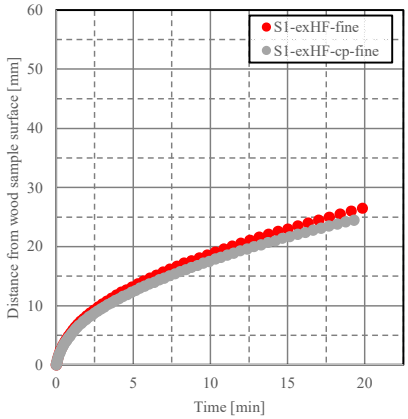

Graph 56: 300°C-ISO profile for "S1-exHF-fine", & "S1-exHF-cp-fine"

The behaviour for the charring front shows a logarithmic progression in both simulations and again, the simulation with constant specific heat values has a smaller charring rate.

5.4.4 Simulation time

Table 43 compares the simulation times. Both simulations were run on the same HPC cluster and with the same number of meshes.

Table 43: Simulation time for "S1-exHF-fine" & "S1-exHF-cp-fine"

	Simulation time
S1-exHF-fine	24 [h] 38 [min]
S2-HP-cp- fine	28 [h] 05 [min]

The simulation with the constant specific heat values showed around 1.1 times longer simulation time than the simulation with temperature dependent values.

5.4.5 Summary

Using constant specific heat values instead of temperature dependent values lead to lower HRR, lower temperature profiles inside the timber sample, a lower charring depth and a slower charring rate. The reason for this seems to be the choice of the constant specific heat values which were for higher temperatures.

In the standard simulations, temperature dependent specific heat values for spruce and char were used as found in the literature. Defining such values as constants adds some subjectivity to these parameters, unless some information is present about the most appropriate mean temperature for the simulation situation. If such information is unavailable, then a sensitivity study should be run to define the most adequate temperature for defining the specific heat as constant. In such cases, the effort needed to find an appropriate constant specific heat seems bigger than directly defining the value as temperature dependent in FDS.

The usefulness of the two definitions of the specific heat is discussed in the comparison with the experimental data (5.5 “Comparison with the experimental results”).

5.5 Comparison with the experimental results

This chapter compares the standard simulations with the fine mesh resolution inside the timber sample with the experimental data. First, the comparison of the air velocity measurements above the timber sample is shown, followed by the gas temperature measurements in the tunnel, the surface temperature measurements on the timber sample, the temperature measurements inside the timber sample and finally, the comparison of the charring depth and rate as well as the charring progression.

5.5.1 Air velocity measurements over the timber sample

Graph 57 shows the comparison between the air velocity measurements above the timber sample and the adjacent table 44 the mean values over the whole simulation time.

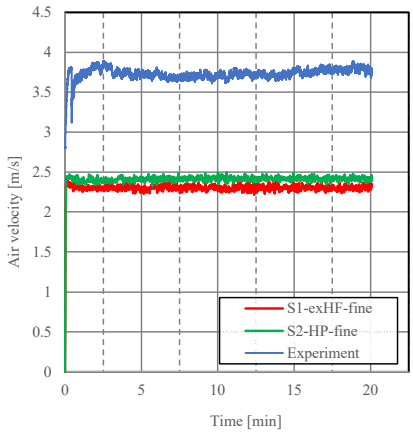

Graph 57: Comparison of the air velocity measurements above the timber sample for "S1-exHF-fine" & "S2-HP-fine" and the experiment

Table 44: Mean air velocities for "S1-exHF-fine" & "S2-HP-fine" and the experiment

	Mean air velocity [m/s]
S1-exHF	2.3
S2-HP	2.4
Experiment	3.7

The comparison shows again a lower value for the mean air velocity in the simulations than for the experiment (cf. “3.5.4 Air velocity measurements over the timber sample”). Comparing the mean values with the ones from the simulations “S1-exHF-coarse” and “S2-HP-coarse” (table 13) shows the same values and also a comparison by graph shows very similar values as can be seen in graph 58.

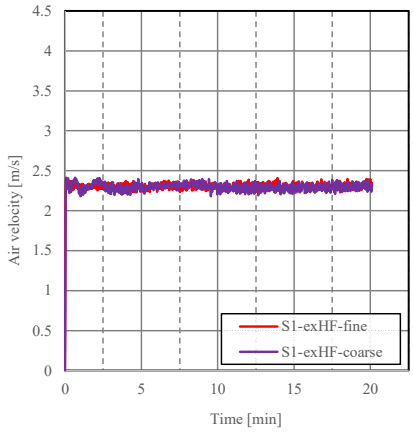

Graph 58: Comparison between air velocity above the timber sample for "S1-exHF-fine" & "S1-exHF-coarse"

The change in mesh resolution inside the solid material did not lead to an amelioration of the simulations results for the air velocity measurements above the timber sample.

5.5.2 Gas temperature measurements

The following three graphs compare the gas temperatures at the start, the end and behind the fire chamber.

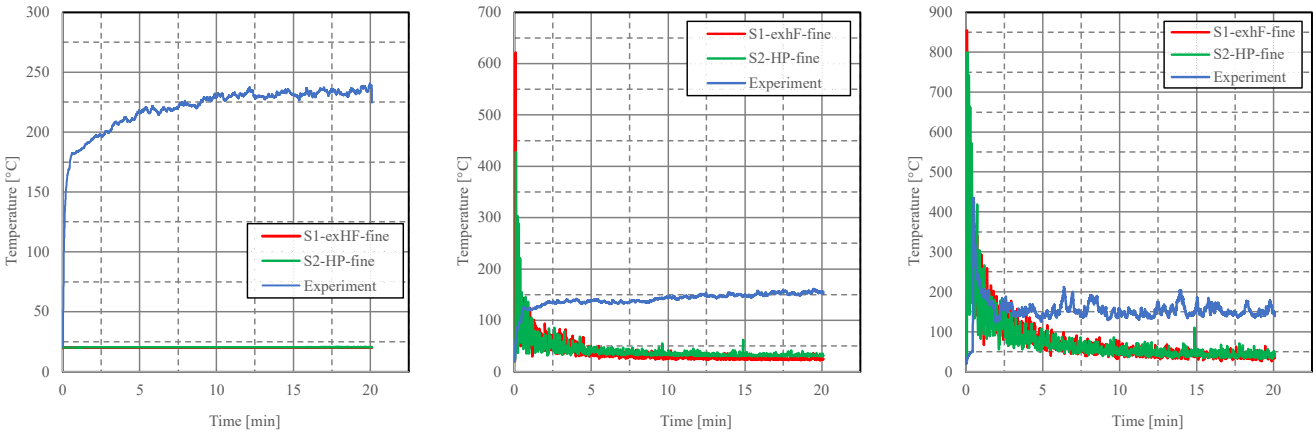

Graph 59: Gas temperatures at the start of the fire chamber (left), at the end of the fire chamber (middle) and behind the fire chamber (right) for "S1-exHF-fine" & "S2-HP-fine" and the experiment

First of all, the simulation now reflects the continuous burning instead of a flickering of the flames (graph 6), which is in general more in agreement with the experimental data. However, the values differ a lot. The difference in temperature measurements at the start of the fire chamber could maybe be due to the difference in the definition of the air flow. In the simulation air was pushed through the tunnel, but in the experiment, it had been pulled through. Maybe the pulling of the air resulted in a stagnation zone before the fire, whereas the pushing in the simulation moved the heat away. The difference for the other two graphs could be caused by the simplified pyrolysis

reaction in the modelling. Another reason could be the not very fine mesh resolution for the fluid which could potentially affect the gas temperature measurements.

5.5.3 Surface temperature measurements

The next two graphs show the comparison of the surface temperature measurements over the simulation time and table 45 summarizes the mean surface temperatures from the graphs.

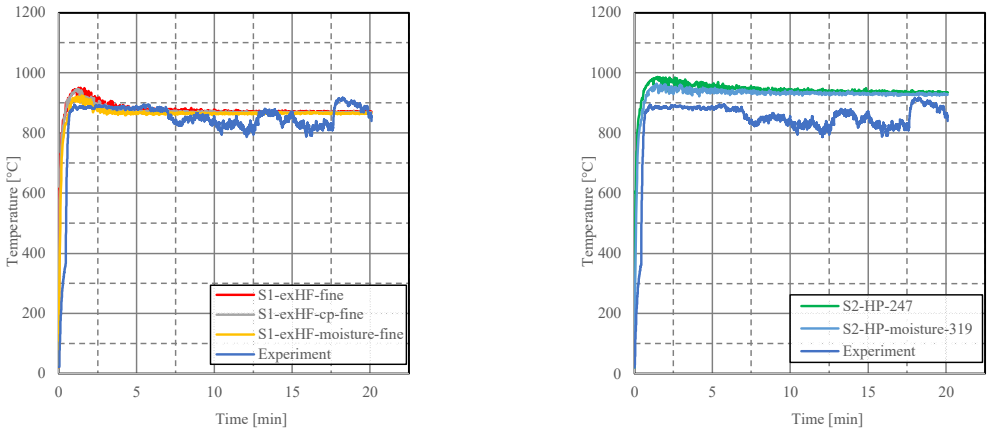

Graph 60: Comparison of the surface temperature measurements between the experiment & the simulation environment with ignition by an external heat flux (left) and between the experiment & the simulation environment with ignition by a heat panel (right)

Table 45: Mean surface temperatures for the experiment and all the simulations

	Mean surface temperature [°C]	***Percentage***
S1-exHF-fine	876.3	105%
S1-exHF-moisture-fine	863.6	103%
S1-exHF-cp-fine	871.1	104%
S2-HP-fine	940.7	113%
S2-HP-moisture-fine	926.7	111%
Experiment	834.7	100%

The comparison of the mean values shows very similar surface temperatures in the experiment as well in the simulations. The values for the simulation environment with ignition by a heat panel shows slightly higher values. The modifications of the standard cases do not lead to a huge change in the results compared to the experimental values.

5.5.4 Temperature measurements inside the timber sample

The following six graphs compare the simulated temperatures inside the timber sample for the simulation environment with ignition by the external heat flux with the ones measured in the experiments for depths of ca. 6 [mm], 12 [mm], 18 [mm], 24 [mm], 30 [mm] and 36 [mm] from the timber surface.

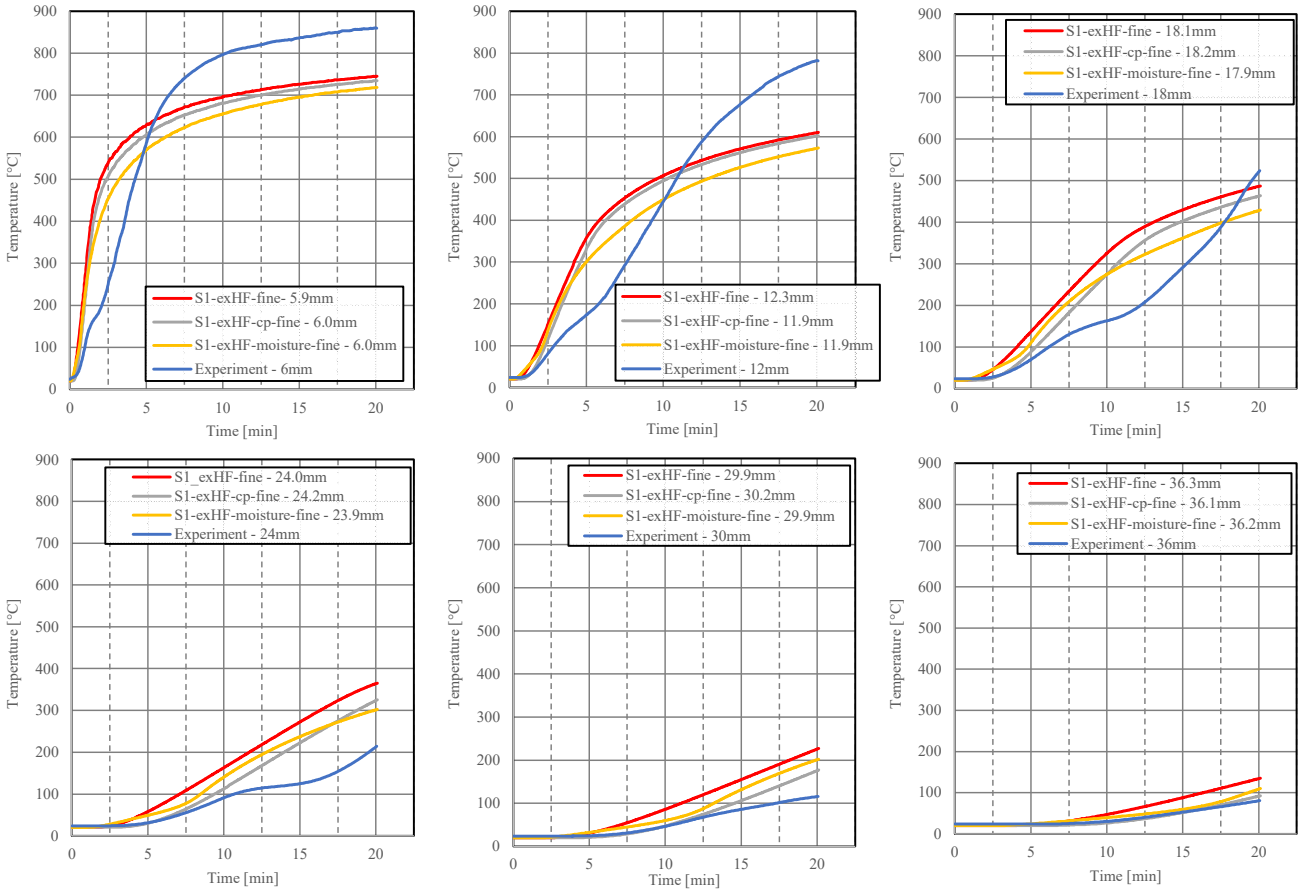

Graph 61: Comparison of temperature recordings inside the timber sample for "S1-exHF-fine", "S1-exHF-cp-fine", "S1-exHF-moisture-fine" and experiment

The comparison shows that the simulation temperature recordings close to the surface result in lower temperatures than those measured in the experiment. At a depth of 18 [mm], the simulation and experimental results end in a similar temperature range. At deeper measuring positions inside the timber sample, the simulations show higher temperatures than the experiment. The reasons for this could be diverse, and might be related to the simplified definition of the charring process, but also the manner in which temperatures were recorded during the experiment, as installing and measuring temperatures inside timber samples during experiments is a complex task.

The comparison between the experimental results and the simulations with the ignition by a heat panel gives the same result and is shown in Appendix I.

5.5.5 Char properties

Table 46 compares the charring depth and rate for the all the simulations and the experiment.

Table 46: Charring depth and rate for all simulations and experiment

	Charring depth [mm]	***Charring rate* [mm/min]**
S1-exHF-fine	26.5	1.33
S1-exHF-moisture-fine	23.9	1.20
S1-exHF-cp-fine	24.9	1.25
S2-HP-fine	28.0	1.41
S2-HP-moisture-fine	25.4	1.28
Experiment	18.0	1.28

The comparison shows that all the results for the charring rates being very close to the experimental value. For the charring dept, the differences are much bigger, between 1.3 and 1.6 times bigger than in the experimental result. There is a possibility that this might be caused by the way the temperatures were recorded in the simulation. In the simulations, direct temperature recordings are done, but in the experiment different types of thermocouples were used, delaying the temperature recording. However, this difference should not affect the charring rate as this was the ratio between the charring depth and the corresponding time to reach that depth.

The next graph compares the progression of the charring front through the timber sample by the 300°C-ISO profile for the three simulations with the ignition done by an external heat flux and the experimental data. The right graph is the result from the experimental analysis with the linear regression from Felder [graph adapted from 31, Fig. 5.2.(b)].

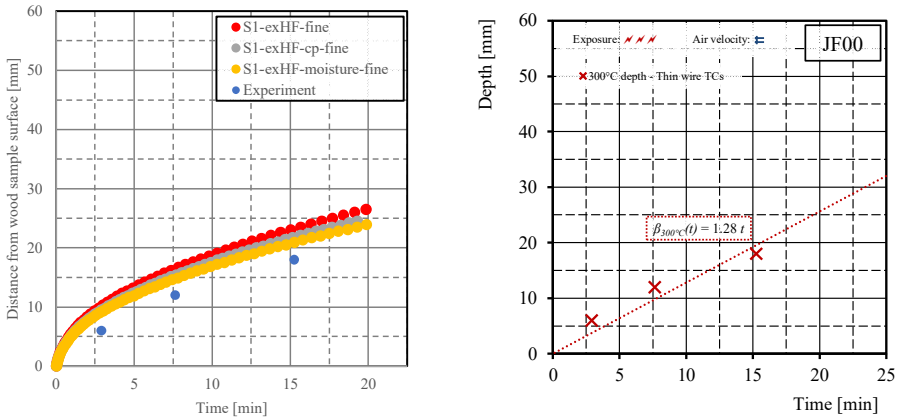

Graph 62: 300°C-ISO profile for the simulations "S1-exHF-fine", " S1-exHF-cp-fine", " S1-exHF-moisture-fine" and the experiment (left) and linear regression for experimental values (right)

The main difference here is the way the charring progresses. In the experiment, a linear progression can be assumed. However, the data points in the simulations show a logarithmic behaviour.

The comparison between the experimental results and the simulations with the ignition by the heat panel gives the same result and is shown in Appendix I.

5.5.6 Summary

As a summary, all the simulations showed reasonably good agreement in terms of surface temperature recordings and charring rates. The charring depth was deeper for all simulation compared to the experiment. The temperature profile inside the timber sample for the simulations and the experiment showed some differences in terms of temperature progression inside the material. However, the gas temperature measurements and the air velocity measurements did not correspond well with the experiment. Reasons for this could be the not fine enough mesh resolution for the fluid or maybe the definition of the air flow inside the tunnel, which have been pushed instead of pulled through.

The standard situation with ignition by an external heat flux resulted in less differences compared to the experimental values than the simulations with ignition by a heat panel. Modifying the standard cases led to lower charring values but the difference with the standard cases were relatively small. As the simulation times were much longer, this slight improvement seems not to be justified. Therefore, for studying the charring depth and charring rate, the standard cases seem to be enough.

However, these standard simulations could also be too simplistic. For example, all the simulations for dry timber led to a swelling of the material because of the simplicity of the pyrolysis model. Reality is more complex and all the processes together result rather in a surface recession. Defining a more detailed pyrolysis process by adding the moisture content to the timber sample changed the simulation result and the sample now shrunk.

5.6 Limitations of the study and further test options

This section discusses the limitations and further test options for the chosen pyrolysis model, for the simulation parameters and for the analysis method. The section finishes with some other additional test options.

5.6.1 Pyrolysis model

The presented simulations used only a one-step global reaction scheme where timber was considered as a lumped product. Another way to define the timber sample would be by its main components, cellulose, hemicellulose and lignin and by using a one-step multi-reaction. The opinion in the literature about how complex a pyrolysis reaction scheme should be to give adequate results is inconsistent. Some researcher concluded that a single reaction scheme is enough for the prediction of the heat release rate and mass loss rate [23], [35]. However, for example, Ding et al. [36] found three parallel reactions are needed for accurate results. Given this inconsistency, a further test option could be to test a one-step multi-reaction with the main components of wood and assess if it is leading to more accurate results compared to the experimental data for the simulated situation.

Moreover, a simple reaction scheme also defines what kind of charring properties can be studied. For example, the simulation with dry timber resulted in a swelling of the sample. This was due to the fact that char has a lower density and that the model assumed conservation of mass [21], [22]. In such simulations, studying the thickness of the charred timber sample would not make sense. Adding the moisture content to the simulation allowed the timber sample to shrink. Therefore, if the goal of the simulation is to study the char layer recession, then secondary reactions should be added into the pyrolysis model.

According to Nyazika et al. [13], one of the most influencing input parameters are the thermophysical properties of the timber sample, but also a key player on the mass loss rate is the heat of pyrolysis and reaction rate. On the other hand, the study from Alonso et al. [37] identified the factors as activation energy, pre-exponential factors and reaction order as being those that influence the pyrolysis model in FDS. Sinha et al. [9] defined thermal conductivity and heat capacity as the most influencing parameters. All of these results and the fact that sensitivity analysis results are model and case dependent to some extent [34] stress the importance for a more in-depth sensitivity analysis on the input parameters of the simulations in this study.

5.6.2 Simulation parameters

This study focused, amongst other themes, on the influence of the mesh resolution inside the timber sample. FDS has another mesh, the one for the fluid. In this study, this mesh was solely defined by a flow field analysis. However, this may not be fine enough for the flaming combustion and the heat feedback between the pyrolysis and flames. Especially if only 15 cells are defining

the height of the tunnel. Therefore, after having found an appropriate mesh size for the solid material, another mesh sensitivity study for the fluid should be run refining the fluid mesh.

5.6.3 Analysis

The position of the recordings inside the wood sample change constantly and very slightly over the simulation time. This is due to the fact that FDS is repositioning them depending on the changing thickness of the material, due to shrinking and swelling of the material. This leads to the addition or removal of layers if the thickness changes too much to keep the number of layers constant for a given spacing. The amount of change depends on the defined pyrolysis model and the spacing between the layers given by the mesh resolution inside the timber sample. For the graphs and the tables shown in this study, a time averaged value for the position was used.
The charring properties in this work are presented with the 300°C-ISO profile. FDS also has the option to record the density of the whole material or of each defined material in the simulation. Such density outputs were also recorded in all the presented simulations in this study (3.5.1 “Implementation”). This data could be used in a further study to analyse the position of the charring depth and hence define the charring rate. Comparing these results with the ones presented in this work could give more inside into the pyrolysis model.
The temperature measurements in the simulations are done by normal temperature recordings. However, the experiment used thermocouples. For a further study, thermocouples instead of temperature measurements could be included into the FDS code given enough information for the simulation implementation are available. This would allow to compare the temperature results more directly.

5.6.4 Other additional test options

A lot of different experiments were performed with the FANCI-setup. For example, experiments with different incident heat flux. In the standard simulation with ignition by an external heat flux such modifications can also be easily simulated, the result analysed and then compared with the experimental data. If the results are reasonably close to the experimental results the simulations could even be used to predict charring properties.

6 Conclusions

The main finding of this work is the importance of an appropriate mesh resolution inside the solid for studying charring properties in timber. The addition of moisture to the pyrolysis model resulted in lower HRR, lower temperatures recordings, a lower charring depth and a slower charring rate as would be expected. It also led to a shrinking of the material's thickness instead of the observed swelling in the simulation results without a moisture content. The use of constant specific heat values instead of temperature dependent ones also led to slightly lower and slower results. This appears to be due to the manner in which the constant values were defined and therefore, shows a user and input data dependency of the simulations. Compared to the experimental results, the modifications in the simulation situations did not lead to huge different outputs compared with the experiment. Therefore, if the focus is only on charring depth and charring rate, the resulting longer simulation time is not justified.
The comparison with the experimental results showed relatively good agreement in terms of charring rate and surface temperature measurements. However, the charring depth was overestimated in all the simulations and the parameter linked to the gaseous phase – like air velocity and gas temperature measurements – did not correspond well with the experimental data. Further studies should be performed to improve these simulation results. For example, a mesh sensitivity study for the gaseous phase during combustion.
The charring parameters were studied on the basis of the temperature profile inside the timber sample, another approach would be to use the density outputs from the simulations.

It should also be noted, that the way the pyrolysis model is defined also setups what kind of output parameters can be studied. For a study of the surface recession during the combustion of timber, a more complex pyrolysis model is needed, including, for example char oxidation.

Simulations are a cheap way to test different environments and situations. However, the findings cannot go beyond the limitations of the model and are dependent upon the simulation situation and the accuracy of the input data. The model also has to be validated with experimental data. Once this is done, it can be used to test different intensities of input parameters, for example, as in the FANCI-experiment to test different incident heat fluxes on the burning process.

At the moment simulating pyrolysis with FDS needs many input parameters and iterative testing and therefore, it is not practical as an everyday tool. With more studies, a better understanding and more efficient work ways will result. The disadvantage of the complexity of CFD simulation with all its submodels and interlinked processes (compared for example to two-zone models) is also their great advantage for studying complex processes like the burning of timber. A FDS simulation gives the user the capability to start with a relatively simple model, then add more processes and perform tests to discover which are the most important processes and parameters and subsequently simplifying everything ending up with an efficient tool.

Acknowledgments

I would like to thank my supervisors for their advice, help and support.

Prof. Dr. Bart Merci for the supportive discussions and the constructive comments on my work.

Prof. Dr. Andrea Frangi for his help broadening my view on timber constructions and the importance of charring properties.

Chamith Karannagodage for the discussion about the challenges of timber burning and his supportive comments during my work.

Dr. Andrea Lucherini for the helpful comments and additional point of view.

Dr. Georgios Maragkos for his help with the simulation environment and his useful remarks.

I would also like to thank Dr. Joachim Schmid for the provision of the experimental data from the FANCI experiment and the additional explanations, as well as, Miriam Kleinhenz for the helpful discussions about the structure of my report and for all the help with solving computer issues.

I also kindly thank Johanna Saladin-Michel for the administration help during my stay at ETH Zürich and the whole IBK group for kindly welcoming me into their group.

Finally, also a huge thank to family and friends for the report revision and supporting me during this work.

References

[1] S. Deeny, B. Lane, R. Hadden, and A. Laurence, “Fire Safety Design in Modern Timber Buildings,” *Struct. Eng. J. Inst. Struct. Eng.*, vol. 96, no. 1, pp. 48–53, 2018.

[2] B. Östman, D. Brandon, and H. Frantzich, “Fire safety engineering in timber buildings,” *Fire Saf. J.*, vol. 91, no. May, pp. 11–20, 2017, doi: 10.1016/j.firesaf.2017.05.002.

[3] J. Schmid and A. Frangi, “Structural timber in compartment fires – the timber charring and heat storage model,” *Open Eng.*, vol. 11, no. 1, pp. 435–452, 2021, doi: 10.1515/eng-2021-0043.

[4] F. Richter, F. X. Jervis, X. Huang, and G. Rein, “Effect of oxygen on the burning rate of wood,” *Combust. Flame*, vol. 234, p. 111591, 2021, doi: 10.1016/j.combustflame.2021.111591.

[5] V. Šálek, K. Cábová, F. Wald, and M. Jahoda, “Numerical modelling of fire test with timber fire protection,” *J. Struct. Fire Eng.*, vol. 13, no. 1, pp. 99–117, 2022, doi: 10.1108/JSFE-04-2021-0017.

[6] C. Wade, M. Spearpoint, C. Fleischmann, G. Baker, and A. Abu, “Predicting the Fire Dynamics of Exposed Timber Surfaces in Compartments Using a Two-Zone Model,” *Fire Technol.*, vol. 54, no. 4, pp. 893–920, 2018, doi: 10.1007/s10694-018-0714-2.

[7] EN 1995-1-2, Eurocode 5, “Design of timber structures. Part 1-2 General – Structural fire design", European standard, CEN, Brussels , 2004.

[8] C. Di Blasi, “Modeling and Simulation of Combustion Processes of Charring and Non-Charring Solid Fuels,” *Prog. Energy Combust. Sci.*, vol. 19, pp. 71–104, 1993.

[9] S. Sinha, A. Jhalani, M. Ravi, and A. Ray Chaudhury, “Modelling of pyrolysis in wood: a review,” *SESI J.*, vol. 10, no. 1, pp. 41–62, 2000.

[10] L. Shi and M. Y. L. Chew, “A review of thermal properties of timber and char at elevated temperatures,” *Indoor Built Environ.*, vol. 0, no. 0, pp. 1–16, 2021, doi: 10.1177/1420326X211035557.

[11] C. Gorska Putynska, “Fire Dynamics in Multi-Scale Timber Compartments,” *Diss. PHD Thesis, Univ. Queensl.,* Brisbane, 2019.

[12] B. Moghtaderi, “The state-of-the-art in pyrolysis modelling of lignocellulosic solid fuels,” *Fire Mater.*, vol. 30, no. 1, pp. 1–34, 2006, doi: 10.1002/fam.891.

[13] T. Nyazika, M. Jimenez, F. Samyn, and S. Bourbigot, “Pyrolysis modeling, sensitivity analysis, and optimization techniques for combustible materials: A review,” *J. Fire Sci.*, vol. 37, no. 4–6, pp. 377–433, 2019, doi: 10.1177/0734904119852740.

[14] A. I. Bartlett, R. M. Hadden, and L. A. Bisby, “A Review of Factors Affecting the Burning Behaviour of Wood for Application to Tall Timber Construction,” *Fire Technol.*, vol. 55, no. 1, pp. 1–49, 2019, doi: 10.1007/s10694-018-0787-y.

[15] F. S. Forest Products Labarotary, “Theories of the combustion of wood and its control,” United States Departtment of Agriculture, *Rep. 2136*, December, 1958, Available: https://ir.library.oregonstate.edu/downloads/3r0%0A74z89g.

[16] A. Buchanan, B. Östman, A. Frangi, *White paper on fire resistance of timber structures*,Us Departtment of Comerce, National Institute of Standards and Technology, 2014.

[17] M. J. Spearpoint and J. G. Quintiere, “Predicting the burning of wood using an integral model,” *Combust. Flame*, vol. 123, no. 3, pp. 308–325, 2000, doi: 10.1016/S0010-2180(00)00162-0.

[18] A. Rinta-Paavola and S. Hostikka, “A model for pyrolysis and oxidation of two common structural timbers,” pp. 1–10, 2019.

[19] F. Richter and G. Rein, “Heterogeneous kinetics of timber charring at the microscale,” *J. Anal. Appl. Pyrolysis*, vol. 138, no. August 2018, pp. 1–9, 2019, doi: 10.1016/j.jaap.2018.11.019.

[20] Y. Z. Li, *CFD modelling of fire development in metro carriages under different ventilation conditions*. 2015.

[21] K. McGrattan, S. Hostikka, R. McDermott, J. Floyd, C. Weinschenk, and K. Overhold, “Fire Dynamics Simulator User ’s Guide (FDS),” *NIST Spec. Publ. 1019*, Sixth Edition, pp. 1-378, 2020.

[22] K. McGrattan, S. Hostikka, R. McDermott, J. Floyd, C. Weinschenk, and K. Overholt, “Fire Dynamics Simulator Technical Reference Guide Volume 1 : Mathematical Model,” *NIST Spec. Publ. 1019,* Sixth Edition, pp. 1–147, 2015.

[23] A. Rinta-Paavola and S. Hostikka, “A model for the pyrolysis of two Nordic structural timbers,” *Fire Mater.*, vol. 46, no. 1, pp. 55–68, 2022, doi: 10.1002/fam.2947.

[24] M. Chaos, “Spectral aspects of bench-scale flammability testing: Application to hardwood pyrolysis,” *Fire Saf. Sci.*, vol. 11, pp. 165–178, 2014, doi: 10.3801/IAFSS.FSS.11-165.

[25] K. W. Ragland, D. J. Aerts, and A. J. Baker, “Properties of wood for combustion analysis,” *Bioresour. Technol.*, vol. 37, no. 2, pp. 161–168, 1991, doi: 10.1016/0960-8524(91)90205-X.

[26] B. Frelund, “A model for heat and mass transfer in timber structures during fire: A theoretical, numerical and experimental study,” *PhD Thesis, Lund University*, 1988.

[27] M. J. Hurley *et al.*, “SFPE handbook of fire protection engineering, fifth edition,” *SFPE Handb. Fire Prot. Eng. Fifth Ed.*, pp. 1–3493, 2016, doi: 10.1007/978-1-4939-2565-0.

[28] M. J. Hurley *et al.*, *SFPE Handbook of Fire Protection Engineering*, Fifth edit. Springer New York, 2016.

[29] J. Faouel, F. Mzali, A. Jemni, and S. Ben Nasrallah, “Thermal conductivity and thermal

diffusivity measurements of wood in the three anatomic directions using the transient hot-bridge method," *Spec. Top. Rev. Porous Media*, vol. 3, no. 3, pp. 229–237, 2012, doi: 10.1615/SpecialTopicsRevPorousMedia.v3.i3.50.

[30] "The Physics Hypertextbook," [Online]. Available https://physics.info/viscosity/ [Accessed: 05-May-2022].

[31] J. Felder, "Timber Members in Natural Fires - Influencing Parameters in Decay Phase," 2019.

[32] FDS6, "birch_tga_1step_20.fds," *Example code in FDS software*.

[33] A. Demirbas, "Effects of moisture and hydrogen content on the heating value of fuels," *Energy Sources, Part A Recover. Util. Environ. Eff.*, vol. 29, no. 7, pp. 649–655, 2007, doi: 10.1080/009083190957801.

[34] K. Moinuddin, Q. S. Razzaque, and A. Thomas, "Numerical simulation of coupled pyrolysis and combustion reactions with directly measured fire properties," *Polymers (Basel).*, vol. 12, no. 9, 2020, doi: 10.3390/POLYM12092075.

[35] S. Hostikka and A. Matala, "Pyrolysis model for predicting the heat release rate of birch wood," *Combust. Sci. Technol.*, vol. 189, no. 8, pp. 1373–1393, 2017, doi: 10.1080/00102202.2017.1295959.

[36] Y. Ding, K. Fukumoto, O. A. Ezekoye, S. Lu, C. Wang, and C. Li, "Experimental and numerical simulation of multi-component combustion of typical charring material," *Combust. Flame*, vol. 211, pp. 417–429, 2020, doi: 10.1016/j.combustflame.2019.10.016.

[37] A. Alonso, M. Lázaro, P. Lázaro, D. Lázaro, and D. Alvear, "Assessing the influence of the input variables employed by fire dynamics simulator (FDS) software to model numerically solid-phase pyrolysis of cardboard," *J. Therm. Anal. Calorim.*, vol. 140, no. 1, pp. 263–273, 2020, doi: 10.1007/s10973-019-08804-6.

[38] "Engineering ToolBox," [Online]. Available: https://www.engineeringtoolbox.com/air-absolute-kinematic-viscosity-d_601.html [Accessed: 05-May-2022]

[39] J. De Saedeleer, "Fire Safety and Legislation - lecture 2," *Lecture, University Ghent*, Fall semester 201/2022.

Appendix A – List of graphs, tables, figures and equations

A.1 List of graphs

A.2 List of tables

A.3 List of figures

Appendix B – Mesh size study

This chapter describes the test series to define the mesh size for the fluid. This is done by studying the influence of the mesh size on the air velocity and on the length of the tunnel. The idea of the last point is that a shorter tunnel would allow to use a finer mesh, as it would take less computational time.

B.1 Simulation environment

Three mesh sizes were tested, 1.25 [cm], 1.0 [cm] and 0.625 [m], each of it in two simulation geometries. One of it was the whole FANCI tunnel with a length of 4.5 [m] and the second geometry was a shortened tunnel with a length of ca. 1.8 [m]. In this shortened tunnel, the timber sample was placed in the middle of the tunnel length.

During the tests, no burning was simulated but only the air flow through the tunnel, with an inlet velocity of 2.5 [m/s].

The simulations are named as shown in table 47.

Table 47: Simulation names of the performed simulations in this mesh size study

Simulation name	***Description***
T1-whole-1.25	Whole FANCI geometry, mesh size 1.25 [cm], only air flow
T2-whole-1.0	Whole FANCI geometry, mesh size 1.0 [cm], only air flow
T3-whole-0.625	Whole FANCI geometry, mesh size 0.625 [cm], only air flow
T4-short-1.25	Shortened FANCI geometry, mesh size 1.25 [cm], only air flow
T5-short-1.0	Shortened FANCI geometry, mesh size 1.0 [cm], only air flow
T6-short-0.625	Shortened FANCI geometry, mesh size 0.625 [cm], only air flow

B.2 Output parameters

There were three areas with air velocity measurement points. Nine measurement points were evenly distributed at the surface of the timber sample, nine others were positioned above the sample, in a parallel plan to it, and three were positioned at mid-height of the tunnel at the outlet.

Additionally, three cuts with animated velocity recordings were also recorded, one through the middle of each of the three axes in the tunnel.

The codes are shown under section B.4 FDS codes.

B.3 Results

The qualitative analysis of the simulation showed a similar flow field for all the simulations. Near the border of the tunnel, there was a range of lower air velocities compared to the middle of the tunnel. Additionally, variations in the air velocity measurements slightly increased along the tunnel (figure 18 & 19). Both geometries, the shorter and the longer tunnel, showed similar flow fields, but it seemed more stretched out for the longer tunnel (figure 18). Figure 18 shows the animated velocity outputs for the simulation with the whole FANCI geometry and a mesh size of 1.0 [cm] ("T2-whole-1.0"). The long tube is the tunnel, viewed from the side and with a vertical cut for the air velocity recordings. The flow direction is from left to right and the still is at 4.6 [min]. The scale for the velocity is from 0.0 – 3.83 [m/s]. The two grey rectangles are two areas which are enlarged in the smaller images below the tunnel. Figure 19 shows the same as figure 19 except this time, it is the result for the simulation with the shorter FANCI geometry ("T5-short-1.0"); the air velocity scale this time is from 0.0 – 3.63 [m/s].

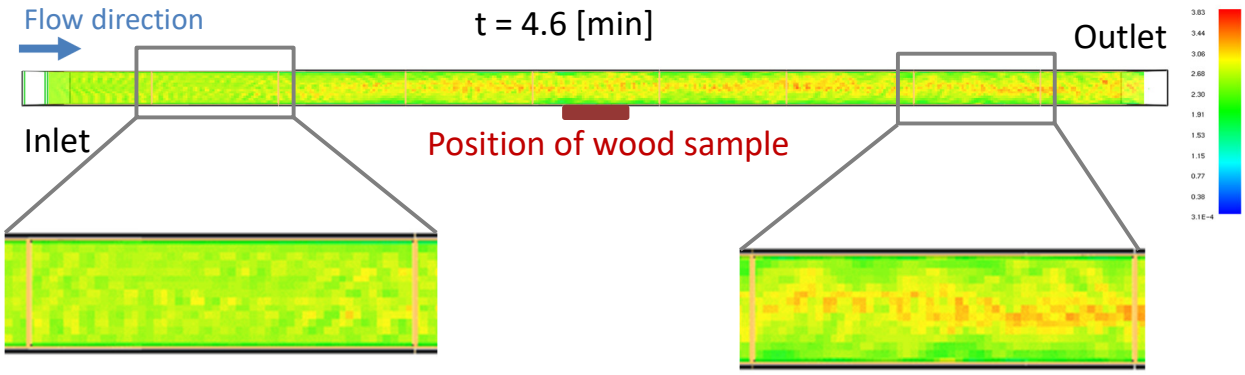

Figure 18: Result of the animated velocity output for simulation with the whole FANCI geometry and a mesh size of 1.0 [cm] ("T2-whole-1.0"); with a velocity scale of 0.0 - 3.83 [m/s] and a simulation time of the still of 4.6 [min]

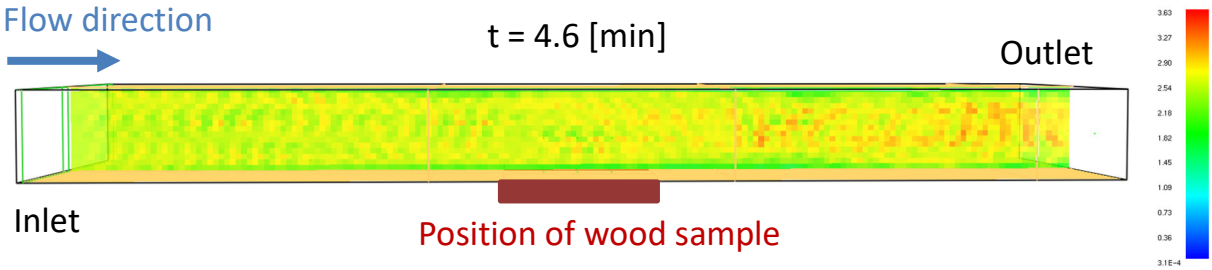

Figure 19: Result of the animated velocity output for simulation with the short FANCI geometry and a mesh size of 1.0 [cm] ("T5-short-1.0"); with a velocity scale of 0.0 - 3.63 [m/s] and a simulation time of the still of 4.6 [min]

For the shorter geometry, all the three simulations had air velocities in the same range, between 0.0 – 3.6 [m/s]. However, for the longer tunnel, there was a slightly bigger difference for the simulation with the finest mesh size. There the range was between 0.0 – 4.2 [m/s]. For the mesh size of 1.0 [cm] it was between 0.0 – 3.8 [m/s] and for the one with 1.25 [cm] it was a slightly smaller range, between 0.0 – 3.7 [m/s]. But generally, the variations in the flow field were not huge and given that no burning is happening at both ends of the tunnel, shortening the geometry seems reasonable.

For the quantitative analysis of the results, the air velocities in each area, meaning on the timber sample, above it and at the outlet, were averaged in time and space. The results can be seen in table 48 and are compared in the following graphs.

Table 48: Mean velocity in different areas of the simulations for the six simulations of the test series

Simulation name	***Area of measurements for the mean air velocity [m/s]***		
	Timber sample surface	*Above wood sample*	*Outlet*
T1-whole-1.25	2.1	2.7	2.8
T2-whole-1.0	2.0	2.9	2.9
T3-whole-0.625	1.8	2.7	3.0
T4-short-1.25	2.0	2.4	2.9
T5-short-1.0	2.0	2.7	2.8
T6-short-0.625	1.7	2.7	2.8

The following three graphs compare all the six simulations split by the mesh size, on the left side is the graph for a mesh size of 1.25 [cm], in the middle for 1.0 [cm] and on the right side for 0.625 [cm].

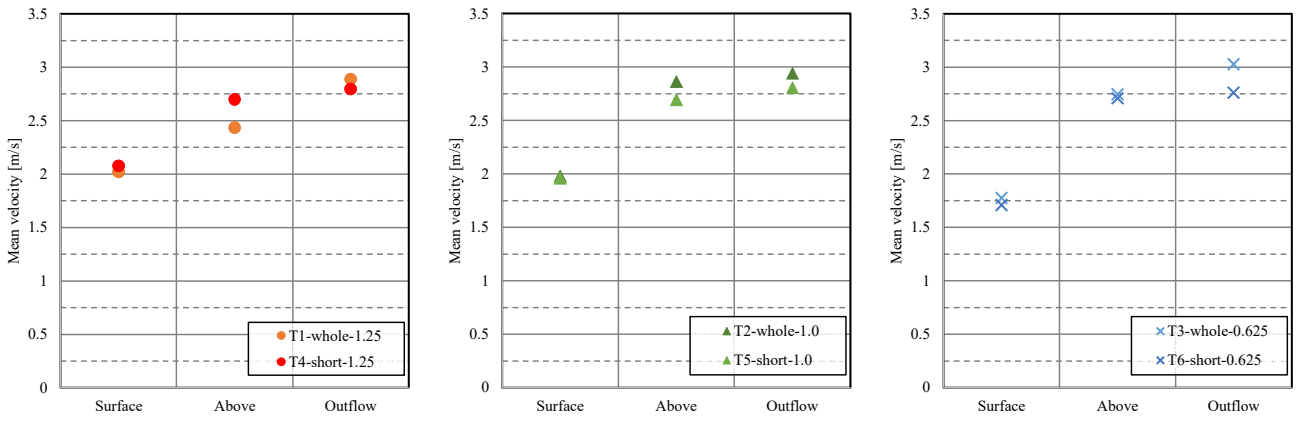

Graph 63: Mean velocities for the six simulations, in the three tested areas, split by mesh size; left for a mesh size of 1.25 [cm], middle for 1.0 [cm] and right for 0.625 [cm]

The comparison shows that there seems a small influence of the geometry on the air velocity. But on the surface of the timber sample, this influence is very small. It seems also that the finer mesh the smaller are the differences in the air velocity measurements.

The next two graphs compare the simulations split by the geometry.

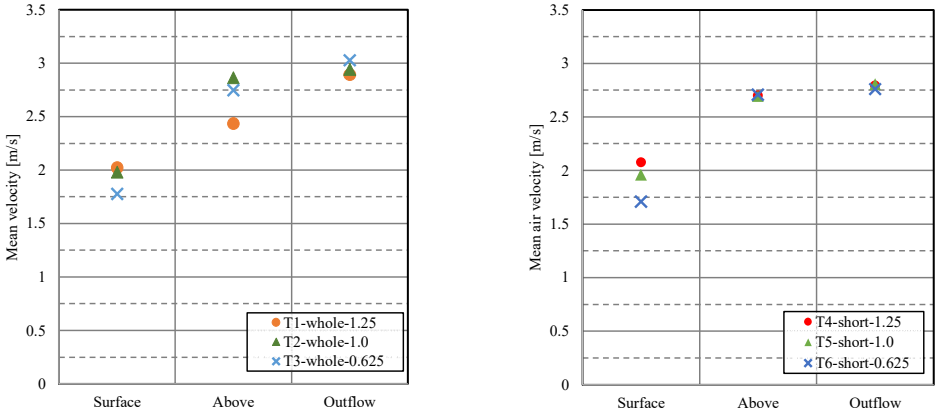

Graph 64: Comparison of the six simulations, in the three areas, split by the geometry; left for the whole FANCI tunnel, right for the shortened tunnel

For the whole geometry, the mesh size of 1.25 [cm] and 0.625 [cm] result in different velocities. The mesh size of 1.0 [cm] range in-between and is a sort of compromise between the two others. For the shortened geometry, the results are much closer, except for the measurements at the surface of the timber sample which is very similar to the results from simulations with the whole geometry.

As a conclusion, the shortened geometry of the FANCI tunnel with a mesh size of 1.0 [cm] seems a reasonable compromise between accuracy and simulation time. It leads 15 cells along the height of the tunnel (table 49).

Table 49: Mesh sizes and corresponding number of cells per height and width of the tunnel

	Mesh size		
	1.25 [cm]	**1.0 [cm]**	**0.625 [cm]**
Nb of cells along the height of the tunnel	12	15	24
Nb of cells along the width of the tunnel	40	50	80

B.4 FDS codes

B.4.1 T1-whole-1.25

This is the FDS code for the simulation with the whole FANCI geometry and a mesh size of 1.25 [cm].

```
-------Simulation name-------
&HEAD CHID='Fanci_5_2_nohf'/
-------Simulation time-------
&TIME T_END=300.0/
-------Mesh-------
&MESH ID='Mesh_01', IJK=108,40,12, XB=0.0,1.35,0.0,0.5,0.0,0.15, MPI_Process = 0/
&MESH ID='Mesh_02', IJK=144,40,12, XB=1.35,3.15,0.0,0.5,0.0,0.15, MPI_Process = 1/
&MESH ID='Mesh_03', IJK=109,40,12, XB=3.15,4.5125,0.0,0.5,0.0,0.15, MPI_Process = 2/
-------Spruce-------
&MATL ID = 'SPRUCE',
        EMISSIVITY = 0.9,
        CONDUCTIVITY = 0.09,
        SPECIFIC_HEAT_RAMP = 'c_ramp_spruce',
        DENSITY = 408.0,
        N_REACTIONS = 1.0,
        A(1) = 4.69E13,
        E(1) = 190500,
        N_S(1) = 1.0,
        MATL_ID(1,1) = 'CHAR',
        NU_MATL(1,1) = 0.16,
        SPEC_ID(1,1) = 'PYROLYZATE',
        NU_SPEC(1,1) = 0.84,
        HEAT_OF_REACTION(1) = 430.0,
        HEAT_OF_COMBUSTION= 14000.0,
        ABSORPTION_COEFFICIENT = 50000.0/
&RAMP ID='c_ramp_spruce', T=30, F=0.92 /
&RAMP ID='c_ramp_spruce', T=230, F=1.8 /
-------Steel (walls of tunnel)-------
&MATL ID='STEEL',
        SPECIFIC_HEAT=0.46,
        CONDUCTIVITY=45.8,
        DENSITY=7850.0,
        EMISSIVITY=0.7/
&SURF ID='STEEL_SURFACE',
        MATL_ID(1,1)='STEEL',
        MATL_MASS_FRACTION(1,1)=1.0,
        THICKNESS(1)=3.0E-3/
-------Inlet air flow-------
&SURF ID='INFLOW',
```

```
        RGB=26,204,26,
        VEL=-2.5/
-------Wood sample-------
&SURF ID='SAMPLE',
        RGB=200,100,0,
        BACKING='INSULATED',
        MATL_ID='SPRUCE',
        THICKNESS=0.12/
-------Geometry of tunnel-------
&OBST ID='Bottom_outlet', XB=0.0,2.1125,0.0,0.5,0.0,0.0, SURF_ID='STEEL_SURFACE'/
&OBST ID='Bottom_inlet', XB=2.375,4.5125,0.0,0.5,0.0,0.0, SURF_ID='STEEL_SURFACE'/
&OBST ID='Bottom_front', XB=2.112,2.38,0.0,0.1375,0.0,0.0, SURF_ID='STEEL_SURFACE'/
&OBST ID='Bottom_back', XB=2.112,2.38,0.3625,0.5,0.0,0.0, SURF_ID='STEEL_SURFACE'/
&OBST ID='Top', XB=0.0,4.5125,0.0,0.5,0.15,0.15, SURF_ID='STEEL_SURFACE'/
&OBST ID='Side_Front', XB=0.0,4.5125,0.0,0.0,0.0,0.15, SURF_ID='STEEL_SURFACE'/
&OBST ID='Side_Back', XB=0.0,4.5125,0.5,0.5,0.0,0.15, SURF_ID='STEEL_SURFACE'/
-------Position air inflow-------
&OBST ID='Side_Inlet', XB=4.5,4.5125,0.0,0.5,0.0,0.15, SURF_ID='INFLOW'/
-------Position wood sample-------
&OBST ID='WOOD_SAMPLE', XB=2.1125,2.375,0.1375,0.3625,0.0,0.0, SURF_ID='SAMPLE'/
-------Tunnel openings-------
&VENT ID='Mesh Vent: Mesh_01 [XMAX]', SURF_ID='OPEN', XB=4.5125,4.5125,0.0,0.5,0.0,0.15/
&VENT ID='Mesh Vent: Mesh_01 [XMIN]', SURF_ID='OPEN', XB=0.0,0.0,0.0,0.5,0.0,0.15/
-------Output air velocity surface of wood sample -------
&DEVC ID='CM-U', QUANTITY='U-VELOCITY', XYZ=2.2375,0.25,0.0/
&DEVC ID='CM-V', QUANTITY='V-VELOCITY', XYZ=2.2375,0.25,0.0/
&DEVC ID='CM-W', QUANTITY='W-VELOCITY', XYZ=2.2375,0.25,0.0/
&DEVC ID='CM', QUANTITY='VELOCITY', XYZ=2.2375,0.25,0.0/

&DEVC ID='CF-U', QUANTITY='U-VELOCITY', XYZ=2.2375,0.1875,0.0/
&DEVC ID='CF-V', QUANTITY='V-VELOCITY', XYZ=2.2375,0.1875,0.0/
&DEVC ID='CF-W', QUANTITY='W-VELOCITY', XYZ=2.2375,0.1875,0.0/
&DEVC ID='CF', QUANTITY='VELOCITY', XYZ=2.2375,0.1875,0.0/

&DEVC ID='CB-U', QUANTITY='U-VELOCITY', XYZ=2.2375,0.3,0.0/
&DEVC ID='CB-V', QUANTITY='V-VELOCITY', XYZ=2.2375,0.3,0.0/
&DEVC ID='CB-W', QUANTITY='W-VELOCITY', XYZ=2.2375,0.3,0.0/
&DEVC ID='CB', QUANTITY='VELOCITY', XYZ=2.2375,0.3,0.0/

&DEVC ID='OM-U', QUANTITY='U-VELOCITY', XYZ=2.175,0.25,0.0/
&DEVC ID='OM-V', QUANTITY='V-VELOCITY', XYZ=2.175,0.25,0.0/
&DEVC ID='OM-W', QUANTITY='W-VELOCITY', XYZ=2.175,0.25,0.0/
&DEVC ID='OM', QUANTITY='VELOCITY', XYZ=2.175,0.25,0.0/
```

```
&DEVC ID='OF-U', QUANTITY='U-VELOCITY', XYZ=2.175,0.1875,0.0/
&DEVC ID='OF-V', QUANTITY='V-VELOCITY', XYZ=2.175,0.1875,0.0/
&DEVC ID='OF-W', QUANTITY='W-VELOCITY', XYZ=2.175,0.1875,0.0/
&DEVC ID='OF', QUANTITY='VELOCITY', XYZ=2.175,0.1875,0.0/

&DEVC ID='OB-U', QUANTITY='U-VELOCITY', XYZ=2.175,0.3,0.0/
&DEVC ID='OB-V', QUANTITY='V-VELOCITY', XYZ=2.175,0.3,0.0/
&DEVC ID='OB-W', QUANTITY='W-VELOCITY', XYZ=2.175,0.3,0.0/
&DEVC ID='OB', QUANTITY='VELOCITY', XYZ=2.175,0.3,0.0/

&DEVC ID='IM-U', QUANTITY='U-VELOCITY', XYZ=2.3,0.25,0.0/
&DEVC ID='IM-V', QUANTITY='V-VELOCITY', XYZ=2.3,0.25,0.0/
&DEVC ID='IM-W', QUANTITY='W-VELOCITY', XYZ=2.3,0.25,0.0/
&DEVC ID='IM', QUANTITY='VELOCITY', XYZ=2.3,0.25,0.0/

&DEVC ID='IF-U', QUANTITY='U-VELOCITY', XYZ=2.3,0.1875,0.0/
&DEVC ID='IF-V', QUANTITY='V-VELOCITY', XYZ=2.3,0.1875,0.0/
&DEVC ID='IF-W', QUANTITY='W-VELOCITY', XYZ=2.3,0.1875,0.0/
&DEVC ID='IF', QUANTITY='VELOCITY', XYZ=2.3,0.1875,0.0/

&DEVC ID='IB-U', QUANTITY='U-VELOCITY', XYZ=2.3,0.3,0.0/
&DEVC ID='IB-V', QUANTITY='V-VELOCITY', XYZ=2.3,0.3,0.0/
&DEVC ID='IB-W', QUANTITY='W-VELOCITY', XYZ=2.3,0.3,0.0/
&DEVC ID='IB', QUANTITY='VELOCITY', XYZ=2.3,0.3,0.0/
-------Output air velocity area above wood sample -------
&DEVC ID='CM-1-U', QUANTITY='U-VELOCITY', XYZ=2.2375,0.25,0.0125/
&DEVC ID='CM-1-V', QUANTITY='V-VELOCITY', XYZ=2.2375,0.25,0.0125/
&DEVC ID='CM-1-W', QUANTITY='W-VELOCITY', XYZ=2.2375,0.25,0.0125/
&DEVC ID='CM-1', QUANTITY='VELOCITY', XYZ=2.2375,0.25,0.0125/

&DEVC ID='CF-1-U', QUANTITY='U-VELOCITY', XYZ=2.2375,0.125,0.0125/
&DEVC ID='CF-1-V', QUANTITY='V-VELOCITY', XYZ=2.2375,0.125,0.0125/
&DEVC ID='CF-1-W', QUANTITY='W-VELOCITY', XYZ=2.2375,0.125,0.0125/
&DEVC ID='CF-1', QUANTITY='VELOCITY', XYZ=2.2375,0.125,0.0125/

&DEVC ID='CB-1-U', QUANTITY='U-VELOCITY', XYZ=2.2375,0.375,0.0125/
&DEVC ID='CB-1-V', QUANTITY='V-VELOCITY', XYZ=2.2375,0.375,0.0125/
&DEVC ID='CB-1-W', QUANTITY='W-VELOCITY', XYZ=2.2375,0.375,0.0125/
&DEVC ID='CB-1', QUANTITY='VELOCITY', XYZ=2.2375,0.375,0.0125/

&DEVC ID='OM-1-U', QUANTITY='U-VELOCITY', XYZ=2.175,0.25,0.0125/
&DEVC ID='OM-1-V', QUANTITY='V-VELOCITY', XYZ=2.175,0.25,0.0125/
&DEVC ID='OM-1-W', QUANTITY='W-VELOCITY', XYZ=2.175,0.25,0.0125/
&DEVC ID='OM-1', QUANTITY='VELOCITY', XYZ=2.175,0.25,0.0125/
```

```
&DEVC ID='OF-1-U', QUANTITY='U-VELOCITY', XYZ=2.175,0.125,0.0125/
&DEVC ID='OF-1-V', QUANTITY='V-VELOCITY', XYZ=2.175,0.125,0.0125/
&DEVC ID='OF-1-W', QUANTITY='W-VELOCITY', XYZ=2.175,0.125,0.0125/
&DEVC ID='OF-1', QUANTITY='VELOCITY', XYZ=2.175,0.125,0.0125/

&DEVC ID='CB-1-U', QUANTITY='U-VELOCITY', XYZ=2.175,0.375,0.0125/
&DEVC ID='CB-1-V', QUANTITY='V-VELOCITY', XYZ=2.175,0.375,0.0125/
&DEVC ID='CB-1-W', QUANTITY='W-VELOCITY', XYZ=2.175,0.375,0.0125/
&DEVC ID='CB-1', QUANTITY='VELOCITY', XYZ=2.175,0.375,0.0125/

&DEVC ID='IM-1-U', QUANTITY='U-VELOCITY', XYZ=2.3,0.25,0.0125/
&DEVC ID='IM-1-V', QUANTITY='V-VELOCITY', XYZ=2.3,0.25,0.0125/
&DEVC ID='IM-1-W', QUANTITY='W-VELOCITY', XYZ=2.3,0.25,0.0125/
&DEVC ID='IM-1', QUANTITY='VELOCITY', XYZ=2.3,0.25,0.0125/

&DEVC ID='IF-1-U', QUANTITY='U-VELOCITY', XYZ=2.3,0.125,0.0125/
&DEVC ID='IF-1-V', QUANTITY='V-VELOCITY', XYZ=2.3,0.125,0.0125/
&DEVC ID='IF-1-W', QUANTITY='W-VELOCITY', XYZ=2.3,0.125,0.0125/
&DEVC ID='IF-1', QUANTITY='VELOCITY', XYZ=2.3,0.125,0.0125/

&DEVC ID='IB-1-U', QUANTITY='U-VELOCITY', XYZ=2.3,0.375,0.0125/
&DEVC ID='IB-1-V', QUANTITY='V-VELOCITY', XYZ=2.3,0.375,0.0125/
&DEVC ID='IB-1-W', QUANTITY='W-VELOCITY', XYZ=2.3,0.375,0.0125/
&DEVC ID='IB-1', QUANTITY='VELOCITY', XYZ=2.3,0.375,0.0125/
-------Output air velocity at outlet-------
&DEVC ID='O-M-U', QUANTITY='U-VELOCITY', XYZ=1.35,0.25,0.075/
&DEVC ID='O-M-V', QUANTITY='V-VELOCITY', XYZ=1.35,0.25,0.075/
&DEVC ID='O-M-W', QUANTITY='W-VELOCITY', XYZ=1.35,0.25,0.075/
&DEVC ID='O-M', QUANTITY='VELOCITY', XYZ=1.35,0.25,0.075/

&DEVC ID='O-F-U', QUANTITY='U-VELOCITY', XYZ=1.35,0.125,0.075/
&DEVC ID='O-F-V', QUANTITY='V-VELOCITY', XYZ=1.35,0.125,0.075/
&DEVC ID='O-F-W', QUANTITY='W-VELOCITY', XYZ=1.35,0.125,0.075/
&DEVC ID='O-F', QUANTITY='VELOCITY', XYZ=1.35,0.125,0.075/

&DEVC ID='O-B-U', QUANTITY='U-VELOCITY', XYZ=1.35,0.375,0.075/
&DEVC ID='O-B-V', QUANTITY='V-VELOCITY', XYZ=1.35,0.375,0.075/
&DEVC ID='O-B-W', QUANTITY='W-VELOCITY', XYZ=1.35,0.375,0.075/
&DEVC ID='O-B', QUANTITY='VELOCITY', XYZ=1.35,0.375,0.075/
-------Animated output velocity-------
&SLCF QUANTITY='VELOCITY', VECTOR=.TRUE., CELL_CENTERED=.TRUE., PBY=0.25/
&SLCF QUANTITY='VELOCITY', VECTOR=.TRUE., CELL_CENTERED=.TRUE., PBX=2.2375/
&SLCF QUANTITY='VELOCITY', VECTOR=.TRUE., CELL_CENTERED=.TRUE., PBZ=0.075/
```

```
-------Animated output temperature-------
&SLCF QUANTITY='TEMPERATURE', CELL_CENTERED=.TRUE., PBZ=0.075/

&TAIL /
```

B.4.2 T2-whole-1.0

This is the FDS code for the simulation with the whole FANCI geometry and a mesh size of 1.0 [cm].

```
-------Simulation name-------
&HEAD CHID='Fanci_7_1_1_nohf'/
-------Simulation time-------
&TIME T_END=300.0/
-------Mesh-------
&MESH ID='Mesh_01', IJK=50,27,15, XB=0.0,0.5,0.0,0.27,0.0,0.15, MPI_Process = 0/
&MESH ID='Mesh_02', IJK=50,23,15, XB=0.0,0.5,0.27,0.5,0.0,0.15, MPI_Process = 1/
&MESH ID='Mesh_03', IJK=50,27,15, XB=0.5,1.0,0.0,0.27,0.0,0.15, MPI_Process = 2/
&MESH ID='Mesh_04', IJK=50,23,15, XB=0.5,1.0,0.27,0.5,0.0,0.15, MPI_Process = 3/
&MESH ID='Mesh_05', IJK=50,27,15, XB=1.0,1.5,0.0,0.27,0.0,0.15, MPI_Process = 4/
&MESH ID='Mesh_06', IJK=50,23,15, XB=1.0,1.5,0.27,0.5,0.0,0.15, MPI_Process = 5/
&MESH ID='Mesh_07', IJK=50,27,15, XB=1.5,2.0,0.0,0.27,0.0,0.15, MPI_Process = 6/
&MESH ID='Mesh_08', IJK=50,23,15, XB=1.5,2.0,0.27,0.5,0.0,0.15, MPI_Process = 7/
&MESH ID='Mesh_09', IJK=50,27,15, XB=2.0,2.5,0.0,0.27,0.0,0.15, MPI_Process = 8/
&MESH ID='Mesh_10', IJK=50,23,15, XB=2.0,2.5,0.27,0.5,0.0,0.15, MPI_Process = 9/
&MESH ID='Mesh_11', IJK=50,27,15, XB=2.5,3.0,0.0,0.27,0.0,0.15, MPI_Process = 10/
&MESH ID='Mesh_12', IJK=50,23,15, XB=2.5,3.0,0.27,0.5,0.0,0.15, MPI_Process = 11/
&MESH ID='Mesh_13', IJK=50,27,15, XB=3.0,3.5,0.0,0.27,0.0,0.15, MPI_Process = 12/
&MESH ID='Mesh_14', IJK=50,23,15, XB=3.0,3.5,0.27,0.5,0.0,0.15, MPI_Process = 13/
&MESH ID='Mesh_15', IJK=50,27,15, XB=3.5,4.0,0.0,0.27,0.0,0.15, MPI_Process = 14/
&MESH ID='Mesh_16', IJK=50,23,15, XB=3.5,4.0,0.27,0.5,0.0,0.15, MPI_Process = 15/
&MESH ID='Mesh_17', IJK=51,27,15, XB=4.0,4.51,0.0,0.27,0.0,0.15, MPI_Process = 16/
&MESH ID='Mesh_18', IJK=51,23,15, XB=4.0,4.51,0.27,0.5,0.0,0.15, MPI_Process = 17/
-------Spruce-------
&MATL ID = 'SPRUCE',
        EMISSIVITY = 0.9,
        CONDUCTIVITY = 0.09,
        SPECIFIC_HEAT_RAMP = 'c_ramp_spruce',
        DENSITY = 408.0,
        N_REACTIONS = 1.0,
        A(1) = 4.69E13,
        E(1) = 190500,
        N_S(1) = 1.0,
        MATL_ID(1,1) = 'CHAR',
        NU_MATL(1,1) = 0.16,
```

```
        SPEC_ID(1,1) = 'PYROLYZATE',
        NU_SPEC(1,1) = 0.84,
        HEAT_OF_REACTION(1) = 430.0,
        HEAT_OF_COMBUSTION= 14000.0,
        ABSORPTION_COEFFICIENT = 50000.0/
&RAMP ID='c_ramp_spruce', T=30, F=0.92 /
&RAMP ID='c_ramp_spruce', T=230, F=1.8 /
-------Steel (walls of tunnel)-------
&MATL ID='STEEL',
        SPECIFIC_HEAT=0.46,
        CONDUCTIVITY=45.8,
        DENSITY=7850.0,
        EMISSIVITY=0.7/
&SURF ID='STEEL_SURFACE',
        MATL_ID(1,1)='STEEL',
        MATL_MASS_FRACTION(1,1)=1.0,
        THICKNESS(1)=3.0E-3/
-------Inlet air flow-------
&SURF ID='INFLOW',
        RGB=26,204,26,
        VEL=-2.5/
-------Wood sample-------
&SURF ID='SAMPLE',
        RGB=200,100,0,
        BACKING='INSULATED',
        MATL_ID='SPRUCE',
        THICKNESS=0.12/
 -------Geometry of tunnel-------
&OBST ID='Bottom_outlet', XB=0.0,2.12,0.0,0.5,0.0,0.0, SURF_ID='STEEL_SURFACE'/
&OBST ID='Bottom_inlet', XB=2.38,4.51,0.0,0.5,0.0,0.0, SURF_ID='STEEL_SURFACE'/
&OBST ID='Bottom_front', XB=2.115,2.385,0.0,0.14,0.0,0.0, SURF_ID='STEEL_SURFACE'/
&OBST ID='Bottom_back', XB=2.115,2.385,0.36,0.5,0.0,0.0, SURF_ID='STEEL_SURFACE'/
&OBST ID='Top', XB=0.0,4.51,0.0,0.5,0.15,0.15, SURF_ID='STEEL_SURFACE'/
&OBST ID='Side_Front', XB=0.0,4.51,0.0,0.0,0.0,0.15, SURF_ID='STEEL_SURFACE'/
&OBST ID='Side_Back', XB=0.0,4.51,0.5,0.5,0.0,0.15, SURF_ID='STEEL_SURFACE'/
-------Position air inflow-------
&OBST ID='Side_Inlet', XB=4.5,4.51,0.0,0.5,0.0,0.15, SURF_ID='INFLOW'/
-------Position wood sample-------
&OBST ID='WOOD_SAMPLE', XB=2.12,2.38,0.14,0.36,0.0,0.0, SURF_ID='SAMPLE'/
-------Tunnel openings-------
&VENT ID='Mesh Vent: Mesh_01 [XMAX]', SURF_ID='OPEN', XB=4.51,4.51,0.0,0.5,0.0,0.15/
&VENT ID='Mesh Vent: Mesh_01 [XMIN]', SURF_ID='OPEN', XB=0.0,0.0,0.0,0.5,0.0,0.15/
-------Output air velocity surface of wood sample -------
&DEVC ID='CM-U', QUANTITY='U-VELOCITY', XYZ=2.25,0.25,0.0/
```

```
&DEVC ID='CM-V', QUANTITY='V-VELOCITY', XYZ=2.25,0.25,0.0/
&DEVC ID='CM-W', QUANTITY='W-VELOCITY', XYZ=2.25,0.25,0.0/
&DEVC ID='CM', QUANTITY='VELOCITY', XYZ=2.25,0.25,0.0/

&DEVC ID='CF-U', QUANTITY='U-VELOCITY', XYZ=2.25,0.20,0.0/
&DEVC ID='CF-V', QUANTITY='V-VELOCITY', XYZ=2.25,0.20,0.0/
&DEVC ID='CF-W', QUANTITY='W-VELOCITY', XYZ=2.25,0.20,0.0/
&DEVC ID='CF', QUANTITY='VELOCITY', XYZ=2.25,0.20,0.0/

&DEVC ID='CB-U', QUANTITY='U-VELOCITY', XYZ=2.25,0.31,0.0/
&DEVC ID='CB-V', QUANTITY='V-VELOCITY', XYZ=2.25,0.31,0.0/
&DEVC ID='CB-W', QUANTITY='W-VELOCITY', XYZ=2.25,0.31,0.0/
&DEVC ID='CB', QUANTITY='VELOCITY', XYZ=2.25,0.31,0.0/

&DEVC ID='OM-U', QUANTITY='U-VELOCITY', XYZ=2.19,0.25,0.0/
&DEVC ID='OM-V', QUANTITY='V-VELOCITY', XYZ=2.19,0.25,0.0/
&DEVC ID='OM-W', QUANTITY='W-VELOCITY', XYZ=2.19,0.25,0.0/
&DEVC ID='OM', QUANTITY='VELOCITY', XYZ=2.19,0.25,0.0/

&DEVC ID='OF-U', QUANTITY='U-VELOCITY', XYZ=2.19,0.20,0.0/
&DEVC ID='OF-V', QUANTITY='V-VELOCITY', XYZ=2.19,0.20,0.0/
&DEVC ID='OF-W', QUANTITY='W-VELOCITY', XYZ=2.19,0.20,0.0/
&DEVC ID='OF', QUANTITY='VELOCITY', XYZ=2.19,0.20,0.0/

&DEVC ID='OB-U', QUANTITY='U-VELOCITY', XYZ=2.19,0.31,0.0/
&DEVC ID='OB-V', QUANTITY='V-VELOCITY', XYZ=2.19,0.31,0.0/
&DEVC ID='OB-W', QUANTITY='W-VELOCITY', XYZ=2.19,0.31,0.0/
&DEVC ID='OB', QUANTITY='VELOCITY', XYZ=2.19,0.31,0.0/

&DEVC ID='IM-U', QUANTITY='U-VELOCITY', XYZ=2.31,0.25,0.0/
&DEVC ID='IM-V', QUANTITY='V-VELOCITY', XYZ=2.31,0.25,0.0/
&DEVC ID='IM-W', QUANTITY='W-VELOCITY', XYZ=2.31,0.25,0.0/
&DEVC ID='IM', QUANTITY='VELOCITY', XYZ=2.31,0.25,0.0/

&DEVC ID='IF-U', QUANTITY='U-VELOCITY', XYZ=2.31,0.20,0.0/
&DEVC ID='IF-V', QUANTITY='V-VELOCITY', XYZ=2.31,0.20,0.0/
&DEVC ID='IF-W', QUANTITY='W-VELOCITY', XYZ=2.31,0.20,0.0/
&DEVC ID='IF', QUANTITY='VELOCITY', XYZ=2.31,0.20,0.0/

&DEVC ID='IB-U', QUANTITY='U-VELOCITY', XYZ=2.31,0.31,0.0/
&DEVC ID='IB-V', QUANTITY='V-VELOCITY', XYZ=2.31,0.31,0.0/
&DEVC ID='IB-W', QUANTITY='W-VELOCITY', XYZ=2.31,0.31,0.0/
&DEVC ID='IB', QUANTITY='VELOCITY', XYZ=2.31,0.31,0.0/
-------Output air velocity area above wood sample -------
&DEVC ID='CM-1-U', QUANTITY='U-VELOCITY', XYZ=2.25,0.25,0.06/
```

```
&DEVC ID='CM-1-V', QUANTITY='V-VELOCITY', XYZ=2.25,0.25,0.06/
&DEVC ID='CM-1-W', QUANTITY='W-VELOCITY', XYZ=2.25,0.25,0.06/
&DEVC ID='CM-1', QUANTITY='VELOCITY', XYZ=2.25,0.25,0.06/

&DEVC ID='CF-1-U', QUANTITY='U-VELOCITY', XYZ=2.25,0.20,0.06/
&DEVC ID='CF-1-V', QUANTITY='V-VELOCITY', XYZ=2.25,0.20,0.06/
&DEVC ID='CF-1-W', QUANTITY='W-VELOCITY', XYZ=2.25,0.20,0.06/
&DEVC ID='CF-1', QUANTITY='VELOCITY', XYZ=2.25,0.20,0.06/

&DEVC ID='CB-1-U', QUANTITY='U-VELOCITY', XYZ=2.25,0.31,0.06/
&DEVC ID='CB-1-V', QUANTITY='V-VELOCITY', XYZ=2.25,0.31,0.06/
&DEVC ID='CB-1-W', QUANTITY='W-VELOCITY', XYZ=2.25,0.31,0.06/
&DEVC ID='CB-1', QUANTITY='VELOCITY', XYZ=2.25,0.31,0.06/

&DEVC ID='OM-1-U', QUANTITY='U-VELOCITY', XYZ=2.19,0.25,0.06/
&DEVC ID='OM-1-V', QUANTITY='V-VELOCITY', XYZ=2.19,0.25,0.06/
&DEVC ID='OM-1-W', QUANTITY='W-VELOCITY', XYZ=2.19,0.25,0.06/
&DEVC ID='OM-1', QUANTITY='VELOCITY', XYZ=2.19,0.25,0.06/

&DEVC ID='OF-1-U', QUANTITY='U-VELOCITY', XYZ=2.19,0.20,0.06/
&DEVC ID='OF-1-V', QUANTITY='V-VELOCITY', XYZ=2.19,0.20,0.06/
&DEVC ID='OF-1-W', QUANTITY='W-VELOCITY', XYZ=2.19,0.20,0.06/
&DEVC ID='OF-1', QUANTITY='VELOCITY', XYZ=2.19,0.20,0.06/

&DEVC ID='OB-1-U', QUANTITY='U-VELOCITY', XYZ=2.19,0.31,0.06/
&DEVC ID='OB-1-V', QUANTITY='V-VELOCITY', XYZ=2.19,0.31,0.06/
&DEVC ID='OB-1-W', QUANTITY='W-VELOCITY', XYZ=2.19,0.31,0.06/
&DEVC ID='OB-1', QUANTITY='VELOCITY', XYZ=2.19,0.31,0.06/

&DEVC ID='IM-1-U', QUANTITY='U-VELOCITY', XYZ=2.31,0.25,0.06/
&DEVC ID='IM-1-V', QUANTITY='V-VELOCITY', XYZ=2.31,0.25,0.06/
&DEVC ID='IM-1-W', QUANTITY='W-VELOCITY', XYZ=2.31,0.25,0.06/
&DEVC ID='IM-1', QUANTITY='VELOCITY', XYZ=2.31,0.25,0.06/

&DEVC ID='IF-1-U', QUANTITY='U-VELOCITY', XYZ=2.31,0.20,0.06/
&DEVC ID='IF-1-V', QUANTITY='V-VELOCITY', XYZ=2.31,0.20,0.06/
&DEVC ID='IF-1-W', QUANTITY='W-VELOCITY', XYZ=2.31,0.20,0.06/
&DEVC ID='IF-1', QUANTITY='VELOCITY', XYZ=2.31,0.20,0.06/

&DEVC ID='IB-1-U', QUANTITY='U-VELOCITY', XYZ=2.31,0.31,0.06/
&DEVC ID='IB-1-V', QUANTITY='V-VELOCITY', XYZ=2.31,0.31,0.06/
&DEVC ID='IB-1-W', QUANTITY='W-VELOCITY', XYZ=2.31,0.31,0.06/
&DEVC ID='IB-1', QUANTITY='VELOCITY', XYZ=2.31,0.31,0.06/
-------Output air velocity at outlet -------
&DEVC ID='O-M-U', QUANTITY='U-VELOCITY', XYZ=0.0,0.25,0.07/
```

```
&DEVC ID='O-M-V', QUANTITY='V-VELOCITY', XYZ=0.0,0.25,0.07/
&DEVC ID='O-M-W', QUANTITY='W-VELOCITY', XYZ=0.0,0.25,0.07/
&DEVC ID='O-M', QUANTITY='VELOCITY', XYZ=0.0,0.25,0.07/

&DEVC ID='O-F-U', QUANTITY='U-VELOCITY', XYZ=0.0,0.20,0.07/
&DEVC ID='O-F-V', QUANTITY='V-VELOCITY', XYZ=0.0,0.20,0.07/
&DEVC ID='O-F-W', QUANTITY='W-VELOCITY', XYZ=0.0,0.20,0.07/
&DEVC ID='O-F', QUANTITY='VELOCITY', XYZ=0.0,0.20,0.07/

&DEVC ID='O-B-U', QUANTITY='U-VELOCITY', XYZ=0.0,0.31,0.07/
&DEVC ID='O-B-V', QUANTITY='V-VELOCITY', XYZ=0.0,0.31,0.07/
&DEVC ID='O-B-W', QUANTITY='W-VELOCITY', XYZ=0.0,0.31,0.07/
&DEVC ID='O-B', QUANTITY='VELOCITY', XYZ=0.0,0.31,0.07/
-------Animated output velocity-------
&SLCF QUANTITY='VELOCITY', VECTOR=.TRUE., CELL_CENTERED=.TRUE., PBY=0.25/
&SLCF QUANTITY='VELOCITY', VECTOR=.TRUE., CELL_CENTERED=.TRUE., PBX=2.25/
&SLCF QUANTITY='VELOCITY', VECTOR=.TRUE., CELL_CENTERED=.TRUE., PBZ=0.07/
-------Animated output temperature-------
&SLCF QUANTITY='TEMPERATURE', CELL_CENTERED=.TRUE., PBZ=0.07/

&TAIL /
```

B.4.3 T3-whole-0.625

This is the FDS code for the simulation with the whole FANCI geometry and a mesh size of 0.625 [cm].

```
-------Simulation name-------
&HEAD CHID='Fanci_6_2_1_nohf'/
-------Simulation time-------
&TIME T_END=300.0/
-------Mesh-------
&MESH ID='Mesh_01', IJK=80,42,24, XB=0.0,0.5,0.0,0.2625,0.0,0.15, MPI_Process = 0/
&MESH ID='Mesh_02', IJK=80,38,24, XB=0.0,0.5,0.2625,0.5,0.0,0.15, MPI_Process = 1/
&MESH ID='Mesh_03', IJK=80,42,24, XB=0.5,1.0,0.0,0.2625,0.0,0.15, MPI_Process = 2/
&MESH ID='Mesh_04', IJK=80,38,24, XB=0.5,1.0,0.2625,0.5,0.0,0.15, MPI_Process = 3/
&MESH ID='Mesh_05', IJK=80,42,24, XB=1.0,1.5,0.0,0.2625,0.0,0.15, MPI_Process = 4/
&MESH ID='Mesh_06', IJK=80,38,24, XB=1.0,1.5,0.2625,0.5,0.0,0.15, MPI_Process = 5/
&MESH ID='Mesh_07', IJK=80,42,24, XB=1.5,2.0,0.0,0.2625,0.0,0.15, MPI_Process = 6/
&MESH ID='Mesh_08', IJK=80,38,24, XB=1.5,2.0,0.2625,0.5,0.0,0.15, MPI_Process = 7/
&MESH ID='Mesh_09', IJK=80,42,24, XB=2.0,2.5,0.0,0.2625,0.0,0.15, MPI_Process = 8/
&MESH ID='Mesh_10', IJK=80,38,24, XB=2.0,2.5,0.2625,0.5,0.0,0.15, MPI_Process = 9/
&MESH ID='Mesh_11', IJK=80,42,24, XB=2.5,3.0,0.0,0.2625,0.0,0.15, MPI_Process = 10/
&MESH ID='Mesh_12', IJK=80,38,24, XB=2.5,3.0,0.2625,0.5,0.0,0.15, MPI_Process = 11/
```

```
&MESH ID='Mesh_13', IJK=80,42,24, XB=3.0,3.5,0.0,0.2625,0.0,0.15, MPI_Process = 12/
&MESH ID='Mesh_14', IJK=80,38,24, XB=3.0,3.5,0.2625,0.5,0.0,0.15, MPI_Process = 13/
&MESH ID='Mesh_15', IJK=80,42,24, XB=3.5,4.0,0.0,0.2625,0.0,0.15, MPI_Process = 14/
&MESH ID='Mesh_16', IJK=80,38,24, XB=3.5,4.0,0.2625,0.5,0.0,0.15, MPI_Process = 15/
&MESH ID='Mesh_17', IJK=81,42,24, XB=4.0,4.50625,0.0,0.2625,0.0,0.15, MPI_Process = 16/
&MESH ID='Mesh_18', IJK=81,38,24, XB=4.0,4.50625,0.2625,0.5,0.0,0.15, MPI_Process = 17/
-------Spruce-------
&MATL ID = 'SPRUCE',
        EMISSIVITY = 0.9,
        CONDUCTIVITY = 0.09,
        SPECIFIC_HEAT_RAMP = 'c_ramp_spruce',
        DENSITY = 408.0,
        N_REACTIONS = 1.0,
        A(1) = 4.69E13,
        E(1) = 190500,
        N_S(1) = 1.0,
        MATL_ID(1,1) = 'CHAR',
        NU_MATL(1,1) = 0.16,
        SPEC_ID(1,1) = 'PYROLYZATE',
        NU_SPEC(1,1) = 0.84,
        HEAT_OF_REACTION(1) = 430.0,
        HEAT_OF_COMBUSTION= 14000.0,
        ABSORPTION_COEFFICIENT = 50000.0/
&RAMP ID='c_ramp_spruce', T=30, F=0.92 /
&RAMP ID='c_ramp_spruce', T=230, F=1.8 /
-------Steel (walls of tunnel)-------
&MATL ID='STEEL',
        SPECIFIC_HEAT=0.46,
        CONDUCTIVITY=45.8,
        DENSITY=7850.0,
        EMISSIVITY=0.7/
&SURF ID='STEEL_SURFACE',
        MATL_ID(1,1)='STEEL',
        MATL_MASS_FRACTION(1,1)=1.0,
        THICKNESS(1)=3.0E-3/
-------Inlet air flow-------
&SURF ID='INFLOW',
        RGB=26,204,26,
        VEL=-2.5/
-------Wood sample-------
&SURF ID='SAMPLE',
        RGB=200,100,0,
        BACKING='INSULATED',
        MATL_ID='SPRUCE',
```

```
        THICKNESS=0.12/
-------Geometry of tunnel-------
&OBST ID='Bottom_outlet', XB=0.0,2.11875,0.0,0.5,0.0,0.0, SURF_ID='STEEL_SURFACE'/
&OBST ID='Bottom_inlet', XB=2.375,4.50625,0.0,0.5,0.0,0.0, SURF_ID='STEEL_SURFACE'/
&OBST ID='Bottom_front', XB=2.1156,2.378,0.0,0.1375,0.0,0.0, SURF_ID='STEEL_SURFACE'/
&OBST ID='Bottom_back', XB=2.1156,2.378,0.3625,0.5,0.0,0.0, SURF_ID='STEEL_SURFACE'/
&OBST ID='Top', XB=0.0,4.50625,0.0,0.5,0.15,0.15, SURF_ID='STEEL_SURFACE'/
&OBST ID='Side_Front', XB=0.0,4.50625,0.0,0.0,0.0,0.15, SURF_ID='STEEL_SURFACE'/
&OBST ID='Side_Back', XB=0.0,4.50625,0.5,0.5,0.0,0.15, SURF_ID='STEEL_SURFACE'/
-------Position air inflow-------
&OBST ID='Side_Inlet', XB=4.5,4.50625,0.0,0.5,0.0,0.15, SURF_ID='INFLOW'/
-------Position wood sample-------
&OBST ID='WOOD_SAMPLE', XB=2.11875,2.375,0.1375,0.3625,0.0,0.0, SURF_ID='SAMPLE'/
-------Tunnel openings-------
&VENT ID='Mesh Vent: Mesh_01 [XMAX]', SURF_ID='OPEN',
XB=4.50625,4.50625,0.0,0.5,0.0,0.15/
&VENT ID='Mesh Vent: Mesh_01 [XMIN]', SURF_ID='OPEN', XB=0.0,0.0,0.0,0.5,0.0,0.15/
-------Output air velocity surface of wood sample -------
&DEVC ID='CM-U', QUANTITY='U-VELOCITY', XYZ=2.24375,0.25,0.0/
&DEVC ID='CM-V', QUANTITY='V-VELOCITY', XYZ=2.24375,0.25,0.0/
&DEVC ID='CM-W', QUANTITY='W-VELOCITY', XYZ=2.24375,0.25,0.0/
&DEVC ID='CM', QUANTITY='VELOCITY', XYZ=2.24375,0.25,0.0/

&DEVC ID='CF-U', QUANTITY='U-VELOCITY', XYZ=2.24375,0.19375,0.0/
&DEVC ID='CF-V', QUANTITY='V-VELOCITY', XYZ=2.24375,0.19375,0.0/
&DEVC ID='CF-W', QUANTITY='W-VELOCITY', XYZ=2.24375,0.19375,0.0/
&DEVC ID='CF', QUANTITY='VELOCITY', XYZ=2.24375,0.19375,0.0/

&DEVC ID='CB-U', QUANTITY='U-VELOCITY', XYZ=2.24375,0.3,0.0/
&DEVC ID='CB-V', QUANTITY='V-VELOCITY', XYZ=2.24375,0.3,0.0/
&DEVC ID='CB-W', QUANTITY='W-VELOCITY', XYZ=2.24375,0.3,0.0/
&DEVC ID='CB', QUANTITY='VELOCITY', XYZ=2.24375,0.3,0.0/

&DEVC ID='OM-U', QUANTITY='U-VELOCITY', XYZ=2.18125,0.25,0.0/
&DEVC ID='OM-V', QUANTITY='V-VELOCITY', XYZ=2.18125,0.25,0.0/
&DEVC ID='OM-W', QUANTITY='W-VELOCITY', XYZ=2.18125,0.25,0.0/
&DEVC ID='OM', QUANTITY='VELOCITY', XYZ=2.1825,0.25,0.0/

&DEVC ID='OF-U', QUANTITY='U-VELOCITY', XYZ=2.18125,0.19375,0.0/
&DEVC ID='OF-V', QUANTITY='V-VELOCITY', XYZ=2.18125,0.19375,0.0/
&DEVC ID='OF-W', QUANTITY='W-VELOCITY', XYZ=2.18125,0.19375,0.0/
&DEVC ID='OF', QUANTITY='VELOCITY', XYZ=2.18125,0.19375,0.0/

&DEVC ID='OB-U', QUANTITY='U-VELOCITY', XYZ=2.18125,0.30625,0.0/
&DEVC ID='OB-V', QUANTITY='V-VELOCITY', XYZ=2.18125,0.30625,0.0/
```

```
&DEVC ID='OB-W', QUANTITY='W-VELOCITY', XYZ=2.18125,0.30625,0.0/
&DEVC ID='OB', QUANTITY='VELOCITY', XYZ=2.18125,0.30625,0.0/

&DEVC ID='IM-U', QUANTITY='U-VELOCITY', XYZ=2.30625,0.25,0.0/
&DEVC ID='IM-V', QUANTITY='V-VELOCITY', XYZ=2.30625,0.25,0.0/
&DEVC ID='IM-W', QUANTITY='W-VELOCITY', XYZ=2.30625,0.25,0.0/
&DEVC ID='IM', QUANTITY='VELOCITY', XYZ=2.30625,0.25,0.0/

&DEVC ID='IF-U', QUANTITY='U-VELOCITY', XYZ=2.30625,0.19375,0.0/
&DEVC ID='IF-V', QUANTITY='V-VELOCITY', XYZ=2.30625,0.19375,0.0/
&DEVC ID='IF-W', QUANTITY='W-VELOCITY', XYZ=2.30625,0.19375,0.0/
&DEVC ID='IF', QUANTITY='VELOCITY', XYZ=2.30625,0.19375,0.0/

&DEVC ID='IB-U', QUANTITY='U-VELOCITY', XYZ=2.30625,0.30625,0.0/
&DEVC ID='IB-V', QUANTITY='V-VELOCITY', XYZ=2.30625,0.30625,0.0/
&DEVC ID='IB-W', QUANTITY='W-VELOCITY', XYZ=2.30625,0.30625,0.0/
&DEVC ID='IB', QUANTITY='VELOCITY', XYZ=2.30625,0.30625,0.0/
-------Output air velocity area above wood sample -------
&DEVC ID='CM-1-U', QUANTITY='U-VELOCITY', XYZ=2.2375,0.25,0.0375/
&DEVC ID='CM-1-V', QUANTITY='V-VELOCITY', XYZ=2.2375,0.25,0.0375/
&DEVC ID='CM-1-W', QUANTITY='W-VELOCITY', XYZ=2.2375,0.25,0.0375/
&DEVC ID='CM-1', QUANTITY='VELOCITY', XYZ=2.2375,0.25,0.0375/

&DEVC ID='CF-1-U', QUANTITY='U-VELOCITY', XYZ=2.2375,0.125,0.0375/
&DEVC ID='CF-1-V', QUANTITY='V-VELOCITY', XYZ=2.2375,0.125,0.0375/
&DEVC ID='CF-1-W', QUANTITY='W-VELOCITY', XYZ=2.2375,0.125,0.0375/
&DEVC ID='CF-1', QUANTITY='VELOCITY', XYZ=2.2375,0.125,0.0375/

&DEVC ID='CB-1-U', QUANTITY='U-VELOCITY', XYZ=2.2375,0.375,0.0375/
&DEVC ID='CB-1-V', QUANTITY='V-VELOCITY', XYZ=2.2375,0.375,0.0375/
&DEVC ID='CB-1-W', QUANTITY='W-VELOCITY', XYZ=2.2375,0.375,0.0375/
&DEVC ID='CB-1', QUANTITY='VELOCITY', XYZ=2.2375,0.375,0.0375/

&DEVC ID='OM-1-U', QUANTITY='U-VELOCITY', XYZ=2.175,0.25,0.0375/
&DEVC ID='OM-1-V', QUANTITY='V-VELOCITY', XYZ=2.175,0.25,0.0375/
&DEVC ID='OM-1-W', QUANTITY='W-VELOCITY', XYZ=2.175,0.25,0.0375/
&DEVC ID='OM-1', QUANTITY='VELOCITY', XYZ=2.175,0.25,0.0375/

&DEVC ID='OF-1-U', QUANTITY='U-VELOCITY', XYZ=2.175,0.125,0.0375/
&DEVC ID='OF-1-V', QUANTITY='V-VELOCITY', XYZ=2.175,0.125,0.0375/
&DEVC ID='OF-1-W', QUANTITY='W-VELOCITY', XYZ=2.175,0.125,0.0375/
&DEVC ID='OF-1', QUANTITY='VELOCITY', XYZ=2.175,0.125,0.0375/

&DEVC ID='OB-1-U', QUANTITY='U-VELOCITY', XYZ=2.175,0.375,0.0375/
&DEVC ID='OB-1-V', QUANTITY='V-VELOCITY', XYZ=2.175,0.375,0.0375/
```

```
&DEVC ID='OB-1-W', QUANTITY='W-VELOCITY', XYZ=2.175,0.375,0.0375/
&DEVC ID='OB-1', QUANTITY='VELOCITY', XYZ=2.175,0.375,0.0375/

&DEVC ID='IM-1-U', QUANTITY='U-VELOCITY', XYZ=2.3,0.25,0.0375/
&DEVC ID='IM-1-V', QUANTITY='V-VELOCITY', XYZ=2.3,0.25,0.0375/
&DEVC ID='IM-1-W', QUANTITY='W-VELOCITY', XYZ=2.3,0.25,0.0375/
&DEVC ID='IM-1', QUANTITY='VELOCITY', XYZ=2.3,0.25,0.0375/

&DEVC ID='IF-1-U', QUANTITY='U-VELOCITY', XYZ=2.3,0.125,0.0375/
&DEVC ID='IF-1-V', QUANTITY='V-VELOCITY', XYZ=2.3,0.125,0.0375/
&DEVC ID='IF-1-W', QUANTITY='W-VELOCITY', XYZ=2.3,0.125,0.0375/
&DEVC ID='IF-1', QUANTITY='VELOCITY', XYZ=2.3,0.125,0.0375/

&DEVC ID='IB-1-U', QUANTITY='U-VELOCITY', XYZ=2.3,0.375,0.0375/
&DEVC ID='IB-1-V', QUANTITY='V-VELOCITY', XYZ=2.3,0.375,0.0375/
&DEVC ID='IB-1-W', QUANTITY='W-VELOCITY', XYZ=2.3,0.375,0.0375/
&DEVC ID='IB-1', QUANTITY='VELOCITY', XYZ=2.3,0.375,0.0375/
-------Output air velocity at outlet -------
&DEVC ID='O-M-U', QUANTITY='U-VELOCITY', XYZ=0.0,0.25,0.075/
&DEVC ID='O-M-V', QUANTITY='V-VELOCITY', XYZ=0.0,0.25,0.075/
&DEVC ID='O-M-W', QUANTITY='W-VELOCITY', XYZ=0.0,0.25,0.075/
&DEVC ID='O-M', QUANTITY='VELOCITY', XYZ=0.0,0.25,0.075/

&DEVC ID='O-F-U', QUANTITY='U-VELOCITY', XYZ=0.0,0.125,0.075/
&DEVC ID='O-F-V', QUANTITY='V-VELOCITY', XYZ=0.0,0.125,0.075/
&DEVC ID='O-F-W', QUANTITY='W-VELOCITY', XYZ=0.0,0.125,0.075/
&DEVC ID='O-F', QUANTITY='VELOCITY', XYZ=0.0,0.125,0.075/

&DEVC ID='O-B-U', QUANTITY='U-VELOCITY', XYZ=0.0,0.375,0.075/
&DEVC ID='O-B-V', QUANTITY='V-VELOCITY', XYZ=0.0,0.375,0.075/
&DEVC ID='O-B-W', QUANTITY='W-VELOCITY', XYZ=0.0,0.375,0.075/
&DEVC ID='O-B', QUANTITY='VELOCITY', XYZ=0.0,0.375,0.075/
-------Animated output velocity-------
&SLCF QUANTITY='VELOCITY', VECTOR=.TRUE., CELL_CENTERED=.TRUE., PBY=0.25/
&SLCF QUANTITY='VELOCITY', VECTOR=.TRUE., CELL_CENTERED=.TRUE., PBX=2.2375/
&SLCF QUANTITY='VELOCITY', VECTOR=.TRUE., CELL_CENTERED=.TRUE., PBZ=0.075/
-------Animated output temperature-------
&SLCF QUANTITY='TEMPERATURE', CELL_CENTERED=.TRUE., PBZ=0.075/

&TAIL /
```

B.4.4 T4-short-1.25

This is the FDS code for the simulation with the shortened FANCI geometry and a mesh size of 1.25 [cm].

```
-------Simulation name-------
&HEAD CHID='Fanci_5_0_nohf_2'/
-------Simulation time-------
&TIME T_END=300.0/
-------Mesh-------
&MESH ID='Mesh_01', IJK=145,40,12, XB=1.35,3.1625,0.0,0.5,0.0,0.15/
-------Spruce-------
&MATL ID = 'SPRUCE',
      EMISSIVITY = 0.9,
      CONDUCTIVITY = 0.09,
      SPECIFIC_HEAT_RAMP = 'c_ramp_spruce',
      DENSITY = 408.0,
      N_REACTIONS = 1.0,
      A(1) = 4.69E13,
      E(1) = 190500,
      N_S(1) = 1.0,
      MATL_ID(1,1) = 'CHAR',
      NU_MATL(1,1) = 0.16,
      SPEC_ID(1,1) = 'PYROLYZATE',
      NU_SPEC(1,1) = 0.84,
      HEAT_OF_REACTION(1) = 430.0,
      HEAT_OF_COMBUSTION= 14000.0,
      ABSORPTION_COEFFICIENT = 50000.0/
&RAMP ID='c_ramp_spruce', T=30, F=0.92 /
&RAMP ID='c_ramp_spruce', T=230, F=1.8 /
-------Steel (walls of tunnel)-------
&MATL ID='STEEL',
      SPECIFIC_HEAT=0.46,
      CONDUCTIVITY=45.8,
      DENSITY=7850.0,
      EMISSIVITY=0.7/
&SURF ID='STEEL_SURFACE',
      MATL_ID(1,1)='STEEL',
      MATL_MASS_FRACTION(1,1)=1.0,
      THICKNESS(1)=3.0E-3/
-------Inlet air flow-------
&SURF ID='INFLOW',
      RGB=26,204,26,
      VEL=-2.5/
```

```
-------Wood sample-------
&SURF ID='SAMPLE',
      RGB=200,100,0,
      BACKING='INSULATED',
      MATL_ID='SPRUCE',
      THICKNESS=0.12/
-------Geometry of tunnel-------
&OBST ID='Bottom_outlet', XB=1.35,2.1125,0.0,0.5,0.0,0.0, SURF_ID='STEEL_SURFACE'/
&OBST ID='Bottom_inlet', XB=2.375,3.15,0.0,0.5,0.0,0.0, SURF_ID='STEEL_SURFACE'/
&OBST ID='Bottom_front', XB=2.112,2.38,0.0,0.1375,0.0,0.0, SURF_ID='STEEL_SURFACE'/
&OBST ID='Bottom_back', XB=2.112,2.38,0.3625,0.5,0.0,0.0, SURF_ID='STEEL_SURFACE'/
&OBST ID='Top', XB=1.35,3.15,0.0,0.5,0.15,0.15, SURF_ID='STEEL_SURFACE'/
&OBST ID='Side_Front', XB=1.35,3.15,0.0,0.0,0.0,0.15, SURF_ID='STEEL_SURFACE'/
&OBST ID='Side_Back', XB=1.35,3.15,0.5,0.5,0.0,0.15, SURF_ID='STEEL_SURFACE'/
-------Geometry of tunnel-------
&OBST ID='Side_Inlet', XB=3.15,3.1625,0.0,0.5,0.0,0.15, SURF_ID='INFLOW'/
-------Position wood sample-------
&OBST ID='WOOD_SAMPLE', XB=2.1125,2.375,0.1375,0.3625,0.0,0.0, SURF_ID='SAMPLE'/
-------Tunnel openings-------
&VENT ID='Mesh Vent: Mesh_01 [XMAX]', SURF_ID='OPEN', XB=3.1625,3.1625,0.0,0.5,0.0,0.15/
&VENT ID='Mesh Vent: Mesh_01 [XMIN]', SURF_ID='OPEN', XB=1.35,1.35,0.0,0.5,0.0,0.15/
-------Output air velocity surface of wood sample -------
&DEVC ID='CM-U', QUANTITY='U-VELOCITY', XYZ=2.2375,0.25,0.0/
&DEVC ID='CM-V', QUANTITY='V-VELOCITY', XYZ=2.2375,0.25,0.0/
&DEVC ID='CM-W', QUANTITY='W-VELOCITY', XYZ=2.2375,0.25,0.0/
&DEVC ID='CM', QUANTITY='VELOCITY', XYZ=2.2375,0.25,0.0/

&DEVC ID='CF-U', QUANTITY='U-VELOCITY', XYZ=2.2375,0.1875,0.0/
&DEVC ID='CF-V', QUANTITY='V-VELOCITY', XYZ=2.2375,0.1875,0.0/
&DEVC ID='CF-W', QUANTITY='W-VELOCITY', XYZ=2.2375,0.1875,0.0/
&DEVC ID='CF', QUANTITY='VELOCITY', XYZ=2.2375,0.1875,0.0/

&DEVC ID='CB-U', QUANTITY='U-VELOCITY', XYZ=2.2375,0.3,0.0/
&DEVC ID='CB-V', QUANTITY='V-VELOCITY', XYZ=2.2375,0.3,0.0/
&DEVC ID='CB-W', QUANTITY='W-VELOCITY', XYZ=2.2375,0.3,0.0/
&DEVC ID='CB', QUANTITY='VELOCITY', XYZ=2.2375,0.3,0.0/

&DEVC ID='OM-U', QUANTITY='U-VELOCITY', XYZ=2.175,0.25,0.0/
&DEVC ID='OM-V', QUANTITY='V-VELOCITY', XYZ=2.175,0.25,0.0/
&DEVC ID='OM-W', QUANTITY='W-VELOCITY', XYZ=2.175,0.25,0.0/
&DEVC ID='OM', QUANTITY='VELOCITY', XYZ=2.175,0.25,0.0/

&DEVC ID='OF-U', QUANTITY='U-VELOCITY', XYZ=2.175,0.1875,0.0/
&DEVC ID='OF-V', QUANTITY='V-VELOCITY', XYZ=2.175,0.1875,0.0/
```

```
&DEVC ID='OF-W', QUANTITY='W-VELOCITY', XYZ=2.175,0.1875,0.0/
&DEVC ID='OF', QUANTITY='VELOCITY', XYZ=2.175,0.1875,0.0/

&DEVC ID='OB-U', QUANTITY='U-VELOCITY', XYZ=2.175,0.3,0.0/
&DEVC ID='OB-V', QUANTITY='V-VELOCITY', XYZ=2.175,0.3,0.0/
&DEVC ID='OB-W', QUANTITY='W-VELOCITY', XYZ=2.175,0.3,0.0/
&DEVC ID='OB', QUANTITY='VELOCITY', XYZ=2.175,0.3,0.0/

&DEVC ID='IM-U', QUANTITY='U-VELOCITY', XYZ=2.3,0.25,0.0/
&DEVC ID='IM-V', QUANTITY='V-VELOCITY', XYZ=2.3,0.25,0.0/
&DEVC ID='IM-W', QUANTITY='W-VELOCITY', XYZ=2.3,0.25,0.0/
&DEVC ID='IM', QUANTITY='VELOCITY', XYZ=2.3,0.25,0.0/

&DEVC ID='IF-U', QUANTITY='U-VELOCITY', XYZ=2.3,0.1875,0.0/
&DEVC ID='IF-V', QUANTITY='V-VELOCITY', XYZ=2.3,0.1875,0.0/
&DEVC ID='IF-W', QUANTITY='W-VELOCITY', XYZ=2.3,0.1875,0.0/
&DEVC ID='IF', QUANTITY='VELOCITY', XYZ=2.3,0.1875,0.0/

&DEVC ID='IB-U', QUANTITY='U-VELOCITY', XYZ=2.3,0.3,0.0/
&DEVC ID='IB-V', QUANTITY='V-VELOCITY', XYZ=2.3,0.3,0.0/
&DEVC ID='IB-W', QUANTITY='W-VELOCITY', XYZ=2.3,0.3,0.0/
&DEVC ID='IB', QUANTITY='VELOCITY', XYZ=2.3,0.3,0.0/
-------Output air velocity area above the wood sample -------
&DEVC ID='CM-1-U', QUANTITY='U-VELOCITY', XYZ=2.2375,0.25,0.075/
&DEVC ID='CM-1-V', QUANTITY='V-VELOCITY', XYZ=2.2375,0.25,0.075/
&DEVC ID='CM-1-W', QUANTITY='W-VELOCITY', XYZ=2.2375,0.25,0.075/
&DEVC ID='CM-1', QUANTITY='VELOCITY', XYZ=2.2375,0.25,0.075/

&DEVC ID='CF-1-U', QUANTITY='U-VELOCITY', XYZ=2.2375,0.125,0.075/
&DEVC ID='CF-1-V', QUANTITY='V-VELOCITY', XYZ=2.2375,0.125,0.075/
&DEVC ID='CF-1-W', QUANTITY='W-VELOCITY', XYZ=2.2375,0.125,0.075/
&DEVC ID='CF-1', QUANTITY='VELOCITY', XYZ=2.2375,0.125,0.075/

&DEVC ID='CB-1-U', QUANTITY='U-VELOCITY', XYZ=2.2375,0.375,0.075/
&DEVC ID='CB-1-V', QUANTITY='V-VELOCITY', XYZ=2.2375,0.375,0.075/
&DEVC ID='CB-1-W', QUANTITY='W-VELOCITY', XYZ=2.2375,0.375,0.075/
&DEVC ID='CB-1', QUANTITY='VELOCITY', XYZ=2.2375,0.375,0.075/

&DEVC ID='OM-1-U', QUANTITY='U-VELOCITY', XYZ=2.175,0.25,0.075/
&DEVC ID='OM-1-V', QUANTITY='V-VELOCITY', XYZ=2.175,0.25,0.075/
&DEVC ID='OM-1-W', QUANTITY='W-VELOCITY', XYZ=2.175,0.25,0.075/
&DEVC ID='OM-1', QUANTITY='VELOCITY', XYZ=2.175,0.25,0.075/

&DEVC ID='OF-1-U', QUANTITY='U-VELOCITY', XYZ=2.175,0.125,0.075/
&DEVC ID='OF-1-V', QUANTITY='V-VELOCITY', XYZ=2.175,0.125,0.075/
```

```
&DEVC ID='OF-1-W', QUANTITY='W-VELOCITY', XYZ=2.175,0.125,0.075/
&DEVC ID='OF-1', QUANTITY='VELOCITY', XYZ=2.175,0.125,0.075/

&DEVC ID='CB-1-U', QUANTITY='U-VELOCITY', XYZ=2.175,0.375,0.075/
&DEVC ID='CB-1-V', QUANTITY='V-VELOCITY', XYZ=2.175,0.375,0.075/
&DEVC ID='CB-1-W', QUANTITY='W-VELOCITY', XYZ=2.175,0.375,0.075/
&DEVC ID='CB-1', QUANTITY='VELOCITY', XYZ=2.175,0.375,0.075/

&DEVC ID='IM-1-U', QUANTITY='U-VELOCITY', XYZ=2.3,0.25,0.075/
&DEVC ID='IM-1-V', QUANTITY='V-VELOCITY', XYZ=2.3,0.25,0.075/
&DEVC ID='IM-1-W', QUANTITY='W-VELOCITY', XYZ=2.3,0.25,0.075/
&DEVC ID='IM-1', QUANTITY='VELOCITY', XYZ=2.3,0.25,0.075/

&DEVC ID='IF-1-U', QUANTITY='U-VELOCITY', XYZ=2.3,0.125,0.075/
&DEVC ID='IF-1-V', QUANTITY='V-VELOCITY', XYZ=2.3,0.125,0.075/
&DEVC ID='IF-1-W', QUANTITY='W-VELOCITY', XYZ=2.3,0.125,0.075/
&DEVC ID='IF-1', QUANTITY='VELOCITY', XYZ=2.3,0.125,0.075/

&DEVC ID='IB-1-U', QUANTITY='U-VELOCITY', XYZ=2.3,0.375,0.075/
&DEVC ID='IB-1-V', QUANTITY='V-VELOCITY', XYZ=2.3,0.375,0.075/
&DEVC ID='IB-1-W', QUANTITY='W-VELOCITY', XYZ=2.3,0.375,0.075/
&DEVC ID='IB-1', QUANTITY='VELOCITY', XYZ=2.3,0.375,0.075/
-------Output air velocity surface of wood sample -------
&DEVC ID='O-M-U', QUANTITY='U-VELOCITY', XYZ=1.35,0.25,0.075/
&DEVC ID='O-M-V', QUANTITY='V-VELOCITY', XYZ=1.35,0.25,0.075/
&DEVC ID='O-M-W', QUANTITY='W-VELOCITY', XYZ=1.35,0.25,0.075/
&DEVC ID='O-M', QUANTITY='VELOCITY', XYZ=1.35,0.25,0.075/

&DEVC ID='O-F-U', QUANTITY='U-VELOCITY', XYZ=1.35,0.125,0.075/
&DEVC ID='O-F-V', QUANTITY='V-VELOCITY', XYZ=1.35,0.125,0.075/
&DEVC ID='O-F-W', QUANTITY='W-VELOCITY', XYZ=1.35,0.125,0.075/
&DEVC ID='O-F', QUANTITY='VELOCITY', XYZ=1.35,0.125,0.075/

&DEVC ID='O-B-U', QUANTITY='U-VELOCITY', XYZ=1.35,0.375,0.075/
&DEVC ID='O-B-V', QUANTITY='V-VELOCITY', XYZ=1.35,0.375,0.075/
&DEVC ID='O-B-W', QUANTITY='W-VELOCITY', XYZ=1.35,0.375,0.075/
&DEVC ID='O-B', QUANTITY='VELOCITY', XYZ=1.35,0.375,0.075/
-------Animated output velocity-------
&SLCF QUANTITY='VELOCITY', VECTOR=.TRUE., CELL_CENTERED=.TRUE., PBY=0.25/
&SLCF QUANTITY='VELOCITY', VECTOR=.TRUE., CELL_CENTERED=.TRUE., PBX=2.2375/
&SLCF QUANTITY='VELOCITY', VECTOR=.TRUE., CELL_CENTERED=.TRUE., PBZ=0.075/
-------Animated output temperature-------
&SLCF QUANTITY='TEMPERATURE', CELL_CENTERED=.TRUE., PBZ=0.075/

&TAIL /
```

B.4.5 T5-short-1.0

This is the FDS code for the simulation with the shortened FANCI geometry and a mesh size of 1.0 [cm].

```
-------Simulation name-------
&HEAD CHID='Fanci_7_0_1_nohf'/
-------Simulation time-------
&TIME T_END=300.0/
-------Mesh-------
&MESH ID='Mesh_01', IJK=14,27,15, XB=1.35,1.5,0.0,0.27,0.0,0.15, MPI_Process = 0/
&MESH ID='Mesh_02', IJK=14,23,15, XB=1.35,1.5,0.27,0.5,0.0,0.15, MPI_Process = 1/
&MESH ID='Mesh_03', IJK=50,27,15, XB=1.5,2.0,0.0,0.27,0.0,0.15, MPI_Process = 2/
&MESH ID='Mesh_04', IJK=50,23,15, XB=1.5,2.0,0.27,0.5,0.0,0.15, MPI_Process = 3/
&MESH ID='Mesh_05', IJK=50,27,15, XB=2.0,2.5,0.0,0.27,0.0,0.15, MPI_Process = 4/
&MESH ID='Mesh_06', IJK=50,23,15, XB=2.0,2.5,0.27,0.5,0.0,0.15, MPI_Process = 5/
&MESH ID='Mesh_07', IJK=66,27,15, XB=2.5,3.16,0.0,0.27,0.0,0.15, MPI_Process = 6/
&MESH ID='Mesh_08', IJK=66,23,15, XB=2.5,3.16,0.27,0.5,0.0,0.15, MPI_Process = 7/
-------Spruce-------
&MATL ID = 'SPRUCE',
        EMISSIVITY = 0.9,
        CONDUCTIVITY = 0.09,
        SPECIFIC_HEAT_RAMP = 'c_ramp_spruce',
        DENSITY = 408.0,
        N_REACTIONS = 1.0,
        A(1) = 4.69E13,
        E(1) = 190500,
        N_S(1) = 1.0,
        MATL_ID(1,1) = 'CHAR',
        NU_MATL(1,1) = 0.16,
        SPEC_ID(1,1) = 'PYROLYZATE',
        NU_SPEC(1,1) = 0.84,
        HEAT_OF_REACTION(1) = 430.0,
        HEAT_OF_COMBUSTION= 14000.0,
        ABSORPTION_COEFFICIENT = 50000.0/
&RAMP ID='c_ramp_spruce', T=30, F=0.92 /
&RAMP ID='c_ramp_spruce', T=230, F=1.8 /
-------Steel (walls of tunnel)-------
&MATL ID='STEEL',
        SPECIFIC_HEAT=0.46,
        CONDUCTIVITY=45.8,
        DENSITY=7850.0,
        EMISSIVITY=0.7/
&SURF ID='STEEL_SURFACE',
        MATL_ID(1,1)='STEEL',
```

```
        MATL_MASS_FRACTION(1,1)=1.0,
        THICKNESS(1)=3.0E-3/
-------Inlet air flow-------
&SURF ID='INFLOW',
        RGB=26,204,26,
        VEL=-2.5/
-------Wood sample-------
&SURF ID='SAMPLE',
        RGB=200,100,0,
        BACKING='INSULATED',
        MATL_ID='SPRUCE',
        THICKNESS=0.12/
-------Geometry of tunnel-------
&OBST ID='Bottom_outlet', XB=1.35,2.12,0.0,0.5,0.0,0.0, SURF_ID='STEEL_SURFACE'/
&OBST ID='Bottom_inlet', XB=2.38,3.16,0.0,0.5,0.0,0.0, SURF_ID='STEEL_SURFACE'/
&OBST ID='Bottom_front', XB=2.115,2.385,0.0,0.14,0.0,0.0, SURF_ID='STEEL_SURFACE'/
&OBST ID='Bottom_back', XB=2.115,2.385,0.36,0.5,0.0,0.0, SURF_ID='STEEL_SURFACE'/
&OBST ID='Top', XB=1.35,3.16,0.0,0.5,0.15,0.15, SURF_ID='STEEL_SURFACE'/
&OBST ID='Side_Front', XB=1.35,3.16,0.0,0.0,0.0,0.15, SURF_ID='STEEL_SURFACE'/
&OBST ID='Side_Back', XB=1.35,3.16,0.5,0.5,0.0,0.15, SURF_ID='STEEL_SURFACE'/
-------Position air inflow-------
&OBST ID='Side_Inlet', XB=3.15,3.16,0.0,0.5,0.0,0.15, SURF_ID='INFLOW'/
-------Position wood sample-------
&OBST ID='WOOD_SAMPLE', XB=2.12,2.38,0.14,0.36,0.0,0.0, SURF_ID='SAMPLE'/
-------Tunnel openings-------
&VENT ID='Mesh Vent: Mesh_01 [XMAX]', SURF_ID='OPEN', XB=3.16,3.16,0.0,0.5,0.0,0.15/
&VENT ID='Mesh Vent: Mesh_01 [XMIN]', SURF_ID='OPEN', XB=1.35,1.35,0.0,0.5,0.0,0.15/
-------Output air velocity surface of wood sample -------
&DEVC ID='CM-U', QUANTITY='U-VELOCITY', XYZ=2.25,0.25,0.0/
&DEVC ID='CM-V', QUANTITY='V-VELOCITY', XYZ=2.25,0.25,0.0/
&DEVC ID='CM-W', QUANTITY='W-VELOCITY', XYZ=2.25,0.25,0.0/
&DEVC ID='CM', QUANTITY='VELOCITY', XYZ=2.25,0.25,0.0/

&DEVC ID='CF-U', QUANTITY='U-VELOCITY', XYZ=2.25,0.20,0.0/
&DEVC ID='CF-V', QUANTITY='V-VELOCITY', XYZ=2.25,0.20,0.0/
&DEVC ID='CF-W', QUANTITY='W-VELOCITY', XYZ=2.25,0.20,0.0/
&DEVC ID='CF', QUANTITY='VELOCITY', XYZ=2.25,0.20,0.0/

&DEVC ID='CB-U', QUANTITY='U-VELOCITY', XYZ=2.25,0.31,0.0/
&DEVC ID='CB-V', QUANTITY='V-VELOCITY', XYZ=2.25,0.31,0.0/
&DEVC ID='CB-W', QUANTITY='W-VELOCITY', XYZ=2.25,0.31,0.0/
&DEVC ID='CB', QUANTITY='VELOCITY', XYZ=2.25,0.31,0.0/

&DEVC ID='OM-U', QUANTITY='U-VELOCITY', XYZ=2.19,0.25,0.0/
```

```
&DEVC ID='OM-V', QUANTITY='V-VELOCITY', XYZ=2.19,0.25,0.0/
&DEVC ID='OM-W', QUANTITY='W-VELOCITY', XYZ=2.19,0.25,0.0/
&DEVC ID='OM', QUANTITY='VELOCITY', XYZ=2.19,0.25,0.0/

&DEVC ID='OF-U', QUANTITY='U-VELOCITY', XYZ=2.19,0.20,0.0/
&DEVC ID='OF-V', QUANTITY='V-VELOCITY', XYZ=2.19,0.20,0.0/
&DEVC ID='OF-W', QUANTITY='W-VELOCITY', XYZ=2.19,0.20,0.0/
&DEVC ID='OF', QUANTITY='VELOCITY', XYZ=2.19,0.20,0.0/

&DEVC ID='OB-U', QUANTITY='U-VELOCITY', XYZ=2.19,0.31,0.0/
&DEVC ID='OB-V', QUANTITY='V-VELOCITY', XYZ=2.19,0.31,0.0/
&DEVC ID='OB-W', QUANTITY='W-VELOCITY', XYZ=2.19,0.31,0.0/
&DEVC ID='OB', QUANTITY='VELOCITY', XYZ=2.19,0.31,0.0/

&DEVC ID='IM-U', QUANTITY='U-VELOCITY', XYZ=2.31,0.25,0.0/
&DEVC ID='IM-V', QUANTITY='V-VELOCITY', XYZ=2.31,0.25,0.0/
&DEVC ID='IM-W', QUANTITY='W-VELOCITY', XYZ=2.31,0.25,0.0/
&DEVC ID='IM', QUANTITY='VELOCITY', XYZ=2.31,0.25,0.0/

&DEVC ID='IF-U', QUANTITY='U-VELOCITY', XYZ=2.31,0.20,0.0/
&DEVC ID='IF-V', QUANTITY='V-VELOCITY', XYZ=2.31,0.20,0.0/
&DEVC ID='IF-W', QUANTITY='W-VELOCITY', XYZ=2.31,0.20,0.0/
&DEVC ID='IF', QUANTITY='VELOCITY', XYZ=2.31,0.20,0.0/

&DEVC ID='IB-U', QUANTITY='U-VELOCITY', XYZ=2.31,0.31,0.0/
&DEVC ID='IB-V', QUANTITY='V-VELOCITY', XYZ=2.31,0.31,0.0/
&DEVC ID='IB-W', QUANTITY='W-VELOCITY', XYZ=2.31,0.31,0.0/
&DEVC ID='IB', QUANTITY='VELOCITY', XYZ=2.31,0.31,0.0/
-------Output air velocity area above wood sample -------
&DEVC ID='CM-1-U', QUANTITY='U-VELOCITY', XYZ=2.25,0.25,0.06/
&DEVC ID='CM-1-V', QUANTITY='V-VELOCITY', XYZ=2.25,0.25,0.06/
&DEVC ID='CM-1-W', QUANTITY='W-VELOCITY', XYZ=2.25,0.25,0.06/
&DEVC ID='CM-1', QUANTITY='VELOCITY', XYZ=2.25,0.25,0.06/

&DEVC ID='CF-1-U', QUANTITY='U-VELOCITY', XYZ=2.25,0.20,0.06/
&DEVC ID='CF-1-V', QUANTITY='V-VELOCITY', XYZ=2.25,0.20,0.06/
&DEVC ID='CF-1-W', QUANTITY='W-VELOCITY', XYZ=2.25,0.20,0.06/
&DEVC ID='CF-1', QUANTITY='VELOCITY', XYZ=2.25,0.20,0.06/

&DEVC ID='CB-1-U', QUANTITY='U-VELOCITY', XYZ=2.25,0.31,0.06/
&DEVC ID='CB-1-V', QUANTITY='V-VELOCITY', XYZ=2.25,0.31,0.06/
&DEVC ID='CB-1-W', QUANTITY='W-VELOCITY', XYZ=2.25,0.31,0.06/
&DEVC ID='CB-1', QUANTITY='VELOCITY', XYZ=2.25,0.31,0.06/

&DEVC ID='OM-1-U', QUANTITY='U-VELOCITY', XYZ=2.19,0.25,0.06/
```

```
&DEVC ID='OM-1-V', QUANTITY='V-VELOCITY', XYZ=2.19,0.25,0.06/
&DEVC ID='OM-1-W', QUANTITY='W-VELOCITY', XYZ=2.19,0.25,0.06/
&DEVC ID='OM-1', QUANTITY='VELOCITY', XYZ=2.19,0.25,0.06/

&DEVC ID='OF-1-U', QUANTITY='U-VELOCITY', XYZ=2.19,0.20,0.06/
&DEVC ID='OF-1-V', QUANTITY='V-VELOCITY', XYZ=2.19,0.20,0.06/
&DEVC ID='OF-1-W', QUANTITY='W-VELOCITY', XYZ=2.19,0.20,0.06/
&DEVC ID='OF-1', QUANTITY='VELOCITY', XYZ=2.19,0.20,0.06/

&DEVC ID='OB-1-U', QUANTITY='U-VELOCITY', XYZ=2.19,0.31,0.06/
&DEVC ID='OB-1-V', QUANTITY='V-VELOCITY', XYZ=2.19,0.31,0.06/
&DEVC ID='OB-1-W', QUANTITY='W-VELOCITY', XYZ=2.19,0.31,0.06/
&DEVC ID='OB-1', QUANTITY='VELOCITY', XYZ=2.19,0.31,0.06/

&DEVC ID='IM-1-U', QUANTITY='U-VELOCITY', XYZ=2.31,0.25,0.06/
&DEVC ID='IM-1-V', QUANTITY='V-VELOCITY', XYZ=2.31,0.25,0.06/
&DEVC ID='IM-1-W', QUANTITY='W-VELOCITY', XYZ=2.31,0.25,0.06/
&DEVC ID='IM-1', QUANTITY='VELOCITY', XYZ=2.31,0.25,0.06/

&DEVC ID='IF-1-U', QUANTITY='U-VELOCITY', XYZ=2.31,0.20,0.06/
&DEVC ID='IF-1-V', QUANTITY='V-VELOCITY', XYZ=2.31,0.20,0.06/
&DEVC ID='IF-1-W', QUANTITY='W-VELOCITY', XYZ=2.31,0.20,0.06/
&DEVC ID='IF-1', QUANTITY='VELOCITY', XYZ=2.31,0.20,0.06/

&DEVC ID='IB-1-U', QUANTITY='U-VELOCITY', XYZ=2.31,0.31,0.06/
&DEVC ID='IB-1-V', QUANTITY='V-VELOCITY', XYZ=2.31,0.31,0.06/
&DEVC ID='IB-1-W', QUANTITY='W-VELOCITY', XYZ=2.31,0.31,0.06/
&DEVC ID='IB-1', QUANTITY='VELOCITY', XYZ=2.31,0.31,0.06/
-------Output air velocity at outlet-------
&DEVC ID='O-M-U', QUANTITY='U-VELOCITY', XYZ=1.35,0.25,0.07/
&DEVC ID='O-M-V', QUANTITY='V-VELOCITY', XYZ=1.35,0.25,0.07/
&DEVC ID='O-M-W', QUANTITY='W-VELOCITY', XYZ=1.35,0.25,0.07/
&DEVC ID='O-M', QUANTITY='VELOCITY', XYZ=1.35,0.25,0.07/

&DEVC ID='O-F-U', QUANTITY='U-VELOCITY', XYZ=1.35,0.12,0.07/
&DEVC ID='O-F-V', QUANTITY='V-VELOCITY', XYZ=1.35,0.12,0.07/
&DEVC ID='O-F-W', QUANTITY='W-VELOCITY', XYZ=1.35,0.12,0.07/
&DEVC ID='O-F', QUANTITY='VELOCITY', XYZ=1.35,0.12,0.07/

&DEVC ID='O-B-U', QUANTITY='U-VELOCITY', XYZ=1.35,0.37,0.07/
&DEVC ID='O-B-V', QUANTITY='V-VELOCITY', XYZ=1.35,0.37,0.07/
&DEVC ID='O-B-W', QUANTITY='W-VELOCITY', XYZ=1.35,0.37,0.07/
&DEVC ID='O-B', QUANTITY='VELOCITY', XYZ=1.35,0.37,0.07/
-------Animated output velocity-------
&SLCF QUANTITY='VELOCITY', VECTOR=.TRUE., CELL_CENTERED=.TRUE., PBY=0.25/
```

```
&SLCF QUANTITY='VELOCITY', VECTOR=.TRUE., CELL_CENTERED=.TRUE., PBX=2.25/
&SLCF QUANTITY='VELOCITY', VECTOR=.TRUE., CELL_CENTERED=.TRUE., PBZ=0.07/
-------Animated output temperature-------
&SLCF QUANTITY='TEMPERATURE', CELL_CENTERED=.TRUE., PBZ=0.07/

&TAIL /
```

B.4.6 T6-short-0.625

This is the FDS code for the simulation with the shortened FANCI geometry and a mesh size of 0.625 [cm].

```
-------Simulation name-------
&HEAD CHID='Fanci_6_0_1_nohf'/
-------Simulation time-------
&TIME T_END=300.0/
-------Mesh-------
&MESH ID='Mesh_01', IJK=24,80,24, XB=1.35,1.5,0.0,0.5,0.0,0.15, MPI_Process = 0/
&MESH ID='Mesh_02', IJK=80,42,24, XB=1.5,2.0,0.0,0.2625,0.0,0.15, MPI_Process = 1/
&MESH ID='Mesh_03', IJK=40,38,24, XB=1.5,2.0,0.2625,0.5,0.0,0.15, MPI_Process = 2/
&MESH ID='Mesh_04', IJK=80,42,24, XB=2.0,2.5,0.0,0.2625,0.0,0.15, MPI_Process = 3/
&MESH ID='Mesh_05', IJK=80,38,24, XB=2.0,2.5,0.2625,0.5,0.0,0.15, MPI_Process = 4/
&MESH ID='Mesh_06', IJK=80,42,24, XB=2.5,3.0,0.0,0.2625,0.0,0.15, MPI_Process = 5/
&MESH ID='Mesh_07', IJK=80,38,24, XB=2.5,3.0,0.2625,0.50,0.0,0.15, MPI_Process = 6/
&MESH ID='Mesh_08', IJK=25,80,24, XB=3.0,3.15625,0.0,0.5,0.0,0.15, MPI_Process = 7/
-------Spruce-------
&MATL ID = 'SPRUCE',
        EMISSIVITY = 0.9,
        CONDUCTIVITY = 0.09,
        SPECIFIC_HEAT_RAMP = 'c_ramp_spruce',
        DENSITY = 408.0,
        N_REACTIONS = 1.0,
        A(1) = 4.69E13,
        E(1) = 190500,
        N_S(1) = 1.0,
        MATL_ID(1,1) = 'CHAR',
        NU_MATL(1,1) = 0.16,
        SPEC_ID(1,1) = 'PYROLYZATE',
        NU_SPEC(1,1) = 0.84,
        HEAT_OF_REACTION(1) = 430.0,
        HEAT_OF_COMBUSTION= 14000.0,
        ABSORPTION_COEFFICIENT = 50000.0/
&RAMP ID='c_ramp_spruce', T=30, F=0.92 /
&RAMP ID='c_ramp_spruce', T=230, F=1.8 /
```

```
-------Steel (walls of tunnel)-------
&MATL ID='STEEL',
      SPECIFIC_HEAT=0.46,
      CONDUCTIVITY=45.8,
      DENSITY=7850.0,
      EMISSIVITY=0.7/
&SURF ID='STEEL_SURFACE',
      MATL_ID(1,1)='STEEL',
      MATL_MASS_FRACTION(1,1)=1.0,
      THICKNESS(1)=3.0E-3/
-------Inlet air flow-------
&SURF ID='INFLOW',
      RGB=26,204,26,
      VEL=-2.5/
-------Wood sample-------
&SURF ID='SAMPLE',
      RGB=200,100,0,
      BACKING='INSULATED',
      MATL_ID='SPRUCE',
      THICKNESS=0.12/
-------Geometry of tunnel-------
&OBST ID='Bottom_outlet', XB=1.35,2.11875,0.0,0.5,0.0,0.0, SURF_ID='STEEL_SURFACE'/
&OBST ID='Bottom_inlet', XB=2.375,3.15625,0.0,0.5,0.0,0.0, SURF_ID='STEEL_SURFACE'/
&OBST ID='Bottom_front', XB=2.1156,2.378,0.0,0.1375,0.0,0.0, SURF_ID='STEEL_SURFACE'/
&OBST ID='Bottom_back', XB=2.1156,2.378,0.3625,0.5,0.0,0.0, SURF_ID='STEEL_SURFACE'/
&OBST ID='Top', XB=1.35,3.15625,0.0,0.5,0.15,0.15, SURF_ID='STEEL_SURFACE'/
&OBST ID='Side_Front', XB=1.35,3.15625,0.0,0.0,0.0,0.15, SURF_ID='STEEL_SURFACE'/
&OBST ID='Side_Back', XB=1.35,3.15625,0.5,0.5,0.0,0.15, SURF_ID='STEEL_SURFACE'/
-------Position air inflow-------
&OBST ID='Side_Inlet', XB=3.15,3.15625,0.0,0.5,0.0,0.15, SURF_ID='INFLOW'/
-------Position wood sample-------
&OBST ID='WOOD_SAMPLE', XB=2.11875,2.375,0.1375,0.3625,0.0,0.0, SURF_ID='SAMPLE'/
-------Tunnel openings-------
&VENT ID='Mesh Vent: Mesh_01 [XMAX]', SURF_ID='OPEN',
XB=3.15625,3.15625,0.0,0.5,0.0,0.15/
&VENT ID='Mesh Vent: Mesh_01 [XMIN]', SURF_ID='OPEN', XB=1.35,1.35,0.0,0.5,0.0,0.15/
-------Output air velocity surface of wood sample -------
&DEVC ID='CM-U', QUANTITY='U-VELOCITY', XYZ=2.24375,0.25,0.0/
&DEVC ID='CM-V', QUANTITY='V-VELOCITY', XYZ=2.24375,0.25,0.0/
&DEVC ID='CM-W', QUANTITY='W-VELOCITY', XYZ=2.24375,0.25,0.0/
&DEVC ID='CM', QUANTITY='VELOCITY', XYZ=2.24375,0.25,0.0/

&DEVC ID='CF-U', QUANTITY='U-VELOCITY', XYZ=2.24375,0.19375,0.0/
&DEVC ID='CF-V', QUANTITY='V-VELOCITY', XYZ=2.24375,0.19375,0.0/
```

```
&DEVC ID='CF-W', QUANTITY='W-VELOCITY', XYZ=2.24375,0.19375,0.0/
&DEVC ID='CF', QUANTITY='VELOCITY', XYZ=2.24375,0.19375,0.0/

&DEVC ID='CB-U', QUANTITY='U-VELOCITY', XYZ=2.24375,0.3,0.0/
&DEVC ID='CB-V', QUANTITY='V-VELOCITY', XYZ=2.24375,0.3,0.0/
&DEVC ID='CB-W', QUANTITY='W-VELOCITY', XYZ=2.24375,0.3,0.0/
&DEVC ID='CB', QUANTITY='VELOCITY', XYZ=2.24375,0.3,0.0/

&DEVC ID='OM-U', QUANTITY='U-VELOCITY', XYZ=2.18125,0.25,0.0/
&DEVC ID='OM-V', QUANTITY='V-VELOCITY', XYZ=2.18125,0.25,0.0/
&DEVC ID='OM-W', QUANTITY='W-VELOCITY', XYZ=2.18125,0.25,0.0/
&DEVC ID='OM', QUANTITY='VELOCITY', XYZ=2.1825,0.25,0.0/

&DEVC ID='OF-U', QUANTITY='U-VELOCITY', XYZ=2.18125,0.19375,0.0/
&DEVC ID='OF-V', QUANTITY='V-VELOCITY', XYZ=2.18125,0.19375,0.0/
&DEVC ID='OF-W', QUANTITY='W-VELOCITY', XYZ=2.18125,0.19375,0.0/
&DEVC ID='OF', QUANTITY='VELOCITY', XYZ=2.18125,0.19375,0.0/

&DEVC ID='OB-U', QUANTITY='U-VELOCITY', XYZ=2.18125,0.30625,0.0/
&DEVC ID='OB-V', QUANTITY='V-VELOCITY', XYZ=2.18125,0.30625,0.0/
&DEVC ID='OB-W', QUANTITY='W-VELOCITY', XYZ=2.18125,0.30625,0.0/
&DEVC ID='OB', QUANTITY='VELOCITY', XYZ=2.18125,0.30625,0.0/

&DEVC ID='IM-U', QUANTITY='U-VELOCITY', XYZ=2.30625,0.25,0.0/
&DEVC ID='IM-V', QUANTITY='V-VELOCITY', XYZ=2.30625,0.25,0.0/
&DEVC ID='IM-W', QUANTITY='W-VELOCITY', XYZ=2.30625,0.25,0.0/
&DEVC ID='IM', QUANTITY='VELOCITY', XYZ=2.30625,0.25,0.0/

&DEVC ID='IF-U', QUANTITY='U-VELOCITY', XYZ=2.30625,0.19375,0.0/
&DEVC ID='IF-V', QUANTITY='V-VELOCITY', XYZ=2.30625,0.19375,0.0/
&DEVC ID='IF-W', QUANTITY='W-VELOCITY', XYZ=2.30625,0.19375,0.0/
&DEVC ID='IF', QUANTITY='VELOCITY', XYZ=2.30625,0.19375,0.0/

&DEVC ID='IB-U', QUANTITY='U-VELOCITY', XYZ=2.30625,0.30625,0.0/
&DEVC ID='IB-V', QUANTITY='V-VELOCITY', XYZ=2.30625,0.30625,0.0/
&DEVC ID='IB-W', QUANTITY='W-VELOCITY', XYZ=2.30625,0.30625,0.0/
&DEVC ID='IB', QUANTITY='VELOCITY', XYZ=2.30625,0.30625,0.0/
-------Output air velocity area above wood sample -------
&DEVC ID='CM-1-U', QUANTITY='U-VELOCITY', XYZ=2.2375,0.25,0.0375/
&DEVC ID='CM-1-V', QUANTITY='V-VELOCITY', XYZ=2.2375,0.25,0.0375/
&DEVC ID='CM-1-W', QUANTITY='W-VELOCITY', XYZ=2.2375,0.25,0.0375/
&DEVC ID='CM-1', QUANTITY='VELOCITY', XYZ=2.2375,0.25,0.0375/

&DEVC ID='CF-1-U', QUANTITY='U-VELOCITY', XYZ=2.2375,0.125,0.0375/
&DEVC ID='CF-1-V', QUANTITY='V-VELOCITY', XYZ=2.2375,0.125,0.0375/
```

```
&DEVC ID='CF-1-W', QUANTITY='W-VELOCITY', XYZ=2.2375,0.125,0.0375/
&DEVC ID='CF-1', QUANTITY='VELOCITY', XYZ=2.2375,0.125,0.0375/

&DEVC ID='CB-1-U', QUANTITY='U-VELOCITY', XYZ=2.2375,0.375,0.0375/
&DEVC ID='CB-1-V', QUANTITY='V-VELOCITY', XYZ=2.2375,0.375,0.0375/
&DEVC ID='CB-1-W', QUANTITY='W-VELOCITY', XYZ=2.2375,0.375,0.0375/
&DEVC ID='CB-1', QUANTITY='VELOCITY', XYZ=2.2375,0.375,0.0375/

&DEVC ID='OM-1-U', QUANTITY='U-VELOCITY', XYZ=2.175,0.25,0.0375/
&DEVC ID='OM-1-V', QUANTITY='V-VELOCITY', XYZ=2.175,0.25,0.0375/
&DEVC ID='OM-1-W', QUANTITY='W-VELOCITY', XYZ=2.175,0.25,0.0375/
&DEVC ID='OM-1', QUANTITY='VELOCITY', XYZ=2.175,0.25,0.0375/

&DEVC ID='OF-1-U', QUANTITY='U-VELOCITY', XYZ=2.175,0.125,0.0375/
&DEVC ID='OF-1-V', QUANTITY='V-VELOCITY', XYZ=2.175,0.125,0.0375/
&DEVC ID='OF-1-W', QUANTITY='W-VELOCITY', XYZ=2.175,0.125,0.0375/
&DEVC ID='OF-1', QUANTITY='VELOCITY', XYZ=2.175,0.125,0.0375/

&DEVC ID='OB-1-U', QUANTITY='U-VELOCITY', XYZ=2.175,0.375,0.0375/
&DEVC ID='OB-1-V', QUANTITY='V-VELOCITY', XYZ=2.175,0.375,0.0375/
&DEVC ID='OB-1-W', QUANTITY='W-VELOCITY', XYZ=2.175,0.375,0.0375/
&DEVC ID='OB-1', QUANTITY='VELOCITY', XYZ=2.175,0.375,0.0375/

&DEVC ID='IM-1-U', QUANTITY='U-VELOCITY', XYZ=2.3,0.25,0.0375/
&DEVC ID='IM-1-V', QUANTITY='V-VELOCITY', XYZ=2.3,0.25,0.0375/
&DEVC ID='IM-1-W', QUANTITY='W-VELOCITY', XYZ=2.3,0.25,0.0375/
&DEVC ID='IM-1', QUANTITY='VELOCITY', XYZ=2.3,0.25,0.0375/

&DEVC ID='IF-1-U', QUANTITY='U-VELOCITY', XYZ=2.3,0.125,0.0375/
&DEVC ID='IF-1-V', QUANTITY='V-VELOCITY', XYZ=2.3,0.125,0.0375/
&DEVC ID='IF-1-W', QUANTITY='W-VELOCITY', XYZ=2.3,0.125,0.0375/
&DEVC ID='IF-1', QUANTITY='VELOCITY', XYZ=2.3,0.125,0.0375/

&DEVC ID='IB-1-U', QUANTITY='U-VELOCITY', XYZ=2.3,0.375,0.0375/
&DEVC ID='IB-1-V', QUANTITY='V-VELOCITY', XYZ=2.3,0.375,0.0375/
&DEVC ID='IB-1-W', QUANTITY='W-VELOCITY', XYZ=2.3,0.375,0.0375/
&DEVC ID='IB-1', QUANTITY='VELOCITY', XYZ=2.3,0.375,0.0375/
-------Output air velocity at outlet-------
&DEVC ID='O-M-U', QUANTITY='U-VELOCITY', XYZ=1.35,0.25,0.075/
&DEVC ID='O-M-V', QUANTITY='V-VELOCITY', XYZ=1.35,0.25,0.075/
&DEVC ID='O-M-W', QUANTITY='W-VELOCITY', XYZ=1.35,0.25,0.075/
&DEVC ID='O-M', QUANTITY='VELOCITY', XYZ=1.35,0.25,0.075/

&DEVC ID='O-F-U', QUANTITY='U-VELOCITY', XYZ=1.35,0.125,0.075/
&DEVC ID='O-F-V', QUANTITY='V-VELOCITY', XYZ=1.35,0.125,0.075/
```

```
&DEVC ID='O-F-W', QUANTITY='W-VELOCITY', XYZ=1.35,0.125,0.075/
&DEVC ID='O-F', QUANTITY='VELOCITY', XYZ=1.35,0.125,0.075/

&DEVC ID='O-B-U', QUANTITY='U-VELOCITY', XYZ=1.35,0.375,0.075/
&DEVC ID='O-B-V', QUANTITY='V-VELOCITY', XYZ=1.35,0.375,0.075/
&DEVC ID='O-B-W', QUANTITY='W-VELOCITY', XYZ=1.35,0.375,0.075/
&DEVC ID='O-B', QUANTITY='VELOCITY', XYZ=1.35,0.375,0.075/
-------Animated output velocity-------
&SLCF QUANTITY='VELOCITY', VECTOR=.TRUE., CELL_CENTERED=.TRUE., PBY=0.25/
&SLCF QUANTITY='VELOCITY', VECTOR=.TRUE., CELL_CENTERED=.TRUE., PBX=2.2375/
&SLCF QUANTITY='VELOCITY', VECTOR=.TRUE., CELL_CENTERED=.TRUE., PBZ=0.075/
-------Animated output temperature-------
&SLCF QUANTITY='TEMPERATURE', CELL_CENTERED=.TRUE., PBZ=0.075/

&TAIL /
```

Appendix C – Calculation of Reynolds number

The Reynolds number Re can be calculated by the following equation [37]:

$$Re = \frac{u*D_h}{v} \quad (22)$$

Where:

- u Air velocity, 2.0 [m/s]
- D_h Hydraulic diameter of tunnel, [m]
- v Kinematic viscosity of air, at 20 [°C], 15.06*10^{-6} [m^2/s] [38]

The hydraulic diameter can be calculated with equation 23 and is 0.23 [m].

$$D_h = \frac{4*\mathrm{A}}{P} \quad (23)$$

Where:

- A Cross-section of tunnel, 0.075 [m^2]
- P Perimeter of tunnel, 1.3 [m]

By that, the Reynolds number becomes 30544 which is higher than 5000 and therefore is characterize as a turbulent flow.

Appendix D – Calibration of the heat panel ("S2-HP")

D.1 Estimation of heat flux from the heat panel

To get a rough idea of the emitting heat flux from the heat panel, an estimation of it is done by the following equations. The incident heat flux I [kW/m^2] on a surface by a radiative panel can be calculated by [39, p. 30]

$$I = \varphi * \alpha * I_{EC} \quad (24)$$

Where:

- I Receiving heat flux on a surface, [kW/m^2]
- φ Configuration factor, [-]
- α Ratio of radiant surface divided by area of enclosed rectangle, [-]
- I_{EC} Emitted heat flux from a heating source, [kW/m^2]

For the simulation situation, the receiving heat flux on a surface is known but the emitted heat flux is to calculate, therefore:

$$I_{EC} = \frac{I}{\varphi * \alpha} \quad (25)$$

The receiving heat flux I is equal to the estimated incident heat flux in the experiment which is 96.4 [kW/m^2] and α is equal to 1. The configuration factor is estimated by the following equation which is for emitting rectangle positioned opposite a receiving point [38, p. 30].

$$\varphi_1 = \frac{1}{2\pi}\left[\frac{X}{\sqrt{X^2+Z^2}}\arctan\left(\frac{Y}{\sqrt{X^2+Z^2}}\right) + \frac{Y}{\sqrt{Y^2+Z^2}}\arctan\left(\frac{Z}{\sqrt{X^2+Y^2}}\right)\right] \quad (26)$$

Where:

- X Longer side of emitting surface, 0.56 [m]
- Y Distance between the emitting surface and the receiving point, 0.15 [m]
- Z Shorter side from emitting surface, 0.139 [m]

Given that in the equation for configuration factor above the receiving point is positioned at a corner of the emitting surface, the total configuration factor φ is equal to $4 * \varphi_1$. With the above given numbers, $\varphi = 4 * 0.182 = 0.727$. Therefore, the estimated emitting heat flux is 132.6 [kW/m^2].

D.2 Test simulations

The estimated emitting heat flux from the heat panel was tested in the simulation environment of the FANCI experiment as described under chapter 3.5.1 “Implementation” except for one modification. The timber surface was replaced by an inert material (“INERT”) and no burning took place. The incident heat flux at the position of the timber sample surface is measured by the output quantity “NET_HEAT_FLUX”. Three measuring points are positioned on the surface, one in the center of the surface, one closer to the back side wall and one closer to the front side wall. A heat panel was added on the ceiling opposite and centered above the timber sample with dimensions 0.56 [m] by 0.39 [m]. The estimated heat flux was placed as a heating source on that heat panel by the code “NET_HEAT_FLUX”. This forces FDS to keep the combination of radiative and convective heat flux from the heat panel equal to the specified value [21, p. 87].

The first test simulation with a heat panel at 132 [kW/m^2] resulted in a too high incident heat flux on the timber sample. Therefore, heat fluxes at 120 and 125 [kW/m^2] were tested. The FDS codes are displayed under D.3.

The mean of the three recorded positions of the incident heat fluxes on the timber sample surface are shown in table 50.

Table 50: Mean heat flux on the surface depending on the emitting heat flux on the heat panel as well as the corresponding values from the experiment

Emitting heat flux	120 [kW/m^2]	125 [kW/m^2]	Experiment
Mean heat flux on wood surface	98.3	102.8	96.4

The simulation with a heat panel at 120 [kW/m^2] resulted in a very similar incident heat flux as the one from the experiment. Therefore, that value was chosen as the heat flux for the simulation with a heat panel.

D.3 FDS code for testing a heat panel

D.3.1 FDS code for a heat flux of 120 [kW/m^2]

```
Fanci_11_3_nb_1206s_120_20.fds
&HEAD CHID='Fanci_11_3_nb_1206s_120_20'/
&TIME T_END=1206.0/
-------Mesh-------
&MESH ID='Mesh_01', IJK=40,27,15, XB=1.6,2.0,0.0,0.27,0.0,0.15, MPI_Process = 0/
&MESH ID='Mesh_02', IJK=40,23,15, XB=1.6,2.0,0.27,0.5,0.0,0.15, MPI_Process = 1/
&MESH ID='Mesh_03', IJK=50,27,15, XB=2.0,2.5,0.0,0.27,0.0,0.15, MPI_Process = 2/
&MESH ID='Mesh_04', IJK=50,23,15, XB=2.0,2.5,0.27,0.5,0.0,0.15, MPI_Process = 3/
&MESH ID='Mesh_05', IJK=50,27,15, XB=2.5,3.0,0.0,0.27,0.0,0.15, MPI_Process = 4/
&MESH ID='Mesh_06', IJK=50,23,15, XB=2.5,3.0,0.27,0.5,0.0,0.15, MPI_Process = 5/
```

```
&MESH ID='Mesh_07', IJK=50,27,15, XB=3.0,3.5,0.0,0.27,0.0,0.15, MPI_Process = 6/
&MESH ID='Mesh_08', IJK=50,23,15, XB=3.0,3.5,0.27,0.5,0.0,0.15, MPI_Process = 7/
&MESH ID='Mesh_09', IJK=31,27,15, XB=3.5,3.81,0.0,0.27,0.0,0.15, MPI_Process = 8/
&MESH ID='Mesh_10', IJK=31,23,15, XB=3.5,3.81,0.27,0.5,0.0,0.15, MPI_Process = 9/
-------Steel (walls of tunnel)-------
&MATL ID='STEEL',
      SPECIFIC_HEAT=0.46,
      CONDUCTIVITY=45.8,
      DENSITY=7850.0,
      EMISSIVITY=0.7/
&SURF ID='STEEL_SURFACE',
      MATL_ID(1,1)='STEEL',
      MATL_MASS_FRACTION(1,1)=1.0,
      THICKNESS(1)=3.0E-3/
-------Inlet air flow-------
&SURF ID='INFLOW',
      RGB=26,204,26,
      VEL=-2.0/
-------Heat panel-------
&SURF ID='HEAT_PANEL_SURFACE',
      COLOR='RED',
      NET_HEAT_FLUX=120/
-------Geometry of tunnel-------
&OBST ID='Bottom_outlet', XB=1.6,2.12,0.0,0.5,0.0,0.0, SURF_ID='STEEL_SURFACE'/
&OBST ID='Bottom_inlet', XB=2.38,3.81,0.0,0.5,0.0,0.0, SURF_ID='STEEL_SURFACE'/
&OBST ID='Bottom_front', XB=2.115,2.385,0.0,0.14,0.0,0.0, SURF_ID='STEEL_SURFACE'/
&OBST ID='Bottom_back', XB=2.115,2.385,0.36,0.5,0.0,0.0, SURF_ID='STEEL_SURFACE'/
&OBST ID='Top_outlet', XB=1.6,1.97,0.0,0.5,0.15,0.15, SURF_ID='STEEL_SURFACE'/
&OBST ID='Top_inlet', XB=2.53,3.81,0.0,0.5,0.15,0.15, SURF_ID='STEEL_SURFACE'/
&OBST ID='Top_front', XB=1.965,2.535,0.0,0.05,0.15,0.15, SURF_ID='STEEL_SURFACE'/
&OBST ID='Top_back', XB=1.965,2.535,0.44,0.5,0.15,0.15, SURF_ID='STEEL_SURFACE'/
&OBST ID='Side_Front', XB=1.6,3.81,0.0,0.0,0.0,0.15, SURF_ID='STEEL_SURFACE'/
&OBST ID='Side_Back', XB=1.6,3.81,0.5,0.5,0.0,0.15, SURF_ID='STEEL_SURFACE'/
&OBST ID='Side_Inlet', XB=3.8,3.81,0.0,0.5,0.0,0.15, SURF_ID='INFLOW'/
-------Wood sample turned inert-------
&OBST ID='WOOD_SAMPLE', XB=2.12,2.38,0.14,0.36,0.0,0.0, SURF_ID='INERT'/
-------Position of heat panel-------
&VENT ID='HEAT_PANEL_FLOW', XB=1.97,2.53,0.05,0.44,0.15,0.15,
SURF_ID='HEAT_PANEL_SURFACE', IOR=-3 /
-------Tunnel openings-------
&VENT ID='Mesh Vent: Mesh_01 [XMAX]', SURF_ID='OPEN', XB=3.81,3.81,0.0,0.5,0.0,0.15/
&VENT ID='Mesh Vent: Mesh_01 [XMIN]', SURF_ID='OPEN', XB=1.6,1.6,0.0,0.5,0.0,0.15/
-------Recording NET_HEAT_FLUX-------
&DEVC ID='HF_M', QUANTITY='NET HEAT FLUX', XYZ=2.25,0.25,0.0, IOR=3/
```

```
&DEVC ID='HF_B', QUANTITY='NET HEAT FLUX', XYZ=2.25,0.31,0.0, IOR=3/
&DEVC ID='HF_F', QUANTITY='NET HEAT FLUX', XYZ=2.25,0.20,0.0, IOR=3/
-------Other heat flux recording on wood surface-------
&DEVC ID='IHF_M', QUANTITY='INCIDENT HEAT FLUX', XYZ=2.25,0.25,0.0, IOR=3/
&DEVC ID='IHF_B', QUANTITY='INCIDENT HEAT FLUX', XYZ=2.25,0.31,0.0, IOR=3/
&DEVC ID='IHF_F', QUANTITY='INCIDENT HEAT FLUX', XYZ=2.25,0.20,0.0, IOR=3/
&DEVC ID='GHF_M', QUANTITY='GAUGE HEAT FLUX', XYZ=2.25,0.25,0.0, IOR=3/
&DEVC ID='GHF_B', QUANTITY='GAUGE HEAT FLUX', XYZ=2.25,0.31,0.0, IOR=3/
&DEVC ID='GHF_F', QUANTITY='GAUGE HEAT FLUX', XYZ=2.25,0.20,0.0, IOR=3/
-------Temperature recording on wood surface-------
&DEVC ID='T_M', QUANTITY='TEMPERATURE', XYZ=2.25,0.25,0.0, IOR=3/
&DEVC ID='T_B', QUANTITY='TEMPERATURE', XYZ=2.25,0.31,0.0, IOR=3/
&DEVC ID='T_F', QUANTITY='TEMPERATURE', XYZ=2.25,0.20,0.0, IOR=3/
-------Animated output air velocity-------
&SLCF QUANTITY='VELOCITY', VECTOR=.TRUE., CELL_CENTERED=.TRUE., PBY=0.25/
&SLCF QUANTITY='VELOCITY', VECTOR=.TRUE., CELL_CENTERED=.TRUE., PBX=2.25/
&SLCF QUANTITY='VELOCITY', VECTOR=.TRUE., CELL_CENTERED=.TRUE., PBZ=0.07/
-------Animated output temperature-------
&SLCF QUANTITY='TEMPERATURE', CELL_CENTERED=.TRUE., PBZ=0.07/

&TAIL /
```

D.3.2 FDS code for a heat flux of 125 [kW/m^2]

This is the same code as in the subsection before, except for the following subchapter:

```
-------Heat panel-------
&SURF ID='HEAT_PANEL_SURFACE',
      COLOR='RED',
      NET_HEAT_FLUX=125/
```

D.3.2 FDS code for a heat flux of 132 [kW/m^2]

This is the same code as in the subsection before, except for the following subchapter:

```
-------Heat panel-------
&SURF ID='HEAT_PANEL_SURFACE',
      COLOR='RED',
      NET_HEAT_FLUX=132/
```

Appendix E – FDS codes

The following sections describe the different simulation codes in FDS. The first section summarizes the codes with ignition by an external heat flux and the second section the codes for ignition by a heat panel.

E.1 "S1-exHF-fine"

The following code is for the standard case with ignition by an external heat flux over the timber sample.

Fanci_12_5_1206s_20_outputs1.fds

```
-------Simulation name-------
&HEAD CHID=' Fanci_12_5_1206s_20_outputs1/
-------Simulation time-------
&TIME T_END=1206.0/
-------Mesh-------
&MESH ID='Mesh_01', IJK=40,27,15, XB=1.6,2.0,0.0,0.27,0.0,0.15, MPI_Process = 0/
&MESH ID='Mesh_02', IJK=40,23,15, XB=1.6,2.0,0.27,0.5,0.0,0.15, MPI_Process = 1/
&MESH ID='Mesh_03', IJK=50,27,15, XB=2.0,2.5,0.0,0.27,0.0,0.15, MPI_Process = 2/
&MESH ID='Mesh_04', IJK=50,23,15, XB=2.0,2.5,0.27,0.5,0.0,0.15, MPI_Process = 3/
&MESH ID='Mesh_05', IJK=50,27,15, XB=2.5,3.0,0.0,0.27,0.0,0.15, MPI_Process = 4/
&MESH ID='Mesh_06', IJK=50,23,15, XB=2.5,3.0,0.27,0.5,0.0,0.15, MPI_Process = 5/
&MESH ID='Mesh_07', IJK=50,27,15, XB=3.0,3.5,0.0,0.27,0.0,0.15, MPI_Process = 6/
&MESH ID='Mesh_08', IJK=50,23,15, XB=3.0,3.5,0.27,0.5,0.0,0.15, MPI_Process = 7/
&MESH ID='Mesh_09', IJK=31,27,15, XB=3.5,3.81,0.0,0.27,0.0,0.15, MPI_Process = 8/
&MESH ID='Mesh_10', IJK=31,23,15, XB=3.5,3.81,0.27,0.5,0.0,0.15, MPI_Process = 9/
-------Gas combustion-------
&REAC FUEL='PYROLYZATE', C=1, H=3.584, O=1.55, N=0, SOOT_YIELD=0.015,
HEAT_OF_COMBUSTION= 14000 /
-------Fuel (gaseous)-------
&SPEC ID = 'PYROLYZATE',
      FORMULA='C1H3.584O1.55',
      CONDUCTIVITY= 0.09,
      DIFFUSIVITY=4.30E-7,
      VISCOSITY=0.00059,
      RADCAL_ID='METHANOL' /
-------Spruce-------
&MATL ID = 'SPRUCE',
      EMISSIVITY = 0.9,
      CONDUCTIVITY = 0.09,
      SPECIFIC_HEAT_RAMP = 'c_ramp_spruce',
      DENSITY = 408.0,
      N_REACTIONS = 1.0,
      A(1) = 4.69E13,
      E(1) = 190500,
```

```
        N_S(1) = 1.0,
        MATL_ID(1,1) = 'CHAR',
        NU_MATL(1,1) = 0.16,
        SPEC_ID(1,1) = 'PYROLYZATE',
        NU_SPEC(1,1) = 0.84,
        HEAT_OF_REACTION(1) = 430.0,
        HEAT_OF_COMBUSTION= 14000.0,
        ABSORPTION_COEFFICIENT = 50000.0/
&RAMP ID='c_ramp_spruce', T=30, F=0.92 /
&RAMP ID='c_ramp_spruce', T=230, F=1.8 /
-------Char-------
&MATL ID='CHAR',
        EMISSIVITY = 0.85,
        DENSITY = 59,
        CONDUCTIVITY = 0.22,
        SPECIFIC_HEAT_RAMP = 'c_ramp_char'/
&RAMP ID='c_ramp_char', T=20, F=0.682 /
&RAMP ID='c_ramp_char', T=60, F=0.889 /
&RAMP ID='c_ramp_char', T=100, F=1.037 /
&RAMP ID='c_ramp_char', T=140, F=1.148 /
&RAMP ID='c_ramp_char', T=180, F=1.234 /
&RAMP ID='c_ramp_char', T=220, F=1.304 /
&RAMP ID='c_ramp_char', T=260, F=1.362 /
&RAMP ID='c_ramp_char', T=300, F=1.411 /
&RAMP ID='c_ramp_char', T=350, F=1.462 /
&RAMP ID='c_ramp_char', T=400, F=1.507 /
&RAMP ID='c_ramp_char', T=450, F=1.547 /
-------Steel (walls of tunnel)-------
&MATL ID='STEEL',
        SPECIFIC_HEAT=0.46,
        CONDUCTIVITY=45.8,
        DENSITY=7850.0,
        EMISSIVITY=0.7/
&SURF ID='STEEL_SURFACE',
        MATL_ID(1,1)='STEEL',
        MATL_MASS_FRACTION(1,1)=1.0,
        THICKNESS(1)=3.0E-3/
-------Inlet air flow-------
&SURF ID='INFLOW',
        RGB=26,204,26,
        VEL=-2.0/
-------Wood sample-------
&SURF ID='SAMPLE',
        RGB=200,100,0,
```

```
        BACKING='INSULATED',
        MATL_ID='SPRUCE',
        THICKNESS=0.12,
        STRETCH_FACTOR(1)=1,
        EXTERNAL_FLUX = 96.3963/
-------Geometry of tunnel-------
&OBST ID='Bottom_outlet', XB=1.6,2.12,0.0,0.5,0.0,0.0, SURF_ID='STEEL_SURFACE'/
&OBST ID='Bottom_inlet', XB=2.38,3.81,0.0,0.5,0.0,0.0, SURF_ID='STEEL_SURFACE'/
&OBST ID='Bottom_front', XB=2.115,2.385,0.0,0.14,0.0,0.0, SURF_ID='STEEL_SURFACE'/
&OBST ID='Bottom_back', XB=2.115,2.385,0.36,0.5,0.0,0.0, SURF_ID='STEEL_SURFACE'/
&OBST ID='Top', XB=1.6,3.81,0.0,0.5,0.15,0.15, SURF_ID='STEEL_SURFACE'/
&OBST ID='Side_Front', XB=1.6,3.81,0.0,0.0,0.0,0.15, SURF_ID='STEEL_SURFACE'/
&OBST ID='Side_Back', XB=1.6,3.81,0.5,0.5,0.0,0.15, SURF_ID='STEEL_SURFACE'/
-------Position air inflow-------
&OBST ID='Side_Inlet', XB=3.8,3.81,0.0,0.5,0.0,0.15, SURF_ID='INFLOW'/
-------Position wood sample-------
&OBST ID='WOOD_SAMPLE', XB=2.12,2.38,0.14,0.36,0.0,0.0, SURF_ID='SAMPLE'/
-------Tunnel openings-------
&VENT ID='Mesh Vent: Mesh_01 [XMAX]', SURF_ID='OPEN', XB=3.81,3.81,0.0,0.5,0.0,0.15/
&VENT ID='Mesh Vent: Mesh_01 [XMIN]', SURF_ID='OPEN', XB=1.6,1.6,0.0,0.5,0.0,0.15/
-------Output temperature inside wood sample-------
&PROF ID='Temp', XYZ=2.25, 0.25, 0.005, QUANTITY='TEMPERATURE', IOR=3 /
-------Output temperature on wood surface(1)-------
&DEVC XYZ=2.25, 0.25, 0.005, QUANTITY='WALL TEMPERATURE', IOR=3, ID='Wall_temp_devc' /
-------Output density inside wood sample-------
&PROF ID='Density', XYZ=2.25, 0.25, 0.005, QUANTITY='DENSITY', IOR=3 /
&PROF ID='Spruce_density', XYZ=2.25, 0.25, 0.005, QUANTITY='SPRUCE', IOR=3 /
&PROF ID='Char_density', XYZ=2.25, 0.25, 0.005, QUANTITY='CHAR', IOR=3 /
-------Output solid density on wood surface-------
&DEVC ID='Solid_density_spruce', XYZ=2.25, 0.25, 0.0, QUANTITY='SOLID DENSITY',
MATL_ID='SPRUCE', IOR=3 /
&DEVC ID='Solid_density_char', XYZ=2.25, 0.25, 0.0, QUANTITY='SOLID DENSITY',
MATL_ID='CHAR', IOR=3 /
-------Output surface density on wood surface-------
&DEVC ID='Surface_density', XYZ=2.25, 0.25, 0.0, IOR = 3, QUANTITY = 'SURFACE DENSITY' /
&DEVC ID='Surface_density_spruce', XYZ=2.25, 0.25, 0.0, IOR = 3, QUANTITY = 'SURFACE
DENSITY', MATL_ID='SPRUCE' /
&DEVC ID='Surface_density_char', XYZ=2.25, 0.25, 0.0, IOR = 3, QUANTITY = 'SURFACE DENSITY',
MATL_ID='CHAR' /
-------Output temperatures on wood surface(2)-------
&DEVC ID='CM-T', QUANTITY='TEMPERATURE', XYZ=2.25,0.25,0.0/
&DEVC ID='CF-T', QUANTITY='TEMPERATURE', XYZ=2.25,0.20,0.0/
&DEVC ID='CB-T', QUANTITY='TEMPERATURE', XYZ=2.25,0.30,0.0/
&DEVC ID='OM-T', QUANTITY='TEMPERATURE', XYZ=2.19,0.25,0.0/
```

```
&DEVC ID='OF-T', QUANTITY='TEMPERATURE', XYZ=2.19,0.20,0.0/
&DEVC ID='OB-T', QUANTITY='TEMPERATURE', XYZ=2.19,0.30,0.0/
&DEVC ID='IM-T', QUANTITY='TEMPERATURE', XYZ=2.31,0.25,0.0/
&DEVC ID='IF-T', QUANTITY='TEMPERATURE', XYZ=2.31,0.20,0.0/
&DEVC ID='IB-T', QUANTITY='TEMPERATURE', XYZ=2.31,0.30,0.0/
-------Output gas temperatures-------
&DEVC ID='C1-T', QUANTITY='TEMPERATURE', XYZ=2.0,0.25,0.07/ at end of fire chamber
&DEVC ID='C2-T', QUANTITY='TEMPERATURE', XYZ=1.8,0.25,0.07/ a little further away from fire
chamber
&DEVC ID='C3-T', QUANTITY='TEMPERATURE', XYZ=1.7,0.25,0.07/ a little further away from fire
chamber
&DEVC ID='C4-T', QUANTITY='TEMPERATURE', XYZ=1.6,0.25,0.07/ a little further away from fire
chamber
&DEVC ID='C01-T', QUANTITY='TEMPERATURE', XYZ=2.7,0.25,0.07/ before fire chamber
&DEVC ID='C02-T', QUANTITY='TEMPERATURE', XYZ=2.5,0.25,0.07/ before fire chamber
&DEVC ID='CM0-T', QUANTITY='TEMPERATURE', XYZ=2.25,0.25,0.07/ center of fire chamber
-------Output velocity-------
&DEVC ID='CIA-V-U', QUANTITY='U-VELOCITY', XYZ=3.70,0.25,0.07/
&DEVC ID='CIA-V-V', QUANTITY='V-VELOCITY', XYZ=3.70,0.25,0.07/
&DEVC ID='CIA-V-W', QUANTITY='W-VELOCITY', XYZ=3.70,0.25,0.07/
&DEVC ID='CIA-V', QUANTITY='VELOCITY', XYZ=3.70,0.25,0.07/

&DEVC ID='CIB-V-U', QUANTITY='U-VELOCITY', XYZ=3.50,0.25,0.07/
&DEVC ID='CIB-V-V', QUANTITY='V-VELOCITY', XYZ=3.50,0.25,0.07/
&DEVC ID='CIB-V-W', QUANTITY='W-VELOCITY', XYZ=3.50,0.25,0.07/
&DEVC ID='CIB-V', QUANTITY='VELOCITY', XYZ=3.50,0.25,0.07/

&DEVC ID='CIC-V-U', QUANTITY='U-VELOCITY', XYZ=3.30,0.25,0.07/
&DEVC ID='CIC-V-V', QUANTITY='V-VELOCITY', XYZ=3.30,0.25,0.07/
&DEVC ID='CIC-V-W', QUANTITY='W-VELOCITY', XYZ=3.30,0.25,0.07/
&DEVC ID='CIC-V', QUANTITY='VELOCITY', XYZ=3.30,0.25,0.07/

&DEVC ID='CI1-V-U', QUANTITY='U-VELOCITY', XYZ=3.10,0.25,0.07/
&DEVC ID='CI1-V-V', QUANTITY='V-VELOCITY', XYZ=3.10,0.25,0.07/
&DEVC ID='CI1-V-W', QUANTITY='W-VELOCITY', XYZ=3.10,0.25,0.07/
&DEVC ID='CI1-V', QUANTITY='VELOCITY', XYZ=3.10,0.25,0.07/

&DEVC ID='CI2-V-U', QUANTITY='U-VELOCITY', XYZ=2.90,0.25,0.07/
&DEVC ID='CI2-V-V', QUANTITY='V-VELOCITY', XYZ=2.90,0.25,0.07/
&DEVC ID='CI2-V-W', QUANTITY='W-VELOCITY', XYZ=2.90,0.25,0.07/
&DEVC ID='CI2-V', QUANTITY='VELOCITY', XYZ=2.90,0.25,0.07/

&DEVC ID='CI3-V-U', QUANTITY='U-VELOCITY', XYZ=2.70,0.25,0.07/
&DEVC ID='CI3-V-V', QUANTITY='V-VELOCITY', XYZ=2.70,0.25,0.07/
```

```
&DEVC ID='CI3-V-W', QUANTITY='W-VELOCITY', XYZ=2.70,0.25,0.07/
&DEVC ID='CI3-V', QUANTITY='VELOCITY', XYZ=2.70,0.25,0.07/

&DEVC ID='CI4-V-U', QUANTITY='U-VELOCITY', XYZ=2.50,0.25,0.07/
&DEVC ID='CI4-V-V', QUANTITY='V-VELOCITY', XYZ=2.50,0.25,0.07/
&DEVC ID='CI4-V-W', QUANTITY='W-VELOCITY', XYZ=2.50,0.25,0.07/
&DEVC ID='CI4-V', QUANTITY='VELOCITY', XYZ=2.50,0.25,0.07/

&DEVC ID='CM-V-U', QUANTITY='U-VELOCITY', XYZ=2.25,0.25,0.07/
&DEVC ID='CM-V-V', QUANTITY='V-VELOCITY', XYZ=2.25,0.25,0.07/
&DEVC ID='CM-V-W', QUANTITY='W-VELOCITY', XYZ=2.25,0.25,0.07/
&DEVC ID='CM-V', QUANTITY='VELOCITY', XYZ=2.25,0.25,0.07/

&DEVC ID='CO1-V-U', QUANTITY='U-VELOCITY', XYZ=2.0,0.25,0.07/
&DEVC ID='CO1-V-V', QUANTITY='V-VELOCITY', XYZ=2.0,0.25,0.07/
&DEVC ID='CO1-V-W', QUANTITY='W-VELOCITY', XYZ=2.0,0.25,0.07/
&DEVC ID='CO1-V', QUANTITY='VELOCITY', XYZ=2.0,0.25,0.07/

&DEVC ID='CO2-V-U', QUANTITY='U-VELOCITY', XYZ=1.8,0.25,0.07/
&DEVC ID='CO2-V-V', QUANTITY='V-VELOCITY', XYZ=1.8,0.25,0.07/
&DEVC ID='CO2-V-W', QUANTITY='W-VELOCITY', XYZ=1.8,0.25,0.07/
&DEVC ID='CO2-V', QUANTITY='VELOCITY', XYZ=1.8,0.25,0.07/

&DEVC ID='CO3-V-U', QUANTITY='U-VELOCITY', XYZ=1.6,0.25,0.07/
&DEVC ID='CO3-V-V', QUANTITY='V-VELOCITY', XYZ=1.6,0.25,0.07/
&DEVC ID='CO3-V-W', QUANTITY='W-VELOCITY', XYZ=1.6,0.25,0.07/
&DEVC ID='CO3-V', QUANTITY='VELOCITY', XYZ=1.6,0.25,0.07/
-------Output thickness-------
&DEVC XYZ=2.25, 0.25, 0.0, IOR=3, QUANTITY='WALL THICKNESS', ID='Thickness' /
-------Animated output velocity-------
&SLCF QUANTITY='VELOCITY', VECTOR=.TRUE., CELL_CENTERED=.TRUE., PBY=0.25/
&SLCF QUANTITY='VELOCITY', VECTOR=.TRUE., CELL_CENTERED=.TRUE., PBX=2.25/
&SLCF QUANTITY='VELOCITY', VECTOR=.TRUE., CELL_CENTERED=.TRUE., PBZ=0.07/
-------Animated output temperature-------
&SLCF QUANTITY='TEMPERATURE', CELL_CENTERED=.TRUE., PBY=0.25/

&TAIL /
```

E.1.1 “S1-exHF-medium”

This is the code for the simulation with a moderate fine mesh resolution inside the timber sample. It is the same code as under D.1 “S1-exHF-fine” except for the following subchapter:

```
-------Wood sample-------
&SURF ID='SAMPLE',
      RGB=200,100,0,
      BACKING='INSULATED',
      MATL_ID='SPRUCE',
      THICKNESS=0.12,
      STRETCH_FACTOR(1)=1.05,
      EXTERNAL_FLUX = 96.3963/
```

E.1.2 “S1-exHF-coarse” // “S1-exHF”

This is the code for the simulation with a coarse mesh resolution inside the timber sample. It is the same code as under D.1 “S1-exHF-fine” except for the following subchapter:

```
-------Wood sample-------
&SURF ID='SAMPLE',
      RGB=200,100,0,
      BACKING='INSULATED',
      MATL_ID='SPRUCE',
      THICKNESS=0.12,
      EXTERNAL_FLUX = 96.3963/
```

E.1.3 “S1-exHF-moisture-fine”

This is the code for the simulation with moisture content. It is the same code as under D.1 “S1-exHF-fine” except for the following subchapters:

```
-------Gas combustion-------
&REAC FUEL='PYROLYZATE', C=1, H=3.584, O=1.55, N=0, SOOT_YIELD=0.015,
HEAT_OF_COMBUSTION= 14163.0 /
-------Spruce-------
&MATL ID = 'SPRUCE',
      EMISSIVITY = 0.9,
      CONDUCTIVITY = 0.2,
      SPECIFIC_HEAT_RAMP = 'c_ramp_spruce',
      DENSITY = 317.8,
      N_REACTIONS = 1.0,
      A(1) = 4.69E13,
```

```
        E(1) = 190500,
        N_S(1) = 1.0,
        MATL_ID(1,1) = 'CHAR',
        NU_MATL(1,1) = 0.16,
        SPEC_ID(1,1) = 'PYROLYZATE',
        NU_SPEC(1,1) = 0.84,
        HEAT_OF_REACTION(1) = 430.0,
        HEAT_OF_COMBUSTION= 14163.0,
        ABSORPTION_COEFFICIENT = 50000.0/
&RAMP ID='c_ramp_spruce', T=30, F=0.792 /
&RAMP ID='c_ramp_spruce', T=70, F=0.857 /
&RAMP ID='c_ramp_spruce', T=110, F=0.912 /
&RAMP ID='c_ramp_spruce', T=150, F=0.959 /
&RAMP ID='c_ramp_spruce', T=190, F=0.999 /
&RAMP ID='c_ramp_spruce', T=230, F=1.035 /
-------Wood sample-------
&SURF ID='SAMPLE',
        RGB=200,100,0,
        BACKING='INSULATED',
        MATL_ID='SPRUCE',
        THICKNESS=0.12,
        MATL_ID(1,1) = 'SPRUCE',
        MATL_ID(1,2) = 'MOISTURE',
        MATL_MASS_FRACTION(1,:) = 0.88,0.12,
        STRETCH_FACTOR(1)=1,
        EXTERNAL_FLUX = 96.3963/
```

And these new subchapters:

```
-------Water vapor-------
&SPEC ID='WATER VAPOR' /
-------Moisture-------
&MATL ID = 'MOISTURE'
        EMISSIVITY = 1.0
        DENSITY = 1000.
        CONDUCTIVITY = 0.6
        SPECIFIC_HEAT = 4.19
        N_REACTIONS = 1
        A = 1E13
        E = 1.0E5
        N_S = 1
        SPEC_ID = 'WATER VAPOR'
        NU_SPEC = 1.0
        HEAT_OF_REACTION = 2260. /
```

E.1.4 “S1-exHF-cp-fine”

This is the code for the simulation with constant specific heat for spruce and char. It is the same code as under D.1 “S1-exHF-fine” except for the following subchapters:

```
-------Spruce-------
&MATL ID = 'SPRUCE',
        EMISSIVITY = 0.9,
        CONDUCTIVITY = 0.09,
        SPECIFIC_HEAT = 1.8,
        DENSITY = 408.0,
        N_REACTIONS = 1.0,
        A(1) = 4.69E13,
        E(1) = 190500,
        N_S(1) = 1.0,
        MATL_ID(1,1) = 'CHAR',
        NU_MATL(1,1) = 0.16,
        SPEC_ID(1,1) = 'PYROLYZATE',
        NU_SPEC(1,1) = 0.84,
        HEAT_OF_REACTION(1) = 430.0,
        HEAT_OF_COMBUSTION= 14000.0,
        ABSORPTION_COEFFICIENT = 50000.0/
-------Char-------
&MATL ID='CHAR',
        EMISSIVITY = 0.85,
        DENSITY = 59,
        CONDUCTIVITY = 0.22,
        SPECIFIC_HEAT = 1.5/
```

E.2 “S2-HP-fine”

This is the standard code for the simulation with ignition by a heat panel. The code is the same as under D.1 “S1-exHF-fine” except for the following subchapters:

```
-------Wood sample-------
&SURF ID='SAMPLE',
      RGB=200,100,0,
      BACKING='INSULATED',
      MATL_ID='SPRUCE',
      THICKNESS=0.12,
      STRETCH_FACTOR(1)=1/
-------Geometry of tunnel-------
&OBST ID='Bottom_outlet', XB=1.6,2.12,0.0,0.5,0.0,0.0, SURF_ID='STEEL_SURFACE'/
&OBST ID='Bottom_inlet', XB=2.38,3.81,0.0,0.5,0.0,0.0, SURF_ID='STEEL_SURFACE'/
&OBST ID='Bottom_front', XB=2.115,2.385,0.0,0.14,0.0,0.0, SURF_ID='STEEL_SURFACE'/
&OBST ID='Bottom_back', XB=2.115,2.385,0.36,0.5,0.0,0.0, SURF_ID='STEEL_SURFACE'/
&OBST ID='Top_outlet', XB=1.6,1.97,0.0,0.5,0.15,0.15, SURF_ID='STEEL_SURFACE'/
&OBST ID='Top_inlet', XB=2.53,3.81,0.0,0.5,0.15,0.15, SURF_ID='STEEL_SURFACE'/
&OBST ID='Top_front', XB=1.965,2.535,0.0,0.05,0.15,0.15, SURF_ID='STEEL_SURFACE'/
&OBST ID='Top_back', XB=1.965,2.535,0.44,0.5,0.15,0.15, SURF_ID='STEEL_SURFACE'/
&OBST ID='Side_Front', XB=1.6,3.81,0.0,0.0,0.0,0.15, SURF_ID='STEEL_SURFACE'/
&OBST ID='Side_Back', XB=1.6,3.81,0.5,0.5,0.0,0.15, SURF_ID='STEEL_SURFACE'/
```

And these new subchapters:

```
-------Heat panel-------
&SURF ID='HEAT_PANEL_SURFACE',
      COLOR='RED',
      NET_HEAT_FLUX=120/
-------Position of heat panel-------
&VENT ID='HEAT_PANEL_FLOW', XB=1.97,2.53,0.05,0.44,0.15,0.15,
SURF_ID='HEAT_PANEL_SURFACE', IOR=-3 /
```

E.2.1 "S2-HP-moisture-fine"

This is the code for the simulation with moisture content. The code is the same as under D.2 "S2-HP-fine" except for the following subchapters:

```
-------Gas combustion-------
&REAC FUEL='PYROLYZATE', C=1, H=3.584, O=1.55, N=0, SOOT_YIELD=0.015, HEAT_OF_COMBUSTION= 14163.0 /
-------Spruce-------
&MATL ID = 'SPRUCE',
      EMISSIVITY = 0.9,
      CONDUCTIVITY = 0.2,
      SPECIFIC_HEAT_RAMP = 'c_ramp_spruce',
      DENSITY = 317.8,
      N_REACTIONS = 1.0,
      A(1) = 4.69E13,
      E(1) = 190500,
      N_S(1) = 1.0,
      MATL_ID(1,1) = 'CHAR',
      NU_MATL(1,1) = 0.16,
      SPEC_ID(1,1) = 'PYROLYZATE',
      NU_SPEC(1,1) = 0.84,
      HEAT_OF_REACTION(1) = 430.0,
      HEAT_OF_COMBUSTION= 14163.0,
      ABSORPTION_COEFFICIENT = 50000.0/
&RAMP ID='c_ramp_spruce', T=30, F=0.792 /
&RAMP ID='c_ramp_spruce', T=70, F=0.857 /
&RAMP ID='c_ramp_spruce', T=110, F=0.912 /
&RAMP ID='c_ramp_spruce', T=150, F=0.959 /
&RAMP ID='c_ramp_spruce', T=190, F=0.999 /
&RAMP ID='c_ramp_spruce', T=230, F=1.035 /
-------Wood sample-------
&SURF ID='SAMPLE',
      RGB=200,100,0,
      BACKING='INSULATED',
      MATL_ID='SPRUCE',
      THICKNESS=0.12,
      MATL_ID(1,1) = 'SPRUCE',
      MATL_ID(1,2) = 'MOISTURE',
      MATL_MASS_FRACTION(1,:) = 0.88,0.12,
      STRETCH_FACTOR(1)=1/
```

And these new subchapters:

```
-------Water vapor-------
&SPEC ID='WATER VAPOR' /
-------Moisture-------
&MATL ID = 'MOISTURE'
      EMISSIVITY = 1.0
      DENSITY = 1000.
      CONDUCTIVITY = 0.6
      SPECIFIC_HEAT = 4.19
      N_REACTIONS = 1
      A = 1E13
      E = 1.0E5
      N_S = 1
      SPEC_ID = 'WATER VAPOR'
      NU_SPEC = 1.0
      HEAT_OF_REACTION = 2260. /
```

Appendix F – Surface temperature recordings from test JF00

The following graph shows the recorded temperature on the surface of the timber sample during the test JF00 with the FANCI apparatus [31, modified Fig. 5.2(a)]. The two lines show the two measuring points. It can be seen that for the red line measuring in TS_2, there was a problem during the recording. Given that, only the temperature measurements from TS_1 was used for the comparison with the simulation in this study.

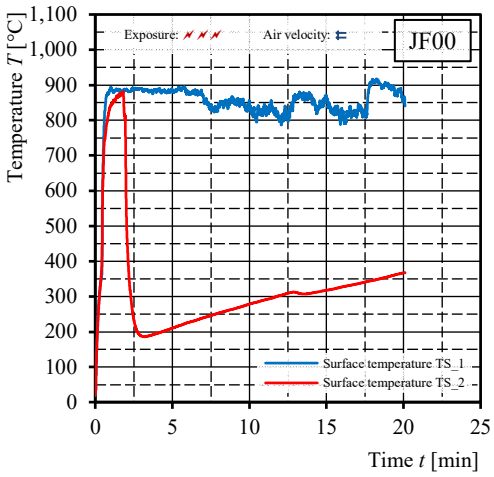

Graph 65: Surface temperature measurements from experiment JF00 [31, modified Fig. 5.2(a)]

Appendix G – Additional simulation results

G.1 Air velocity recordings above timber sample

The first graph shows the air velocity recordings above the timber sample for the simulations with ignition by an external heat flux “S1-exHF-medium”, “S1-exHF-coarse”, “S1-exHF-moisture-fine” and “S1-exHF-cp-fine” together with the experimental results. The lines for the simulation results are overlapping. The second graph shows the results for the simulation with ignition by a heat panel including moisture “S2-HP-moisture-fine” and the experimental results.

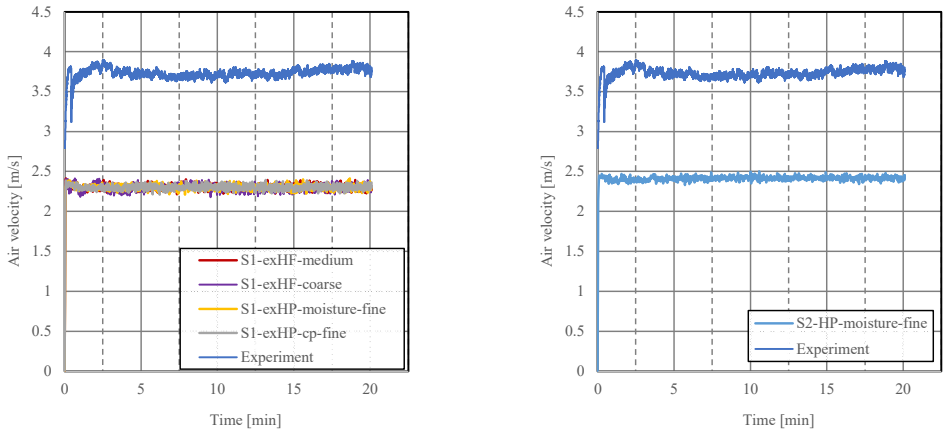

Graph 66: Results from air velocity measurements above timber sample for different simulations and for the experiment

G.2 Gas temperature measurements at the start, the end and behind the fire chamber

The first three graphs show the gas temperature measurements at the start, the end and behind the fire chamber for the simulations with ignition by an external heat flux “S1-exHF-medium”, “S1-exHF-coarse”, “S1-exHF-moisture-fine” and “S1-exHF-cp-fine” and the next three the same results for the simulation with ignition by a heat panel “S2-HP-moisture-fine”, together with the experimental results.

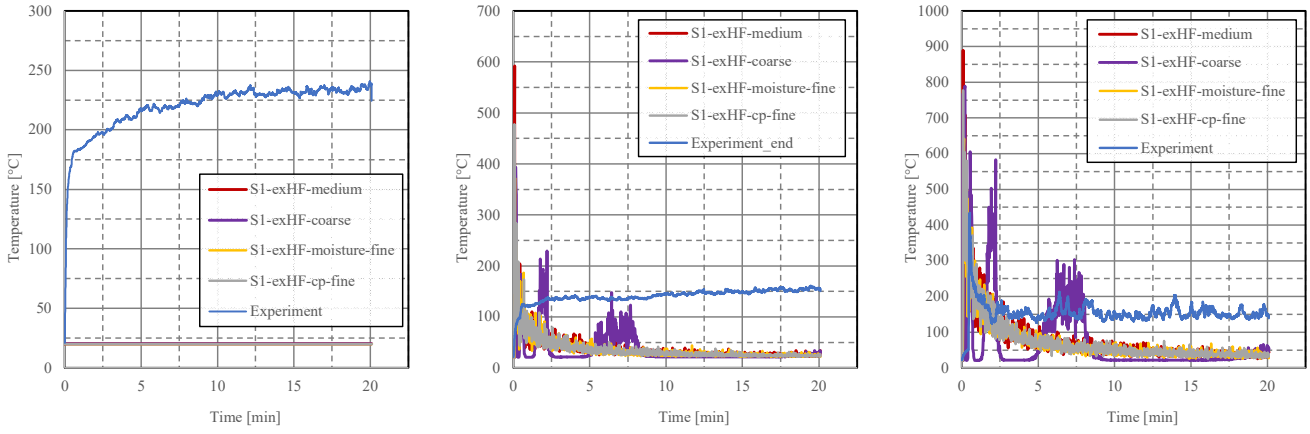

Graph 67: Gas temperature measurements at the start (left), at the end (middle) and behind the fire chamber (left) for simulations with ignition by an external heat flux and the experiment

The results for the simulations “S1-exHF-medium”, “S1-exHF-moisture-fine” and “S1-exHF-cp-fine” are overlapping in all three graphs, and in the results for the position at the start of the fire chamber, also the simulation “S1-exHF-coarse”.

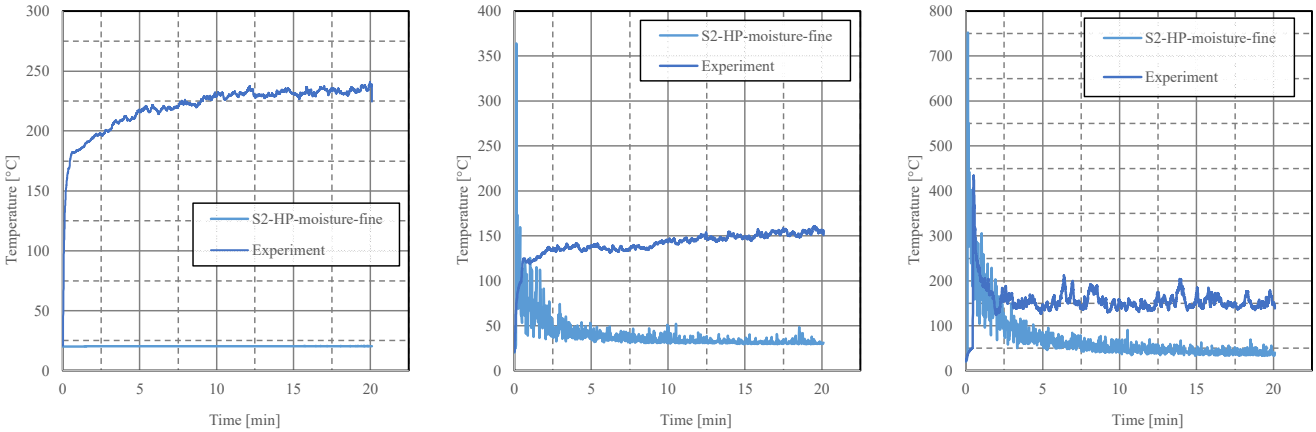

Graph 68: Gas temperature measurements at the start (left), at the end (middle) and behind the fire chamber (left) for the simulation with ignition by a heat panel and moisture and the experiment

Appendix H – Influence of moisture content on simulation results – Further comparisons

H.1 Simulations “S2-HF-fine” & “S2-HF-moisture-fine”

This shows the comparison between the simulation with dry timber and timber with a moisture content for the simulation situation with ignition by a heat panel.

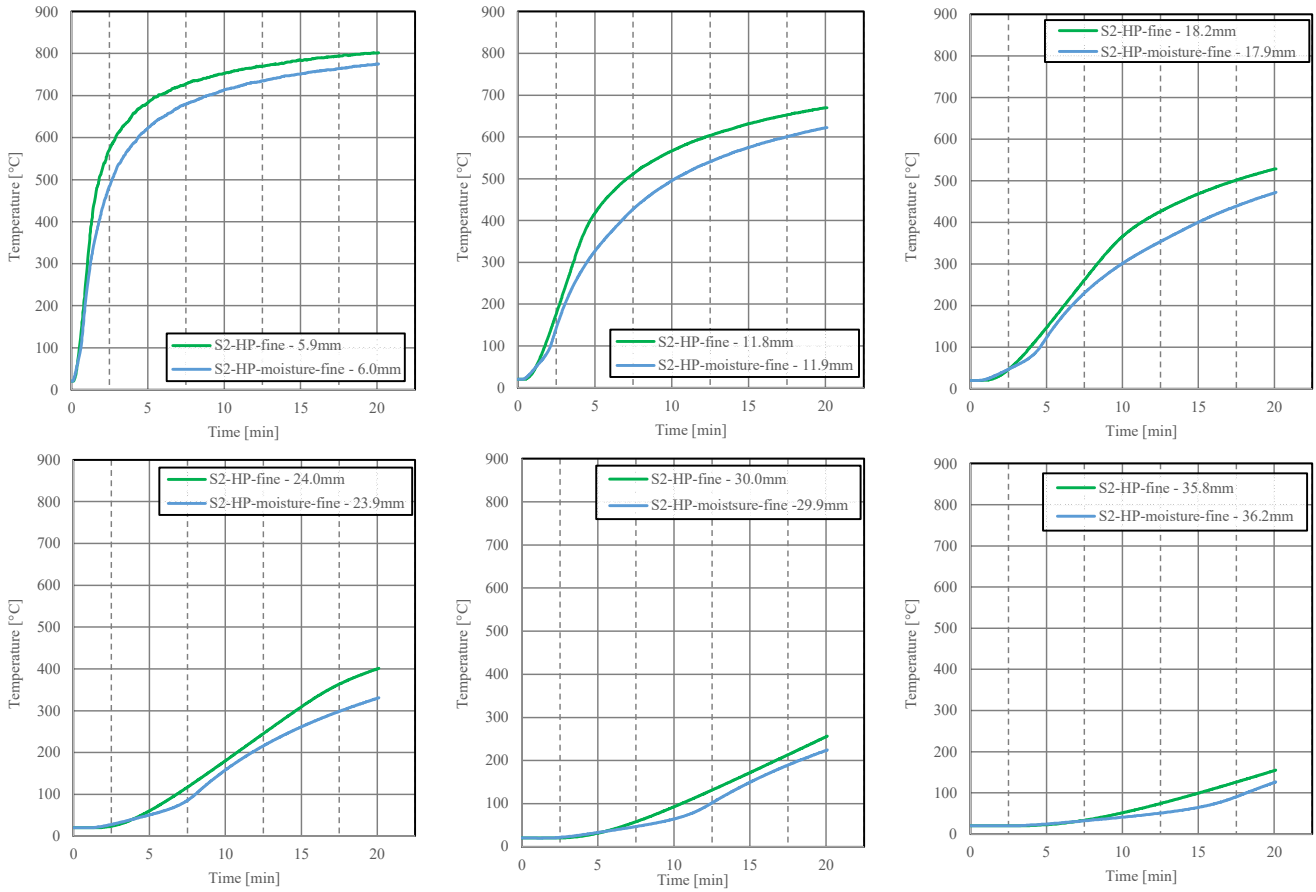

Graph 69: Temperature measurements inside the timber sample for simulations "S2-HP-fine" & "S2-HP-moisture-fine"

Appendix I – Additional comparisons with experimental data

I.1 Temperature measurements in the wood sample

The following graphs compare the simulated temperatures inside the timber sample for the simulations with the ignition by the heat panel with the ones measured in the experiment, for depths of 6 [mm], 12 [mm], 18 [mm], 24 [mm], 30 [mm] and 36 [mm] from the timber surface.

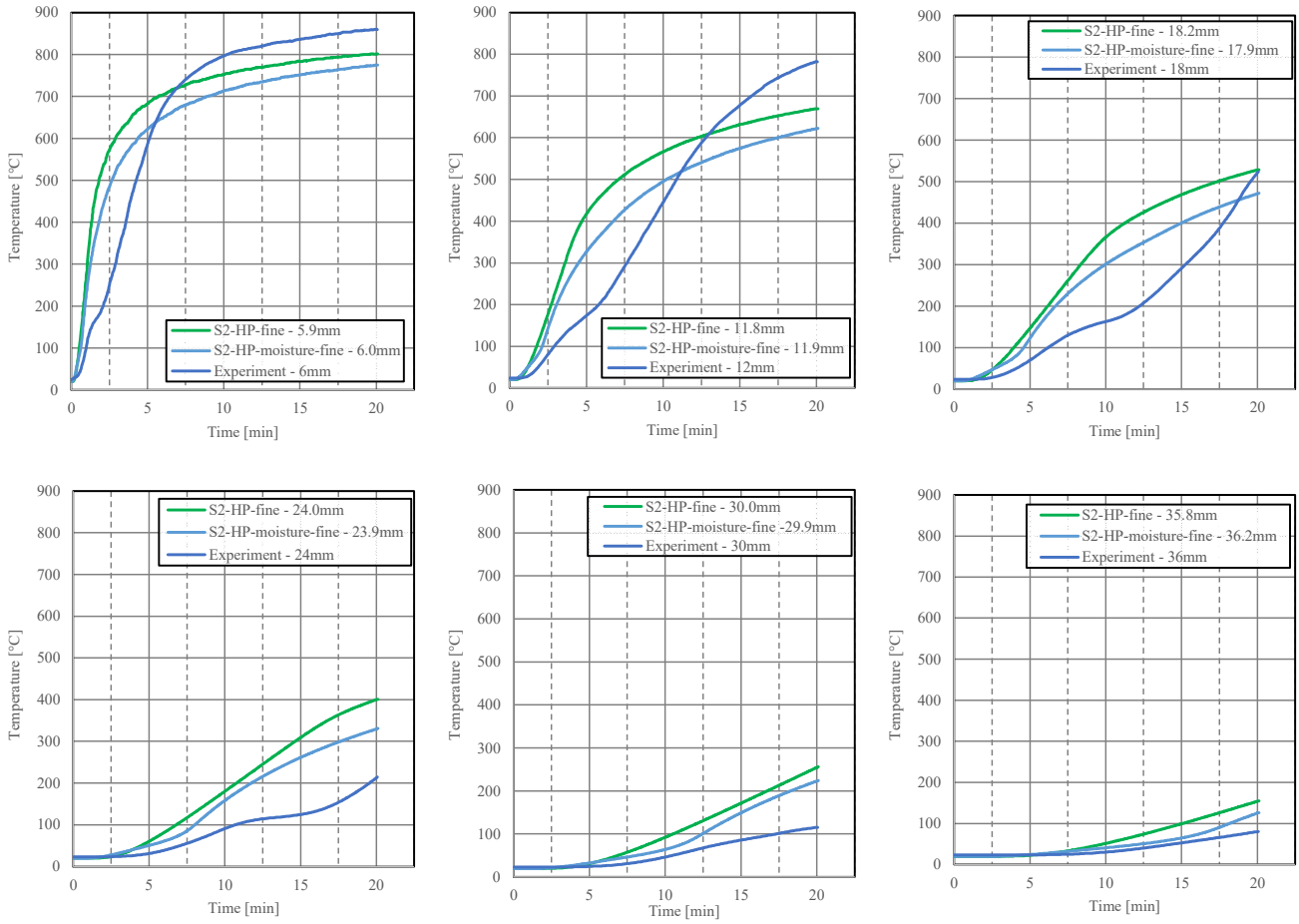

Graph 70: Comparison of temperature measurements inside the timber sample for simulations "S2-HP-fine" & "S2-HP-moisture-fine" with the experimental data

I.2 Char properties

The following graph compares the 300°C-ISO profile from the simulations with ignition by the heat panel with the experimental data.

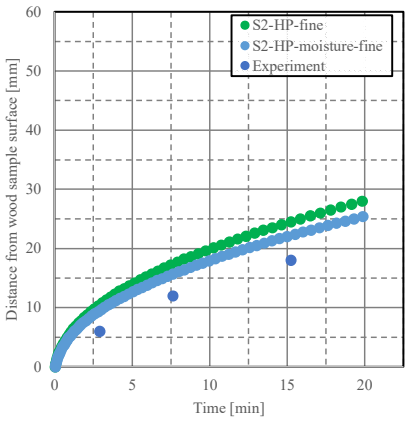

Graph 71: Comparison of the 300°C-ISO profile for the simulations "S2-HP-fine" & " S2-HP-moisture-fine " with the experimental data

Appendix J – Raw data of simulations, analyses and comparisons